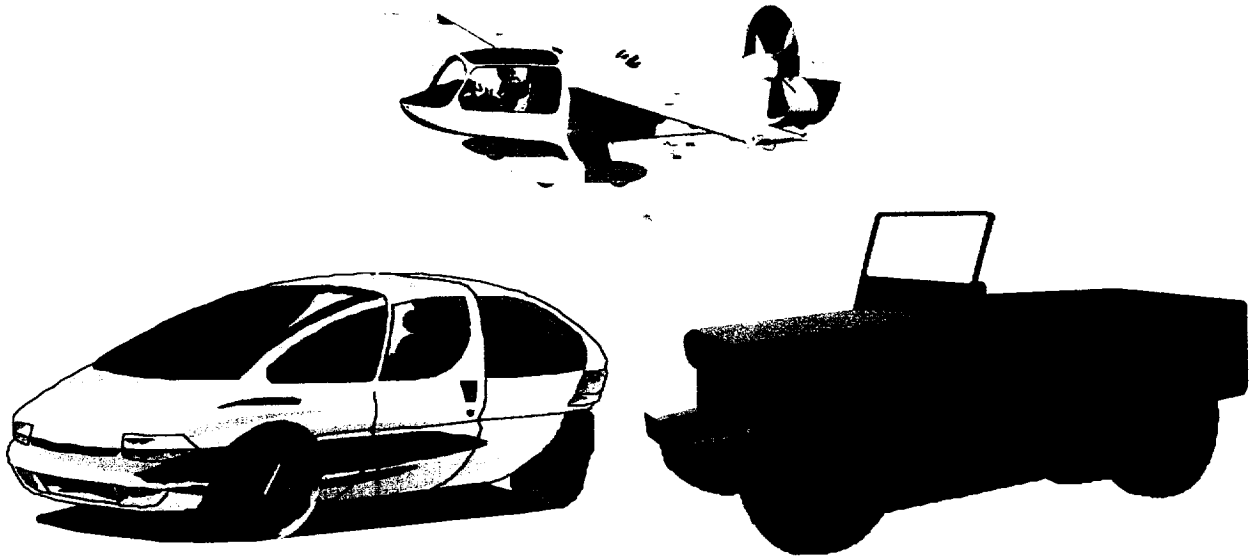


PERSONAL AIR VEHICLE  
&  
FLYING JEEP  
CONCEPTS



A Commentary  
on  
Promising Approaches  
or  
What Goes Around Comes Around  
(about every twenty years)

by

David W. Hall, P.E.  
David Hall Consulting  
965 Morro Avenue  
Unit #C  
Morro Bay, California  
93442

prepared on

Tuesday, July 24, 2001

**DRAFT**

Personal Air Vehicle & Flying Jeep Concepts: A Commentary on Promising Approaches  
Tuesday, July 24, 2001

3:12 PM

**TABLE OF CONTENTS**

<b>Section Title</b>	<b>Page</b>
Introduction	7
Military Fixed-Wing VTOL Approaches	8
Tail Sitters	8
Deflected Slipstream	8
Fan-In-Wing	9
Thrust Augmentors	11
Vectored Thrust	11
Tilt Engines	13
Tilt Wings	14
Other	15
Civilian Fixed-Wing VTOL Approaches	16
Historical Roadable Vehicles	16
Tilt Ducts & Tilt Propulsion	18
Augmentors	22
Autogyro	22
22	
Deflected Slipstream & Thrust Vectoring	23
Other Modern Roadable Aircraft	23
Flying Jeeps	24
Chrysler VZ-6	25
Piasecki VZ-8	25
deLackner <i>Aerocycle</i>	25
Hiller's Second Flying Platform	26
Bell Jet Pack	27
Bertelson <i>Aeromobile</i> 200-2 GEM	27
Curtiss-Wright Model 2500 GEM	28
Summary	28
How the Various V/STOL Approaches Compare	29
V/STOL Considerations	33
General Observations	33
Takeoff and Landing	33
Flight Envelopes	46
Avoid Curve Considerations in Flight Envelope Determination	48
Vertical Lift Stability and Control Considerations	55
Effect of Ground Plane	58
Disc Loading Effects	61
Hover Performance	61
Minimizing Power Required	62
Theoretically Elegant VTOL Concepts—Fluidic Amplification	66
Fan-In-Wing	66
Thrust Augmentor Wing	67
Thrust Augmenter Wing	67
Summary	75
Comments on the Appendices	75

## LIST OF FIGURES

Number	Title	Page
1	Flying Platforms were Explored in the 1950s by the U.S.Army	8
2a	Ryan's VZ-3 Relied on Wing Airflow Momentum Change Aft of a Propeller	9
2b	The Fairchild VZ-5 Relied on Momentum Change Aft of a Propeller	9
3	The Ryan XV-5 was a Fan-In-Wing VTOL Demonstrator, Its Propulsion System is Shown at Center	10
4	The Avro/Canada VZ-9 <i>AvroCar</i> was a Fan-In-Fuselage Approach to VTOL	11
5	The X-14 Used a Different Vectored Thrust Approach Than the <i>Kestrel/Harrier</i>	12
6	The Collins <i>Aerodyne</i> was the Brainchild of Dr. Alexander Lippisch	12
7	The Grumman Model 698 of 1977 was Flown in Scale Model Form	13
8	The Curtiss-Wright VZ-7 Flying Jeep was Designed as an Army Utility Vehicle in the Late 1950s and was Canceled in 1960	13
9	The Doak VZ-4 of 1958 Demonstrated Tilt-Duct Technology	14
10	The Bell X-22A of 1964 Successfully Demonstrated More Sophisticated Tilt-Duct Technology Than the Earlier VZ-4	14
11	The Vertol Model 76 (upper) and Its Successor, the VZ-2 (lower), were the First Tilt-Wing Demonstrators	15
12	The Mississippi State University <i>Marvel</i> STOL Demonstrator was Ahead of Its Time	15
13	Juan Cierva Developed a Successful Autogyro in Spain	16
14a	The Waterman <i>Whatsit</i> Flew in the 1930s	16
14b	The Waterman W-5 <i>Arrowbile</i> of 1937 was Flight Tested	16
15a	The Pit cairn Autogyro of 1935 was an Early PAV	17
15b	The Pit cairn <i>Arrowbile</i> was an Attempt to Make the Autogyro Roadable	17
16	The ConVAir ConVAIRCAR Flew in 1947	17
17	The Fulton Airphibian was the First Certificated Roadable Aircraft, Flying in 1947	18
18	The Taylor Aerocar of 1968 was a Serious Attempt at a Roadable Aircraft	18
19	The Nord Model 500 was Exhibited at the 1967 Paris Airshow	19
20	The Kulair K007 is a tilt Ducted Fan Commuter/Bizjet	19
21		
22	The <i>Vertigo</i> is Available as an R/C Model Kit	20
23	This Novel Tilt-Propeller Design has Already Flown	20
24	A Personal Tilt-Fan VTOL is One Current Scheme Being Explored	20
25a	XM-2 of 1962-68	21
25b	XM-3 of 1966	21
25c	XM-4 of 1970-74	21
25d	M200X of 1985	21
26	Shown at Left is the <i>CityHawk</i> Mockup with a Scale Model at Right	21
27	The LARP is Under Development as an Emergency Rescue Vehicle	22
28	The Moshier Technologies <i>Aurora</i> Used a Four-Poster Augmentor Arrangement	22
29	The <i>CarterCopter</i> is an Example of the Current SOTA in Gyrocopters	22
30a	Thrust Vectoring Scheme	23
30b	Moller M150 <i>Volantor</i>	
30c	Moller M400 <i>Skycar</i>	23
31	The Allied AeroTechnics Incorporated <i>AirBike</i> is a Novel Approach to a PAV	23
32	The Aeromaster Innovations <i>Synergy</i> is an Example of a Modern Roadable Aircraft	24
33	Mr. Williamson's <i>Roadrunner</i> Concept Has A Lot Going For It	24
34	The Chrysler VZ-6 was Unsuccessful	25
35	The Piasecki VZ-8 Operated Well in Ground Effect	25
36	The deLackner <i>Aerocycle</i> Was Feasible in Prototype Form	26
37	Hiller's Second Platform Was Less Successful than the First	26
38	The Bell Jet Pack was a Challenge to Learn to Fly	27
39	The Bertelson <i>Aeromobile</i> 200-2 was Developed by an M.D.	27

<b>Number</b>	<b>Title</b>	<b>Page</b>
40	The Curtiss-Wright Model 2500 GEM Carried Four Passengers	28
41	A Takeoff Parameter Can Be Used to Estimate Takeoff Distances	34
42	Key VTOL Performance Parameters are Interlinked	35
43	A Lot Happens In a Short Period of Time During Takeoff	36
44	An Airplane During Takeoff is Acted Upon by Determinable Forces and Accelerations	36
45	Landing Analysis is Conceptually Similar to Takeoff Analysis	41
46	The Landing Run Freebody Includes Braking	41
47	The Effect of Stopping Deceleration on Ground Roll Can Be Dramatic	46
48	Thrust or Power Required and Available versus Airspeed (left) Yields Excess Thrust or Power for Climb Rate Determination (right)	47
49	A Flight Envelope is Constructed from Other Sets of Performance Curves	48
50	A Variety of Factors Determine the Shape of a Flight Envelope	48
51	Avoid Zones Are Both Kinematically and Aerodynamically Determined	49
52	Angle-of-Attack Plays an Important Role in Avoid Curve Determination	51
53	Lift Engines Run for only a Small Portion of Total Flight Time	54
54	Engine Bypass Ratio and Fan Pressure Ratio Affect Aircraft Design as Shown by This F100/F401 Class Turbofan	56
55	Blowing Hot, High Pressure Gas at a Hard Surface Causes a lot of Things to Happen	59
56	Configuration Plays a Role in Ground Effect Patterns	60
57	Beyond a Certain Distance, Flow Velocities Tend to Become Uniform	60
58	Fountain Effect Can Increase Apparent Lift in Hover	60
59	Hover Time Varies Inversely With Cruise Speed	61
60	High Disc Loading VTOLs Tend to Have Large Engines	61
61	Slipstream Velocity Directly Under a Hovering VTOL Affects Its Performance	63
62	Power Required Reaches a Minimum at the End of Transition from Hover	64
63	Designers Can Improve Low Speed Performance of VTOLs	64
64	VTOL Aircraft Engines Must Be Sized to Take Engine-Out Performance Into Consideration	65
65	Fan Disc Loading is a Strong Determinant of Augmentation Ratio	66
66	Spanwise Augmenter Bays Entrain Large Amounts of Ambient Air	67
67	Relative Geometries Play a Significant Role in Determining Augmentation Ratio	68
68	This Augmenter Layout is Similar to That on the XFV-12A	71
69	Augmenter Bays May be Placed Spanwise Inboard in Small Sets	71
70	Augmenter Bays Can be Arranged Chordwise as well as Spanwise	72
71a	This Four-Poster Augmenter Arrangement is Practical and Efficient	73
71b	Cross-Section Geometric Relationships Define Augmenter Performance	73
72	1979 Marked the Final Year for Substantive Augmenter Development	74

### LIST OF TABLES

<b>Number</b>	<b>Title</b>	<b>Page</b>
1	There Are Advantages and Disadvantages to Each System	30
2	PAV Data Table Foldout	32.5
3	Augmenter Flap Deflector Determines Thrust Available for Direct Acceleration	70

**SYMBOLS**

<b>Symbol</b>	<b>Definition</b>	<b>Units</b>
$A$	Cross-Sectional Area	sq.ft.
$a$	Acceleration	ft/sec <sup>2</sup>
$AR$	Flying Surface Aspect Ratio, wing is default value	-
<b>Symbol</b>	<b>Definition</b>	<b>Units</b>
$C_D$	Drag Coefficient	-
$C_L$	Lift Coefficient	-
$C_\mu$	Thrust Blowing Coefficient	-
$\bar{c}$	Mean Chord	in or ft
$D$	Drag	lbf
$D$	Diameter	in or ft
$d$	Distance	in
$E$	Energy	ft-lbf
$e$	Airplane Efficiency Factor	-
$F$	Engine Thrust, usually thrust generated by a turbofan or turbojet	lbf
$fpr$	Fan Pressure Ratio	-
$g$	Gravitational Acceleration, earth's is default value = 32.2	ft/sec <sup>2</sup>
$h$	Altitude or Height Above Ground	ft
$i$	Incidence Angle, positive leading edge up	°
$K$	Descent Speed Ratio	-
$K_s$	Takeoff Parameter	psf
$L$	Lift	lbf
$\ell$	Tail Arm	in or $\bar{c}$
$\dot{m}$	Mass Flow	slugs/sec
$N$	Normal Force	lbf
$P$	Engine Power	HP
$P$	Ground Roll Parameter	-
$q$	Dynamic Pressure	psf
$R$	Reverse Thrust Ratio	-
$r$	Radius	in or ft
$s$	Distance Along Ground	ft or n.mi.
$S_{referenc}$		Wing Reference Area
	sq.ft.	
$T$	Also Engine Thrust, usually thrust generated by a propeller	lbf
$t$	Time	sec or hrs
$tsfc$	Thrust Specific Fuel Consumption	lbm/lbf/hr
TOGW	TakeOff Gross Weight	lbf
$V$	Airspeed	fps, kts, mph
$W$	Weight	lbf
$\alpha$	Angle-of-Attack	°

$\gamma$	Flightpath Angle	°
$\delta$	Flying or Control Surface Deflection Angle	°
$\phi$	Thrust Augmentation Ratio	-
$\mu$	Friction Coefficient	-
$\eta_{propelle}$		Propeller Efficiency
	-	
$\theta$	Climb Angle	degrees
$\pi$	3.14159...	-
$\rho$	Air Density	slugs/cu.ft.
$\sigma$	Air Density Ratio	-

## Personal Air Vehicle & Flying Jeep Concepts INTRODUCTION

Freeing airplane operations from long runways has been a dream of aircraft designers and users since before runways transformed from short, sod fields to multiple-mile-long strips of concrete. Rotary wing aircraft have achieved that freedom and become operational, but fixed wing aircraft, for the most part, have not. Both the Government and private sectors periodically revisit this dream and the latest Government effort is centered on providing civilian personal air transportation that will markedly improve efficiency over current methods. The private sector has been busy, too, creating a wealth of new design approaches, perhaps fueled as much by frustration at urban commutes as by desire to push the technology envelope or to rejuvenate a sagging perennially general aviation industry.

The NASA/Langley Personal Air Vehicle Exploration (PAVE) and the DARPA Dual Air/Road Transportation System (DARTS) projects were established to investigate the feasibility of creating vehicles which could replace, or at the very least augment, personal ground and air transportation schemes. This overall goal implies integrating several technology areas with practical everyday transportation requirements to design a class of vehicles which will achieve the following goals:

- Vertical, Extremely Short, or Short Takeoff and Landing (VTOL, ESTOL, STOL) capability;
- Operation at block speeds markedly faster than current combinations of land and air transportation, particularly in critical market areas;
- Unit cost comparable to current luxury cars and small general aviation aircraft;
- Excellent reliability;
- Excellent safety; and
- Ability to integrate with existing land and air transportation systems.

There have been several historical technology demonstrations which achieved potentially viable VTOL and/or STOL operation and these will be discussed first, including technology development efforts which have not resulted in operational aircraft and the reasons why not. Next will come discussion of historical personal air vehicles (PAVs) with attention on technological state-of-the-art (SOTA). The focus will initially be civilian applications and a later section will address military applications. Next discussed will be the effects of emerging technologies on these approaches and speculation on which approaches might best suit current operational needs. Final sections will examine technological challenges, and then the political and regulatory climates and what concession, if any, must be made to field this class of vehicles.

Several caveats are in order. First, fixed wing/powered lift approaches will receive the most attention since a wealth of information has been previously published about rotary wing approaches. There will be some discussion of autogyros here, though. Next, no attempt will be made to develop detailed analytical methods, although overall conceptual considerations will be qualitatively discussed. And last, all the data presented here are unclassified and not proprietary.

A companion paper, written in the summer of 2000, is available at [www.redpeace.org/WhitePaper.pdf](http://www.redpeace.org/WhitePaper.pdf) which presents an in-depth discussion of historical VTOL demonstration programs with a focus on larger aircraft for military and regional airline use. The majority of the information in that paper will not be repeated here since this examination will focus on smaller vehicles indicative of those required for personal air transport.

## MILITARY FIXED WING V/STOL APPROACHES Tail Sitters

The 1950s and 1960s saw demonstrations of a variety of approaches to fixed wing vertical takeoff and landing (VTOL) aircraft with the focus being on military usefulness. First examined were tail sitters in both the U.S. and Europe. Of these aircraft, only the Bell Flying Platform (Figure 1) is applicable to the PAV category. Hiller, Bell, and Piasecki all built and flew flying platform prototypes. The VZ-1 flying platform of 1953 used two counter-rotating 5 foot diameter propellers driven by two 40 HP engines. It used what was euphemistically called kinesthetic control—the pilot leaned in the desired direction—and was stable and easy to fly. The only drawback was a gyroscopic righting tendency which limited top speed to around 15 mph.



Figure 1. Flying Platforms were Explored in the 1950s by the U.S.Army.

### Deflected Slipstream

Turning propeller thrust through large angles proved another tempting idea to achieve VTOL flight, or at least STOL or super-STOL flight. Both Ryan and Fairchild built prototypes. The Ryan VZ-3RY *Vertiplane* of 1959 (Figure 2a) was a high wing aircraft using a single T53 turboshaft engine driving two 9 ft diameter propellers in underslung nacelles blowing over large-chord flaps to redirect propeller and wing flow vertically. Residual jet thrust provided attitude control. During flight tests at NASA/Ames Research Center, the aircraft suffered from a thrust deficiency in ground effect but could hover out of ground effect.

The Fairchild VZ-5 (Figure 2b) was a similar layout except that a single T58 drove four propellers. The wing had 50% chord, full-span articulated flaps turning the flow 60°. The remaining 30° required for vertical takeoff was provided by rotating the aircraft to that ground attitude. Both aircraft demonstrated the feasibility of this approach but both had narrow operating margins which could be made worse by poor piloting technique.

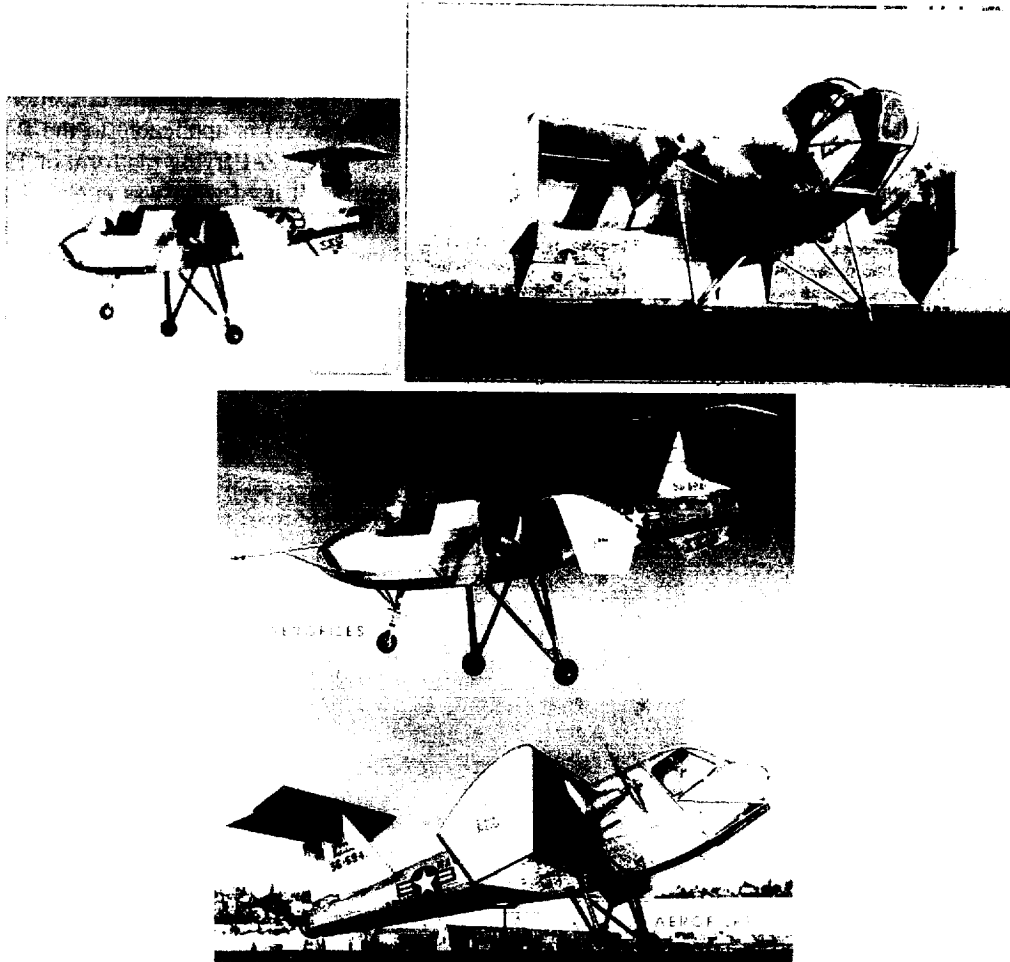


Figure 2a. Ryan's VZ-3 Relied on Wing Airflow Momentum Change Aft of a Propeller.



Figure 2b. The Fairchild VZ-5 Relied on Momentum Change Aft of a Propeller.

### Fan-In-Wing

Ryan built the XV-5A circa 1964 as a demonstrator of the fan-in-wing concept, a way to augment the thrust of cruise engines to generate sufficient thrust for vertical flight. The aircraft never lived up to its promise. Shown in Figure 3 top and lower left is the XV-5A. Figure 3 center shows the thrust diversion scheme used in the General Electric X-353-3 lift system composed of a 76 inch diameter fan with tip turbines immersed in the exhaust flow from a J85 turbojet engine. Figure 3 lower right shows the 1968 incarnation, redesignated XV-5B, which was delivered to NASA/Ames for extensive testing. Although these aircraft were larger than a PAV would be, the technology is potentially applicable given advances in low bypass ratio turbofan SOTA in the last thirty years.

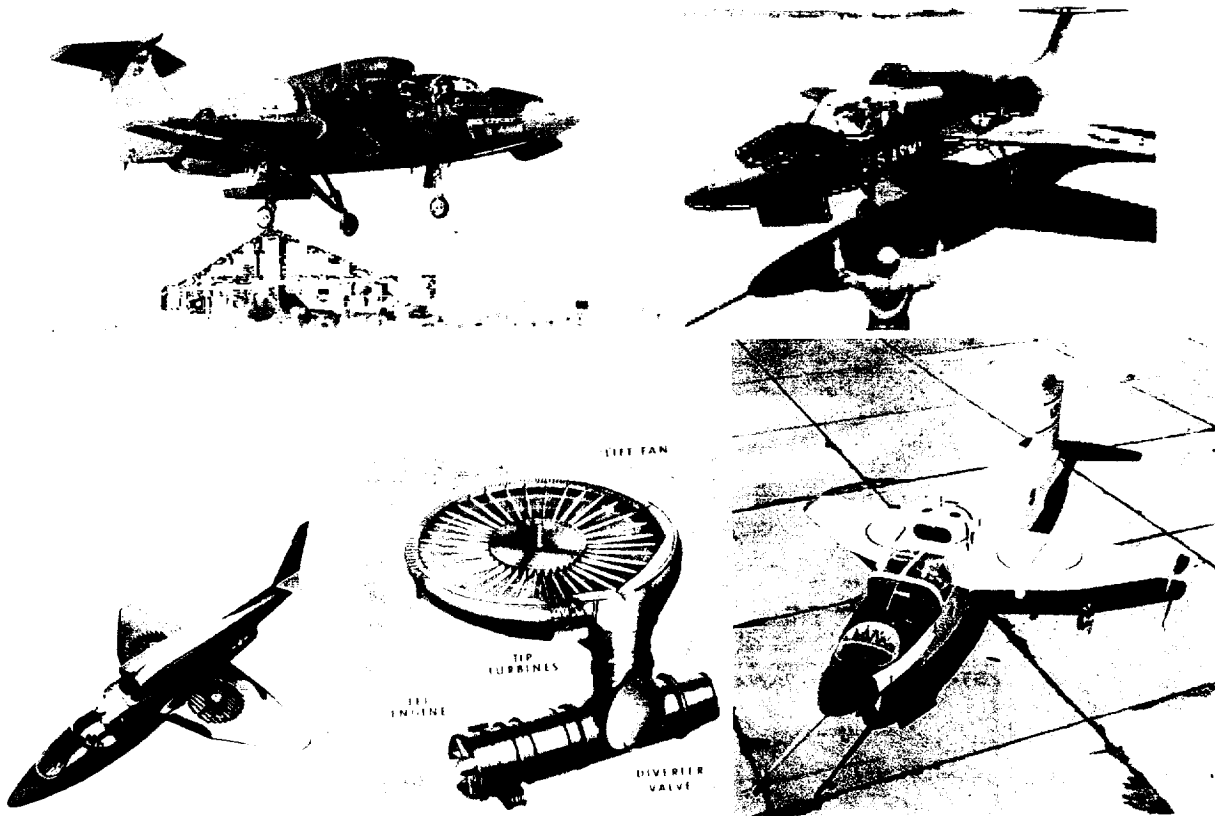
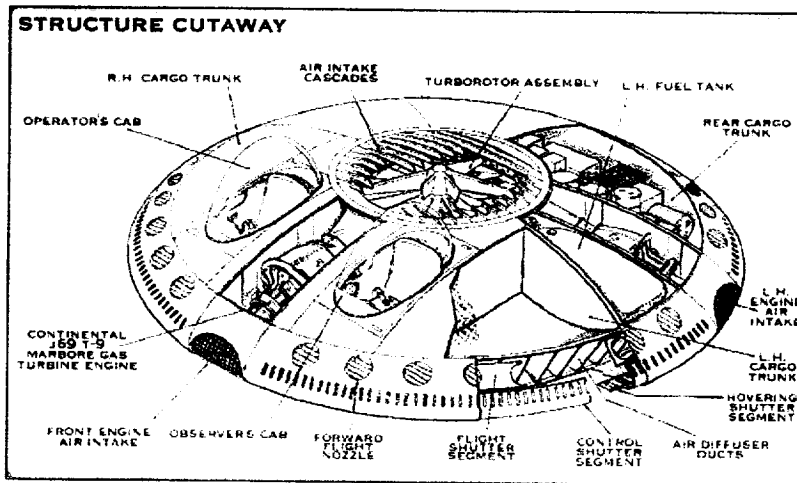
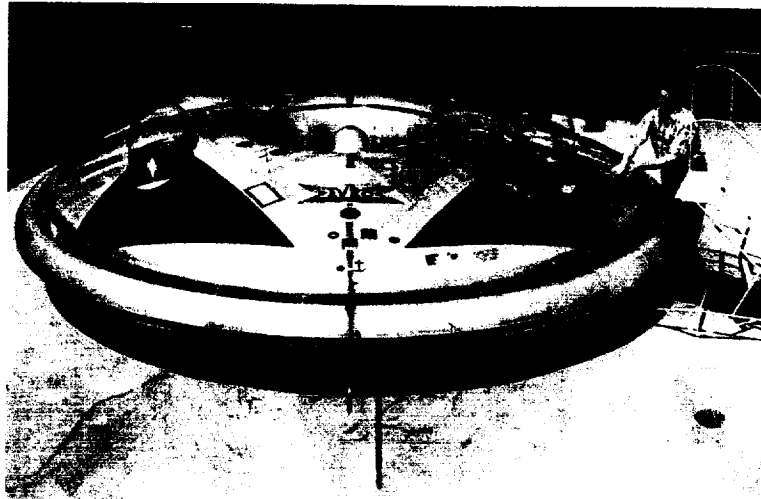


Figure 3. The Ryan XV-5 was a Fan-In-Wing VTOL Demonstrator, Its Propulsion System is Shown in the Center.

Another buried fan concept was the Avro/Canada VZ-9 *AvroCar* of the early 1960s which was a not entirely successful attempt at using ground effect for motion (Figure 4). This aircraft used a large ducted fan for generation of vertical lift in VTOL and in translation driven by three Continental J69 turbojets. Test pilots reported that any air bleedoff for direction changes tended to dip one side of the disc, so precise maneuvering over uneven terrain was a challenge. The aircraft exhibited excellent hover efficiency, however.



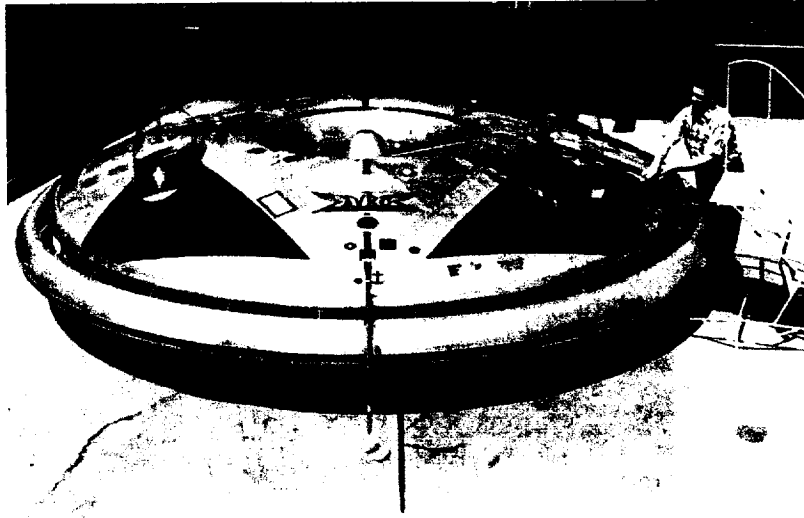


Figure 4. The Avro/Canada VZ-9 AvroCar was a Fan-In-Fuselage Approach to VTOL.

#### Thrust Augmentors

The U.S. Army began funding several theoretically promising V/STOL approaches in 1961. Lockheed won a contract with its Model 330 as the VZ-10, which was redesignated XV-4A, in 1962. The XV-4 used Coanda Effect inside a fuselage cavity running lengthwise from just aft of the cockpit to the vertical tail. This cavity was fed by two 3,300 pound static thrust Pratt & Whitney JT12A-3 engines blowing through slots along either side of the cavity on the top. This aircraft was modified and flown in late 1966 as the XV-4B *Hummingbird* with four GE J85 turbojets mounted vertically in the fuselage for takeoffs and landings and another two mounted horizontally in the wing roots for cruise thrust to explore the lift plus lift/cruise approach. North American modified the XV-4B back to a fuselage augmentor bay with careful tailoring of multiple, short ejector nozzles as an early technology testbed and precursor to their XTV-12A of the 1970s. The XTV-12A was the furthest development of augmentors to date.

#### Vectored Thrust

Early vectored thrust approaches are typified by the Bell X-14 which is shown in hover mode in front of the NASA/Ames Research Center main hangar in Figure 5. The aircraft used wings from a Beechcraft Bonanza and empennage from a Beech T-34. NASA flew the Bell X-14 research aircraft in 1957 and it continued to fly into the 1970s. It weighed about 3,500 pounds and used two GE J85-5 turbojets in its later incarnation as a variable stability research aircraft.

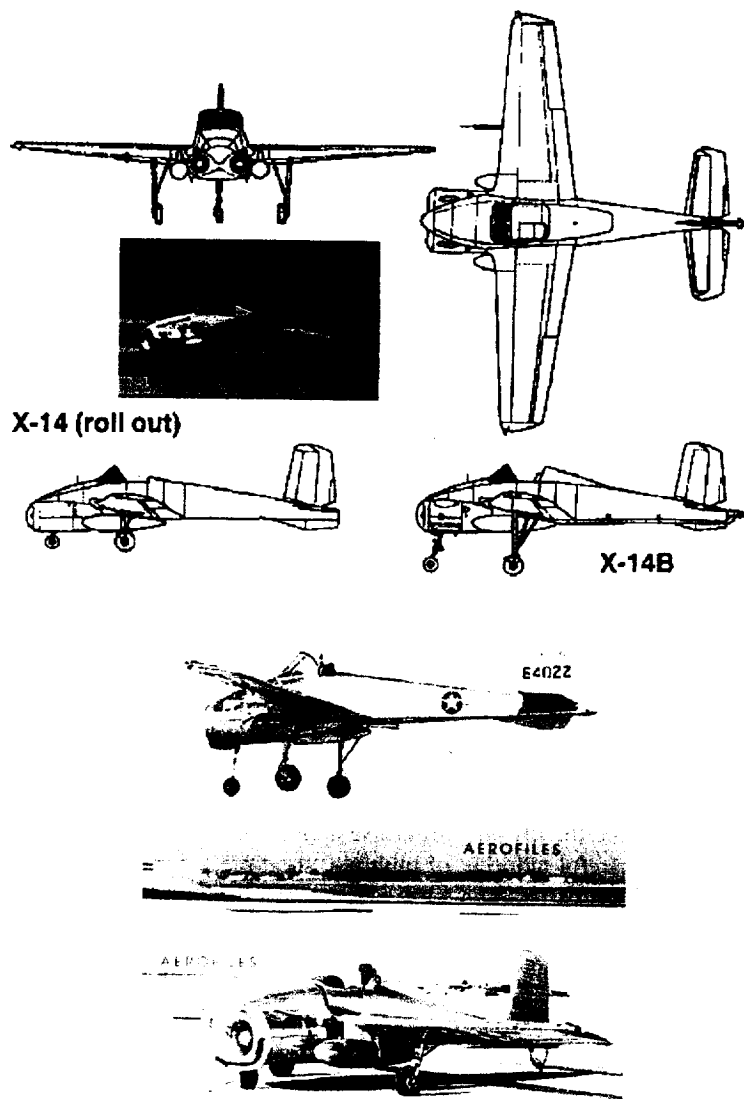


**Figure 5. The X-14 Used a Different Vectored Thrust Approach than the *Kestrel/Harrier*.**

Fitting loosely into this category and of academic interest is the Collins *Aerodyne*, the brainchild of Dr. Alexander Lippisch in the early 1940s (Figure 6). Dr. Lippisch was busy with the exigencies of providing the world's first rocket-powered combat aircraft at the time and didn't get back to the *Aerodyne* concept until the mid-1960s when Rockwell/Collins allowed him to build a 42 foot long prototype which was later tested in the NASA/Ames Research Center's 40x80 foot wind tunnel. Stability and control deficiencies ended the test series and the aircraft was never flown, although Dr. Lippisch continued to work on the concept until his death in the mid-1970s.

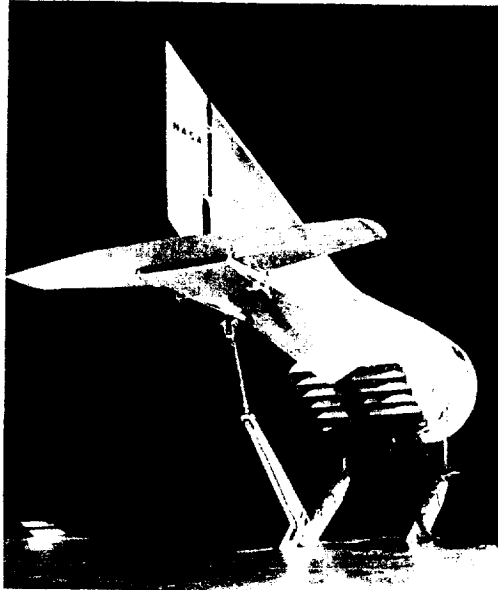


**Figure 6. The Collins Aerodyne was the Brainchild of Dr. Alexander Lippisch.**

Grumman applied a similar thrust vectoring approach in the Model 698 of 1977 (figure 7) which was flown in model form and proved successful.

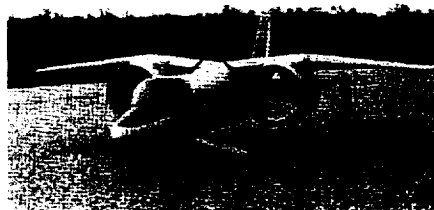


**Figure 7. The Grumman Model 698 of 1977 was Flown in Scale Model Form.**

### **Tilt Engines**

Tilting engine exhaust flow is one way to achieve vertical flight, as just discussed; another is to tilt the entire engine, or possibly even the entire aircraft (Figure 8) or tilt ducted fans (Figures 9 and 10), or even jet engines. Of particular note for the current work is the Curtiss-Wright VZ-7 of Figure 8 which was developed in the 1950s as a prototype flying jeep, and entered flight test in 1957. The VZ-7 used four 80 inch diameter propellers driven by a 425 HP Turbomeca Artouste II. During flight test it flew as long as 25 minutes at a time, but top speed was under 50 mph. The program was terminated in 1960.

The Doak VZ-4 of 1958 had a 3,000 # TOGW and used on Lycoming T53 turboshaft engine driving two 4 foot diameter ducted fans which could tilt through 90°. The overall approach proved promising but was very noisy, the ducted fans at full power sounding like sirens.

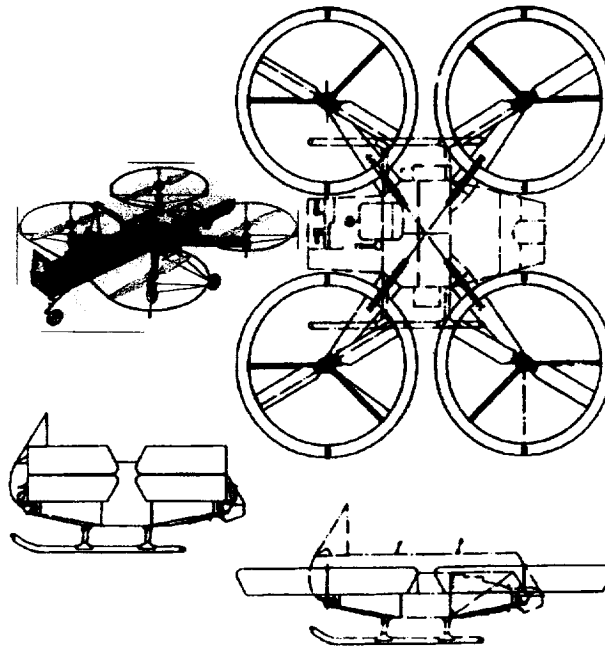


**Figure 8. The Curtiss-Wright VZ-7 Flying Jeep was Designed as an Army Utility Vehicle in the Late 1950s and was Canceled in 1960.**

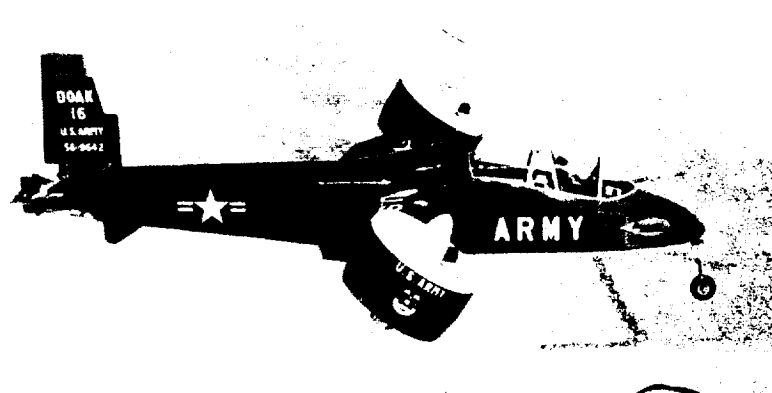


**Figure 9. The Doak VZ-4 of 1958 Demonstrated Tilt-Duct Technology.**

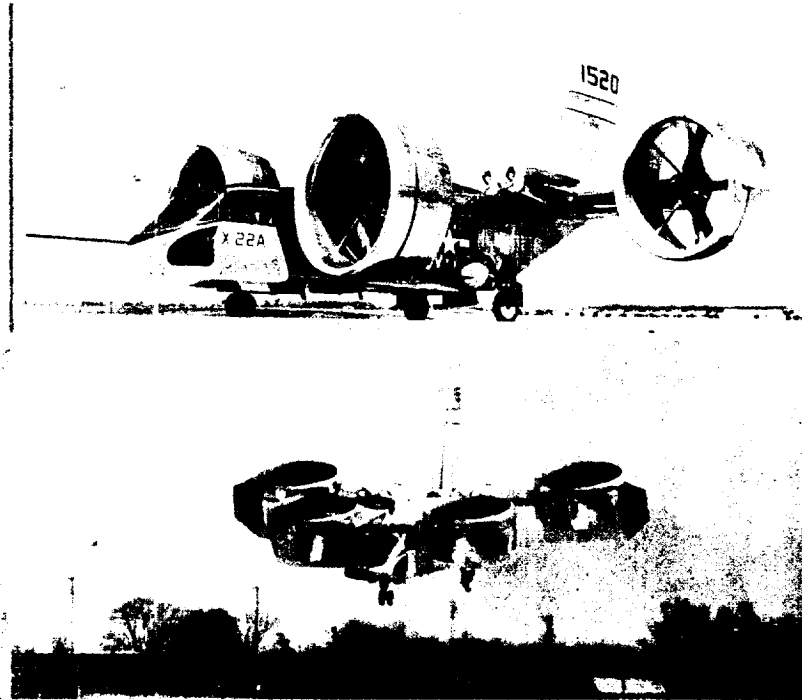


**Figure 10. The Bell X-22A of 1964 Successfully Demonstrated More Sophisticated Tilt-Duct Technology Than the Earlier VZ-4.**

The most successful tilt engine concepts to date have been the Bell tilt rotors. The XV-3 was the first in 1955 followed by the XV-15 in the 1970s and the MV-22 *Osprey* which is just attaining operational status.

### **Tilt Wings**

Vertol, Canadair, and Fairchild all built tilt-wing prototypes, the Vertol Model 76 and VZ-2 flying first in 1957 (Figure 11) followed by the much larger Hiller X-18 and Fairchild/Vought/Hiller XC-142A in 1959. Canadair built its CL-84 in 1965. All prototypes proved the efficacy of tilt-wings but none were carried into production.

The small VZ-2 demonstrator of 1957 may be of sufficient size for some PAVs. The program was funded by the Army Transportation Corps and the aircraft was built under the cognizance of the Office of Naval Research. It was a 3,200# TOGW aircraft using one Lycoming T53 turboshaft to drive two 3-blade propellers and two tail fans. It was tested at NASA/Langley Research Center in the late '50s with disappointing results. The wing exhibited stall problems at 25° to 30° incidence which were aggravated during partial power descents. It also exhibited poor ground effect interactions at altitudes below 15 ft.

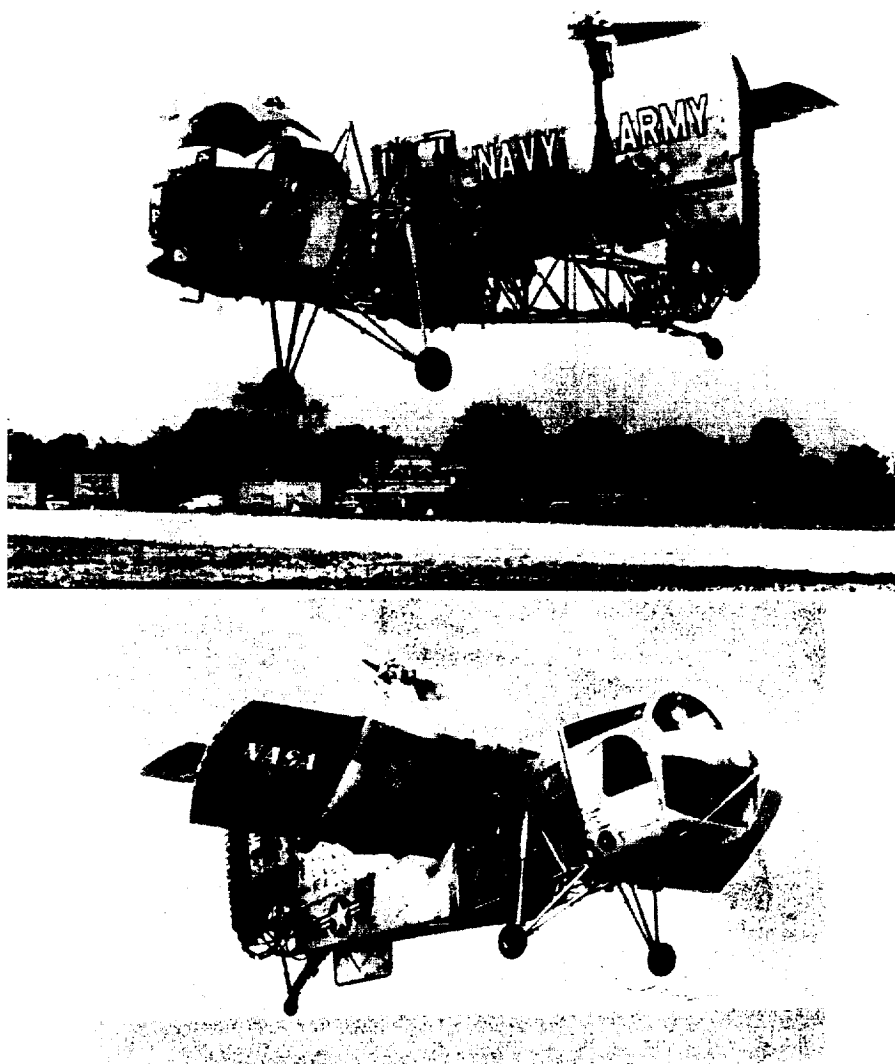


**Figure 11. The Vertol Model 76 (upper) and Its Successor, the VZ-2 (lower), were the First Tilt-Wing Demonstrators.**

#### **Other**

The Raspet research lab at Mississippi State University developed the XV-11A *Marvel* STOL demonstrator (Figure 12) in the mid-1960s. It was ahead of its time in both the high lift system and in the extensive use of composites in primary and secondary structures.

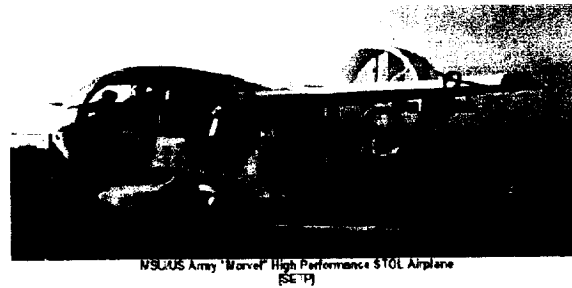


Figure 12. The Mississippi State University *Marvel* STOL Demonstrator was Ahead of Its Time.

### CIVILIAN FIXED WING V/STOL APPROACHES Historical Roadable Vehicles

There have been fits and starts at civilian personal air vehicles since the period just after World War I. At one point, personal fixed-wing VTOL looked like it would be the savior of the U.S. general aviation industry and new-start companies formed to explore various approaches. An early successful attempt at a PAV was the Spanish Cierva autogyro (Figure 13) of 1923 which was marketed domestically by Harold Pitcairn in 1928.

Other early attempts at a conventional takeoff and landing (CTOL) was the Waterman *Whatsit* of 1935 (Figure 14a) which Waldo followed with a flying car prototype, the *Arrowbile*, in 1936 (Figure 14b). Waterman made several attempts at roadable aircraft, the first (Figure 14b) using a 95 HP Menasco B-4. CAA (precursor of FAA) funding came from a largely forgotten Depression-era WPA project to encourage production of a safe, easy-to-fly "everyman's airplane". Waldo's second attempt was in 1938 and exchanged the powerplant for a 100 HP Studebaker engine. His final attempt, rechristened *Aerobile* in 1958 used a Tucker engine.

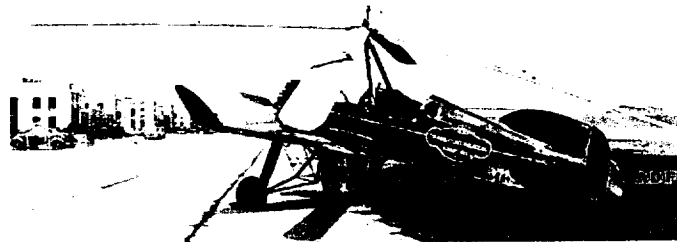
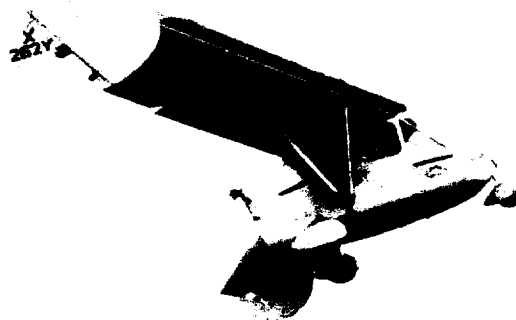


Figure 13. Juan Cierva Developed a Successful Autogyro in Spain.



**Figure 14a.** The Waterman *Whatsit* Flew in the 1930s.



**Figure 14b.** The Waterman W-5 *Arrowbile* of 1937 was Flight Tested.

During this same period, Harold Pit cairn began building autogyros and his PA-18 of 1935 is shown in Figure 15a. It was powered by a 160 HP Kinner radial, as were most succeeding models built during the 1930s. His PA-36 Whirlwing (Figure 15b), the fuselage of which was built by Luscombe, was a roadable version of the earlier autogyro.

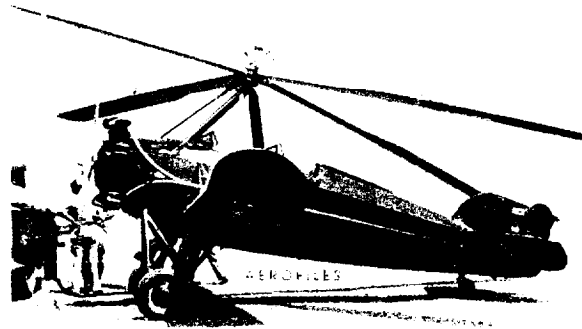


Figure 15a. The Pit cairn Autogyro of 1935 was an Early PAV.



Figure 15b. The Pit cairn *Arrowbile* was an Attempt to Make the Autogyro Roadable.

Daniel Zuck built his Plane-Mobile in 1947 based on his early work on what has become known as free-wing technology where the wing is free to pivot in pitch (variable incidence/fixed angle-of-attack). According to Battelle researchers in the 1970s, one of the reasons Zuck lived a long and prosperous life was that he never attempted to fly his creation. The *ConVAIRCAR* (Figure 16), the *Fulton Airphibian* (Figure 17) of 1947, and the Taylor *Aerocar* (Figure 18) of 1968 are all examples of roadable aircraft from this era. All had similar performance with cruise speeds around 125 mph.

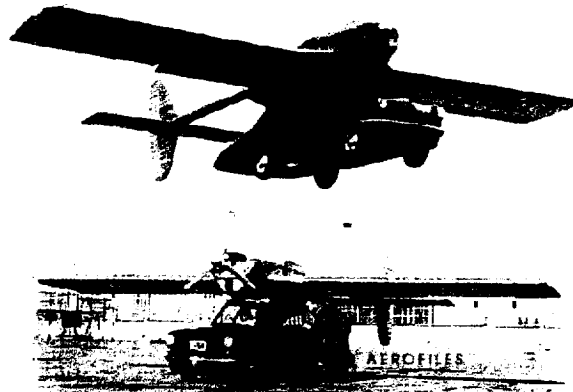


Figure 16. The ConVAir *ConVAIRCAR* Flew in 1947.

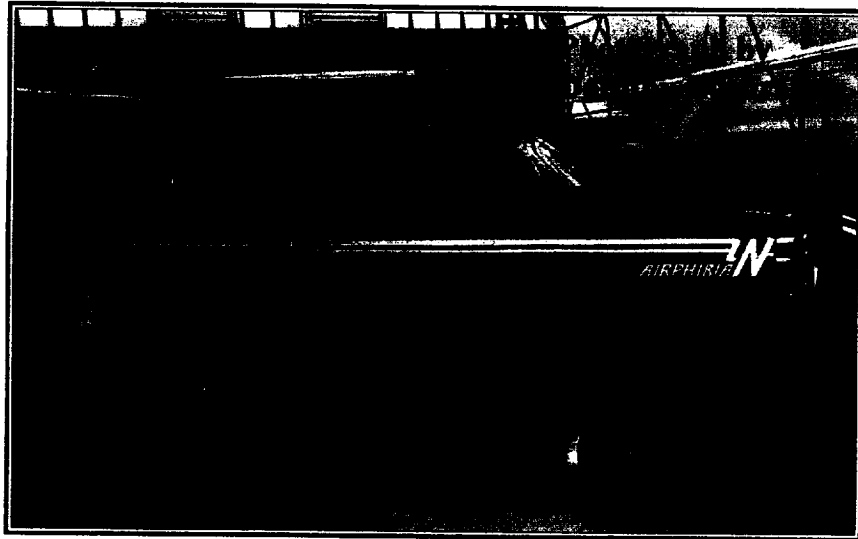


Figure 17. The Fulton *Airphibian* was the first certificated roadable aircraft, flying in 1947.

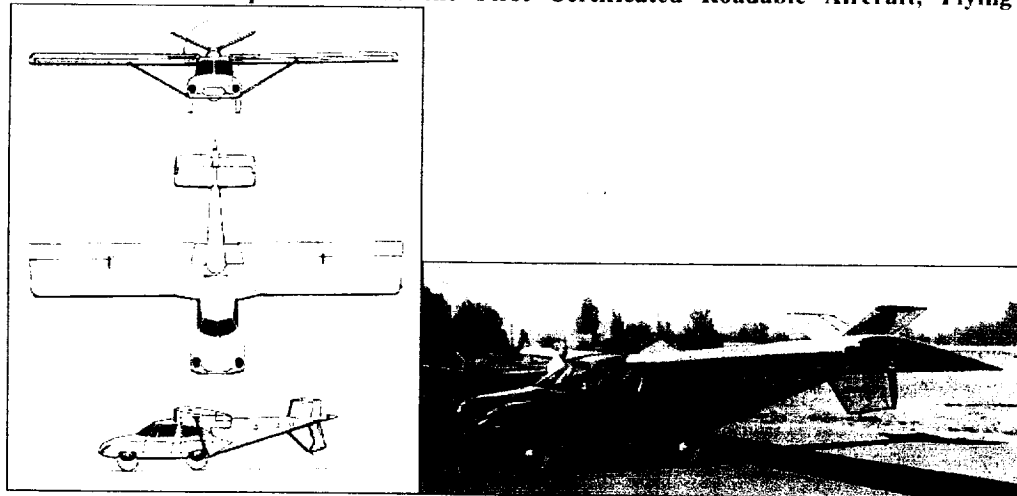


Figure 18. The Taylor *Aerocar* of 1968 was a serious attempt at a roadable aircraft.

### Tilt Ducts & Tilt Propulsion

Tilt duct and its extension, tilt propulsion, technology appears promising for general aviation STOL and VTOL applications and has been demonstrated as early as 1967 with the Nord Model 500 (Figure 19). Another example is the Kulair of Chicago K007 *Convertiplane* (Figure 20) which was designed as an urban commuter.

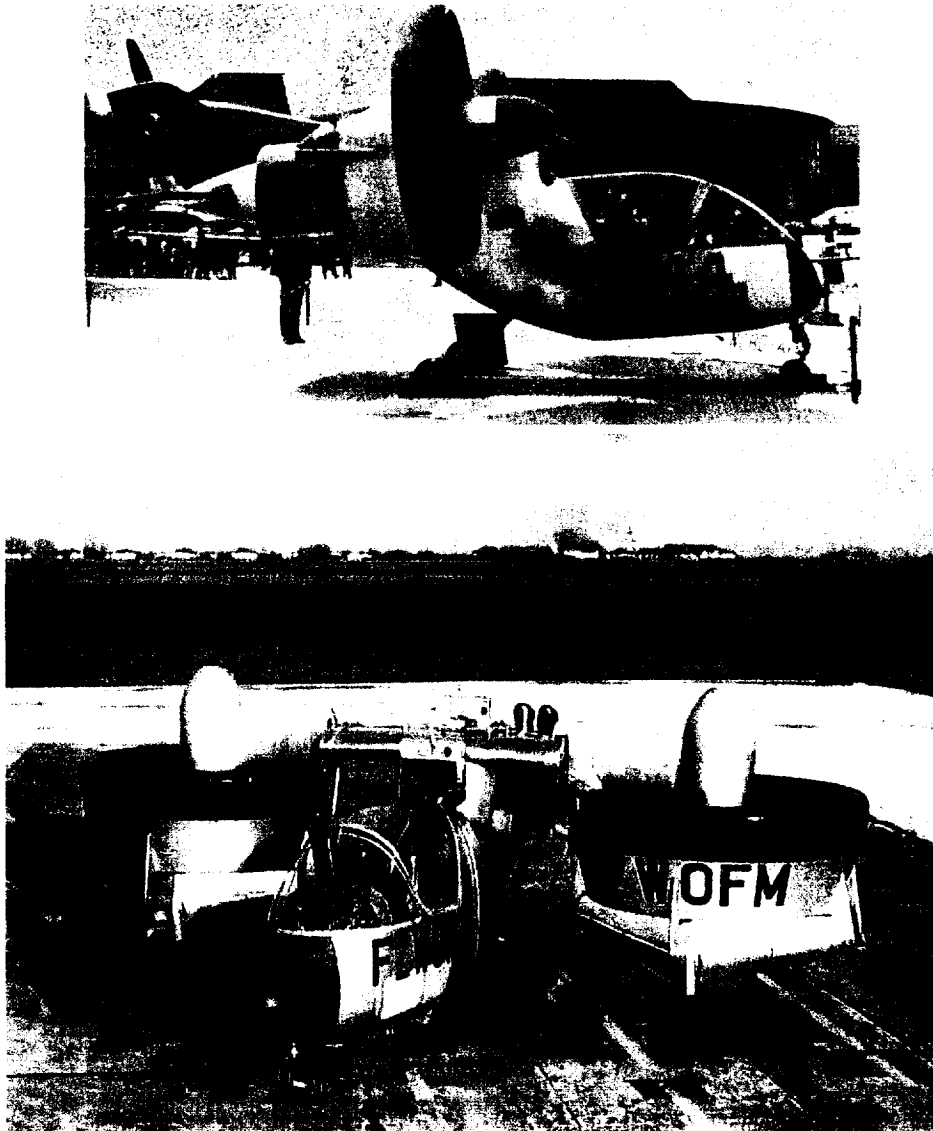


Figure 19. The Nord Model 500 was Exhibited at the 1967 Paris Airshow.

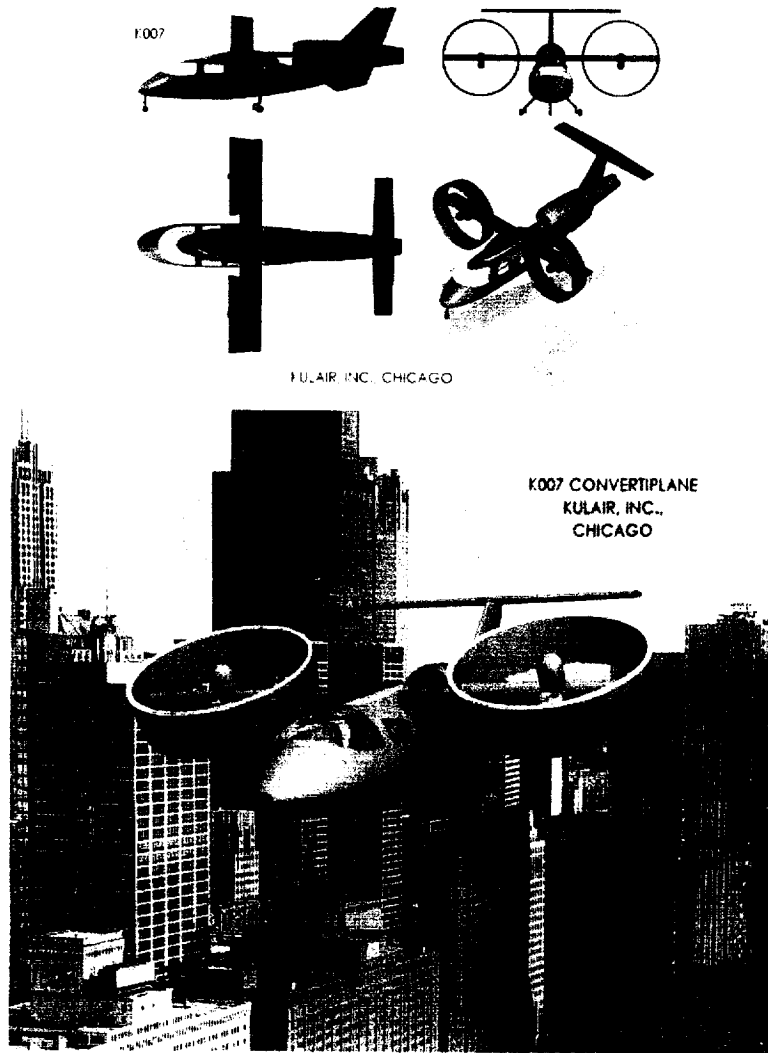


Figure 20. Kulair K007 is a Tilt Ducted Fan Commuter/Bizjet.

Most of the prototypes flown to date have been piloted, but potential PAV propulsion schemes have been applied to Uninhabited Aerial Vehicles (UAVs) with some success for recent DoD competitions and for the radio-controlled (R/C) modeling community. One example is a tilt-ducted fan model called the *Vertigo* which is available in kit form (Figure 22). The *Xantus* of Figure 23 is an application of four-poster tilt-rotors reminiscent of the Bell X-22 tilt-ducted fan of the 1960s. Other companies are prototyping variations of tilt rotors as personal transportation. Figure 24 shows developer Mike Moshier strapped to one called the XFV, which is currently under development in Silicon Valley California.

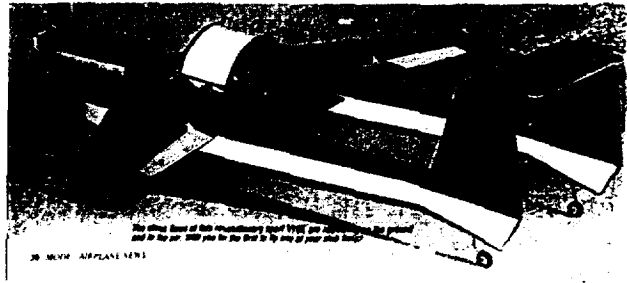


Figure 22. The *Vertigo* is Available as an R/C Model Kit.

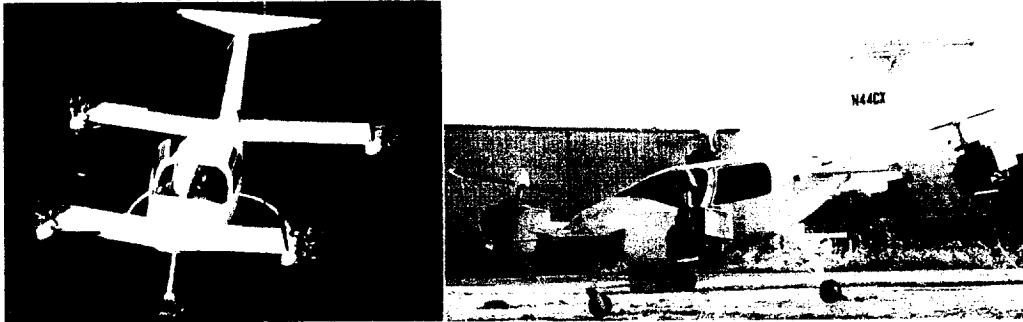


Figure 23. This Novel Tilt-Propeller Design has Already Flown.



Figure 24. A Personal Tilt-Fan VTOL is One Current Scheme Being Explored.

Moller International of Davis California developed a series of PAVs between 1962 and 1989 using a fan-in-fuselage approach. These are shown in Figures 25a through d. All were flying saucer shaped and powered by McCullough motors. In addition, the Israeli company, Romeo Yankee Limited, is developing the CityHawk fan-in-fuselage, two person PAV (Figure 26). A somewhat larger Israeli fan-in-fuselage aircraft is being developed by the DM AeroSafe Group as the Large Aerial Rescue Platform (LARP) shown in Figure 27.



Figure 25a. XM-2 of 1962-68. Figure 25b. XM-3 of 1966. Figure 25c. XM-4 of 1970-74.



Figure 25d. M200X of 1985.



Figure 26. Shown at Left is the *CityHawk* Mockup with a Scale Model at Right.

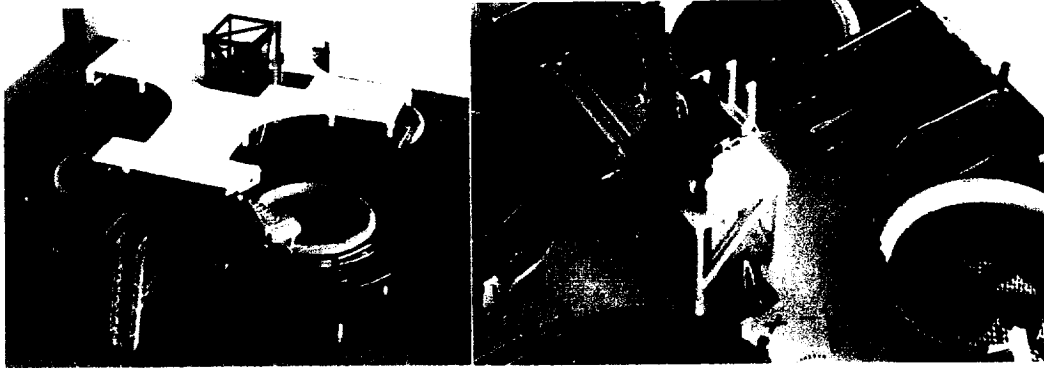


Figure 27. The LARP is Under Development as an Emergency Rescue Vehicle.

### Augmentors

In the mid-1980s, the Moshier Technologies Corporation *Aurora* used a fuselage-mounted four-poster augmentor based on Alperin's work (Figure 28). This was a potentially promising four passenger PAV.

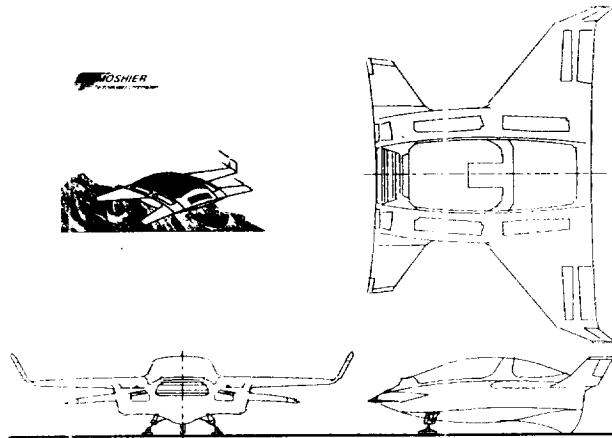
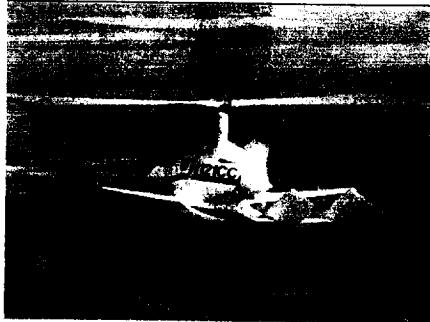


Figure 28. The Moshier Technologies *Aurora* Used a Four-Poster Augmentor Arrangement.

### Autogyro

Benson, McCullough, CarterCopter all developed autogyros between the 1960s and present with the CarterCopter being the latest (Figure 29).



**Figure 29. The CarterCopter is an Example of the Current SOTA in Gyrocopters. Deflected Slipstream & Thrust Vectoring**

Moller International is also developing PAVs using a variation of thrust vectoring, as shown in Figures 30a through c. These aircraft are powered by two 65 hp OMC engines which are single-rotor developments of the Outboard Marine Corporation's rotary engine. Included in these recent designs is an emergency plane-parachute. Also in this category, and in component fabrication and test right now (July 2001), is the Allied AeroTechnics AirBike (Figure 31), probably made for deaf people with a strong death wish.

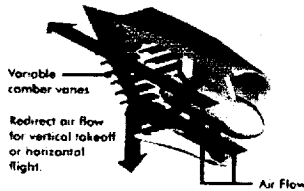


**Figure 30a. Thrust Vectoring Scheme. Figure 30b. Moller M150 Volantor. Figure 30c. Moller M400 Skycar.**



**Figure 31. The Allied AeroTechnics Incorporated *AirBike* is a Novel Approach to a PAV.**

### Other Modern Roadable Aircraft

In this category are several recent designs which appear in the literature and on the world wide web. The *Synergy* from Aeromaster Innovations Incorporated is shown in Figure 32 and is a roadable CTOL PAV seating four passengers and capable of 195 mph in the air and over 75 mph on the road using a Mazda 13B rotary engine. The final aircraft to be discussed here will be the *Roadrunner* from Roger Williamson of San Antonio Texas and it's shown in Figure 33 along with details of its air/ground split.

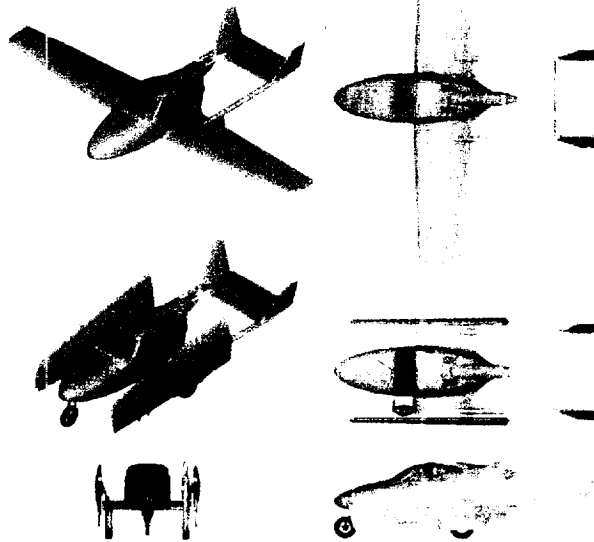


**Figure 32. The Aeromaster Innovations *Synergy* is an Example of a Modern Roadable Aircraft.**



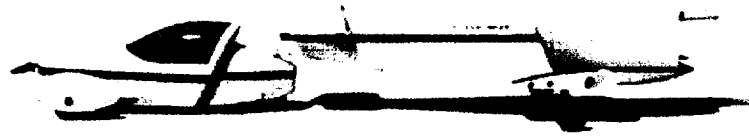


**Figure 33. Mr. Williamson's *Roadrunner* Concept Has A Lot Going For It.**

### **FLYING JEEPS**

The U.S. Army conducted research and development programs in the 1950s and '60s to examine the feasibility of augmenting groundborne jeeps with aerial counterparts. Several of the approaches were discussed in previous sections as examples of specific technical approaches. Others will be discussed here.

#### **Chrysler VZ-6**

In 1969, Chrysler developed the VZ-6 (Figure 34) which used two 8.5 ft diameter ducted fans driven by a single 500 HP reciprocating engine. It had a 2300# TOGW with a crew of one and turned over on its first flight. The Army terminated the project because of control problems.

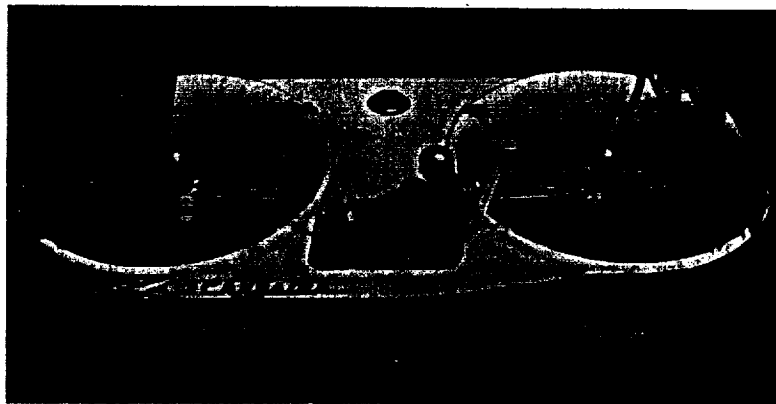


**Figure 34. The Chrysler VZ-6 was Unsuccessful.**

#### **Piasecki VZ-8**

In 1958, Frank Piasecki built the VZ-8 (Figure 35) for the U.S. Army which was also a single place demonstrator. It used two 7.5 ft diameter ducted fans driven by two 180 HP Lycoming reciprocating engines. Fan blades used cyclic control, but the vehicle proved underpowered. It did exhibit excellent operation in ground effect, however, but needed artificial stabilization for flight. The powerplants were later replaced with two 425 HP Turbomeca Artouste turboshafts and performance improved.

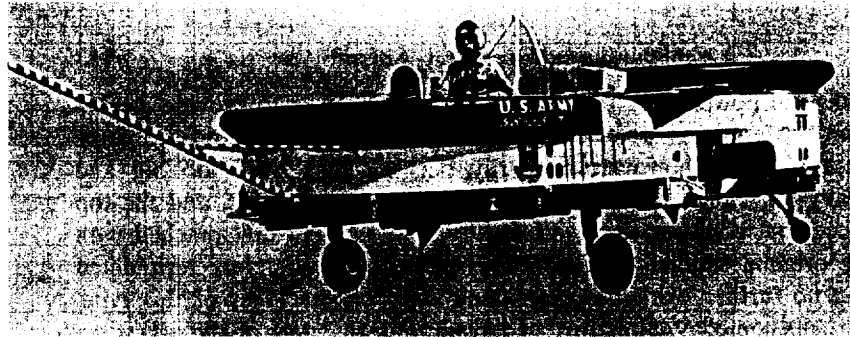


Figure 35. The Piasecki VZ-8 Operated Well in Ground Effect.

### *deLackner Aerocycle*

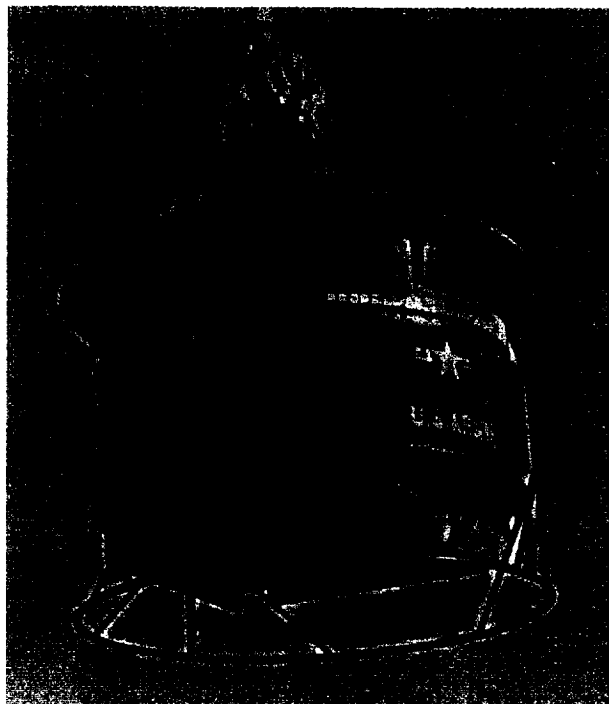
This early '50s design used 15 ft counter-rotating coaxial propellers driven by a 25 HP outboard motor. Later versions used a 40 HP motor when the vehicle proved underpowered in early tests. Kinesthetic control limited top speed to about 20 mph. See Figure 36.



Figure 36. The deLackner Aerocycle Was Feasible in Prototype Form.

### Hiller's Second Flying Platform

Hiller's successor to the VZ-1 (Figure 37) was a larger version designed to overcome the design deficiencies of the earlier model. The second platform used a 8 ft diameter ducts with propellers driven by three interconnected engines. The vehicle proved to be too big, too heavy to control kinesthetically, and had a lower top speed than the VZ-1.



**Figure 37. Hiller's Second Platform Was Less Successful than the First.  
Bell Jet Pack**

In 1959, Bell Aircraft developed their jet pack using a rocket engine at first, then a small turbojet engine, and flew successfully for several years (Figure 38). Later versions used single Williams WR-19 turbofans of 430# thrust. Control was kinesthetic and former test pilots told stories of being lashed at the waist between tall poles and doing forward and backward somersaults until they developed a natural ability to control the beast. Once this happened, pilots reported it as easy to fly but not capable of staying airborne for more than a few minutes at a time.



**Figure 38. The Bell Jet Pack was a Challenge to Learn to Fly.**

#### **Bertelson *Aeromobile* 200-2 GEM**

The Bertelson *Aeromobile* of 1961 (Figure 39) measured 16 ft by 8 ft and used a single 200 HP reciprocating engine to maintain an eight inch operating height off the ground. The vehicle proved practical as a ground effect machine (GEM) but had no altitude capability.



**Figure 39. The Bertelson *Aeromobile* 200-2 was Developed by an M.D.**

#### **Curtiss-Wright Model 2500 GEM**

The Curtiss-Wright Model 2500 as a four-place annular jet GEM with a 2800# TOGW. Note the car-type convertible top in Figure 40.



**Figure 40. The Curtiss-Wright Model 2500 GEM Carried Four Passengers.**

### **Summary**

The foregoing brief discussion of flying jeep prototypes showcases several approaches which bear further investigation given the improvement in propulsion, avionics, and materials SOTAs in the last forty years. Kinesthetic control can now be replaced with affordable, real-time active control systems which will vastly improved usability. Composite structures coupled with modern, high thrust-to-weight turbine engines, will reduce vehicle weight and improve reliability and maintainability in the field.

## HOW THE VARIOUS V/STOL APPROACHES COMPARE

The approaches to vertical flight embraced by aerospace companies over the last five decades appear to be as much the result of political decisions and company favoritism as technical merit. Examples are Bell's preoccupation with tilt-rotors, although given the company's long and illustrious history and success with revolving wings, that makes sense. Similarly, North American Aviation/Columbus Aircraft Division of Rockwell International in the 1970s made a political decision to base all their future work on augmenter-wing applications and ignored other approaches at the eventual expense of the division which had created the *Fury Jet* series, the *Vigilante*, the *Bronco*, and the *Buckeye*.

The period from the early 1950s to the late 1960s was characterized by hardware demonstrations of novel aircraft concepts including most of the VTOL aircraft previously mentioned. The U.S. has not seen an era like that since and probably won't again with piloted aircraft, much to the detriment of the current generation of aerospace engineers and aircraft designers. With the latest round of VTOL and ASTOVL approaches being applied to uninhabited aerial vehicles (UAVs), though, the field is once again open to examine novel methods to achieve vertical flight and the opportunity exists to revisit the work of a generation ago in light of technological breakthroughs in several related fields.

That being the case, how do the vertical flight approaches previously shown compare to one another and is there one approach which is best? Like so many other configuration-related questions, the answer is dependent upon the mission category and operational requirements, but some general observations may be made based upon past tests of each approach. The salient judging criteria for effectiveness include simplicity, elegance, reliability, and system cost.

The use of large aft flaps ala Ryan VZ-3 is a promising approach for STOL operations and, with some headwind, may yield a vertical landing capability.

Fan-in-wing systems suffer from tip turbine losses and duct losses that may be prohibitive. Burying fans in wings and fuselages prohibits those vital internal volumes from being used for carrying passengers and fuel and this may make fan-in-wing concepts larger and heavier than might be possible with other approaches. The fan-in-wing approach as tested in the Ryan XV-5 was lossy using J85 turbojet engines but may be worth a second look with turbofans where overall pressure ratios are lower and cooler fan bypass air can be used to turn the fans. The same comments hold for lift plus lift/cruise engine combinations where the aircraft carries around its VTOL or STOVL propulsion systems as dead weight for most mission legs.

Vectored thrust is still brute force but there's a lot to be said for its simplicity, particularly if thrust vectoring can be combined with low pressure ratio turbofan engines. Akin to this are the tilt-fan and tilt-engine approaches which make increasing sense, particularly when combined with state-of-the-art control methods and free-wings so the engine nacelle/fuselage is free to be vectored to extreme angles. Potentially viable VTOL and ASTOVL performance might be gained from novel combinations of control algorithms, vectored thrust, and variable incidence wings or fuselages. These methods allow a STOL mode whereas fan-in-wing and lift plus lift/cruise engines are predominantly useful for VTOL.

Disc loading with all these approaches is high and that means that the ability to hover for prolonged periods isn't an option, as it is with helicopters which have very low disc loadings; hence, prolonged hovers will require high thrust-to-weight ratios and large fuel reserves.

Tilt wings appear promising and problems with downwash over control surfaces and cross-shafting were successfully dealt with in the XC-142 and CL-84 programs. One potential benefit of tilt-wings is that relatively little wing tilt is necessary to markedly reduce takeoff and landing performance. Recent work shows that 30° of wing tilt will reduce takeoff ground roll from around 1,000 feet to under 300 feet.

The most elegant solution is the augments-wing which captures ambient air by the Coanda effect and uses that to produce the equivalent of lower disc loadings than one would get with vectored thrust and lift engines. In this case, the disc loading can be measured as the combined jet impingement and entrained air footprint on the ground under the aircraft. Augmenters, however, rely on precisely machined nozzles and don't lend themselves to being installed in tapered, swept wings. When they are, end losses and corner losses eat up much of the flow momentum. There is also reasonable concern that manufacturing tolerances won't be maintainable in the field, particularly if systems are damaged in harsh operating conditions.

To summarize, Tables 1 and 2 present comparisons of each of the propulsion approaches discussed in this paper. A more detailed discussion of technology considerations will follow this section. Note that reference wing area doesn't always apply to these PAVs, so when no definable wing exists, the planform area of the vehicle is used in its place. Disc loading is a similarly vague term and is defined here as the TOGW divided by the total face area of the propulsion unit(s). For propellers and ducted fans, this is obvious; for turbofans or turbojets, use the compressor face area.

**Table 1. There Are Advantages and Disadvantages to Each System.**

Type of System	Advantages	Disadvantages
Vectored Thrust	Simple  Uses cruise engine for lift  Thrust vector nozzles can be used in flight and for STOL	High pressure/high temperature erosive footprint  Short hover at light weights  Engine is oversized to attain VTOL
Tilt Rotor	Low energy footprint  STOL operations possible	Cross-shafting necessary  Combined helicopter and airplane controls  Large diameter whirling blades  Wings can be 90° to propeller outflow during VTOL operations  CTOL operations not possible

Type of System	Advantages	Disadvantages
Tilt Wing	Engines swivel with wing so angle-of-attack is programmable  Combined wing and thrust provide lift for super-short takeoffs and landings  CTOL operations possible	Cross-shafting necessary  Tilt-tail may also be necessary depending on local flow field  No turbofan tilt-wings demonstrated yet
Tail Sitters	Low spotting factor	Engines must be oversized to provide high thrust-to-weight ratio for vertical takeoff and landing  Pilots not able to see ground for takeoff and landing motion cues  High pressure/temperature exhaust footprint for jets
Fan-In-Wing	Cooler exhaust footprint than with vectored thrust	Tip turbine and duct flow design critical  VTOL propulsion components don't contribute to most mission segments  STOL operation unlikely
Lift + Cruise Engines	High thrust-to-weight lift engines available  Cruise engine doesn't need to be oversized for VTOL	VTOL propulsion components don't contribute to most mission segments  STOL operation not likely
Lift + Lift/Cruise Engines	High thrust-to-weight lift engines available  Cruise engines don't need to be oversized for VTOL	VTOL propulsion components don't contribute to most mission segments  STOL operation unlikely

Augmentors (Chordwise Orientation)	<p>Untapered shape and 90° corners are efficient</p> <p>Engine doesn't have to be sized strictly for VTOL</p> <p>Elegant in that entrained airflow assists VTOL performance</p> <p>Careful design will permit STOL operation</p>	<p>Complicated ducting runs</p> <p>Some question about production tolerances being sufficient for operations</p> <p>High temperature metals needed for core flows if high pressure ratio engines are used</p> <p>Fuselage or wing root space taken up with augmentor bays and not available for other systems or fuel</p>
Augmentors (Spanwise Orientation)	<p>Elegant in that entrained airflow assists VTOL or STOL performance</p> <p>VTOL system can be tailored to aircraft mold lines</p> <p>Low exhaust footprint</p>	<p>Augmentor bay taper and sweep decreases efficiency</p> <p>Aircraft carries extensive ductwork during all phases of mission</p> <p>Extensive ductwork easily punctured by operational hazards or threats</p>
Tilt-Fan	<p>Low exhaust footprint</p> <p>Single fan installation possible when using pointable fuselage</p>	<p>Cross-shafting necessary for multiple fan installations</p>

The foregoing discussion shows that personal air vehicles have been a subject of more than academic interest since the early days of aviation and continue to be to this day. Many propulsion approaches apply and allow low-end performance to be comparable to conventional small general aviation aircraft. Cost may be higher, but in the same ballpark. Vertical capability is practical, too, with more focus on technology integration and with a higher cost. The salient challenges will be in technology integration, assuring ruggedness and reliability similar to automobiles, and safety as good as airlines. All this is the framework of keeping initial and upkeep costs affordable for the masses.

—foldout table 2 is next—

## V/STOL CONSIDERATIONS General Observations

The foregoing discussion highlights specific examples of V/STOL aircraft, but there are only four ways to achieve vertical flight:

- Thrust tilting;
- Thrust deflector;
- Aircraft tilting; or
- Dual propulsion systems.

And there are four different types of propulsion systems for each of these ways of achieving V/STOL flight:

- Rotors;
- Propellers;
- Ducted fans; or
- Turbofans or turbojets.

Thus, there are sixteen possible combinations. Between the 1940s and the 1970s, fifteen of the sixteen alternatives were tried at one time or another with varying results.

### Takeoff and Landing

Figure 41 presents the effect of a takeoff parameter on takeoff distance for both ground roll and clearing an obstacle. As can be seen by the hatched box in the lower left, aircraft of interest in this work will cluster at low values of the takeoff parameter.<sup>1</sup>

$$K_s = \left( \frac{TOGW}{S_{reference}} \right) \left[ \frac{TOGW}{(F_{installed})_{takeoff}} \right] \left( \frac{1}{C_{L_{takeoff}}} \right) \left( \frac{1}{\sigma} \right)$$

where  $C_{L_{takeoff}} = 0.75C_{L_{max}}$

and, for a propeller driven configuration:

$$(F_{installed})_{takeoff} = \frac{\eta_{propeller}(P_{installed})_{takeoff}}{550V_{average}}$$

where  $V_{average} = 0.7V_{takeoff}$

---

<sup>1</sup> Stinton, Darrol, *The Anatomy of the Aeroplane*. Granada Publishing Limited, London, England, 1966 (ISBN: 0-246-11447-9), pp. 302-303.

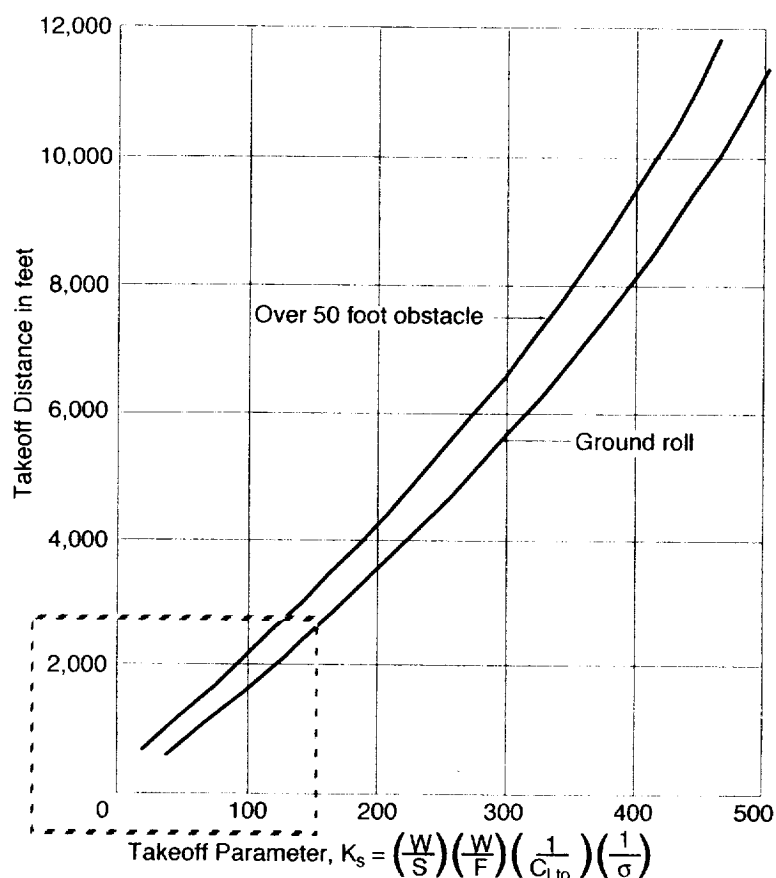


**Figure 41. A Takeoff Parameter Can Be Used to Estimate Takeoff Distances.**

Other parameters besides takeoff distance are important to V/STOL aircraft performance. Figure 42 presents the inter-relationships of several key VTOL design parameters including rotor diameter, disc loading, cruise speed, and lifting jet velocity. For jet lift, the rotor diameter and disc loading are based on engine compressor face dimensions. As might be expected, note the inverse effect of cruise speed on both hover time and disc loading and its direct correlation with exhaust jet velocity.

These charts clearly delineate the mutual exclusivity of high cruise speeds and long hover times unless creative compromises are made. For instance, the work done on fluidic amplification in the 1970s promised aircraft with both. Theory, however, doesn't always work and fluidic amplification, while promising, will require a fair amount of development work to reach operational status. The next sections will explore several areas that separate V/STOL aircraft from other categories.

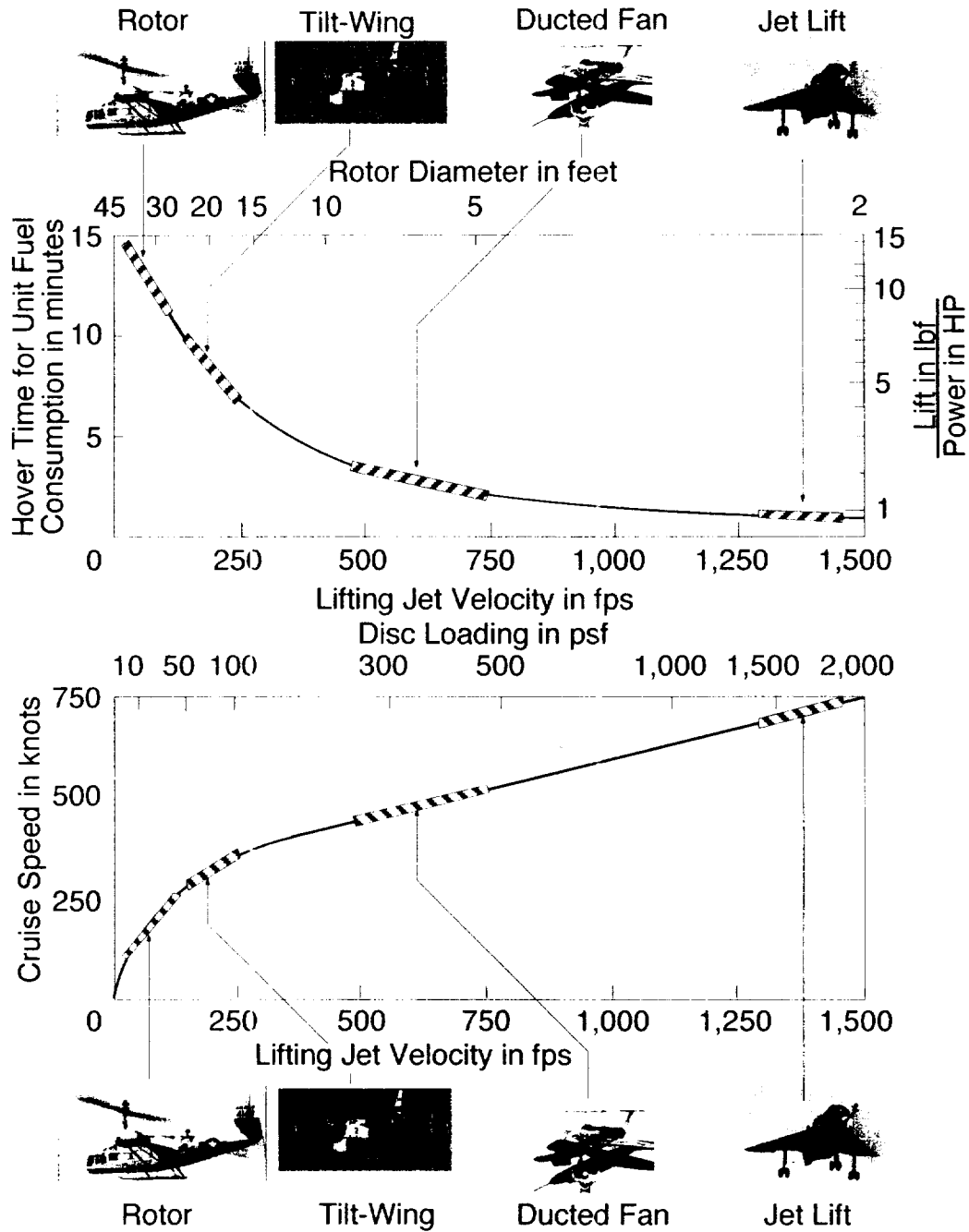
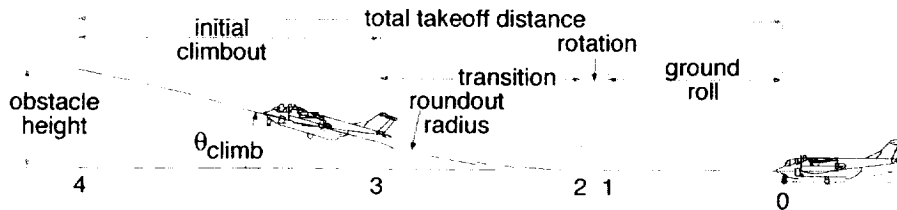


Figure 42. Key VTOL Performance Parameters are Interlinked.

**Idealized STOL Takeoff Equations**

The takeoff segment can be analyzed by separating it into phases as shown in Figure 43.



**Figure 43. A Lot Happens In a Short Period of Time During Takeoff.**

The ground roll portion occurs between beginning takeoff roll (time,  $t=0$ , speed,  $V=0$ ) and beginning rotation. Rotation occurs over approximately three seconds as the pilot rotates the aircraft from ground roll attitude to liftoff attitude. The transition phase occurs between attaining liftoff attitude when all the weight is on the main gear to wing borne flight when the main gear are still on the runway but all the weight is on the wing (lift equals weight). The final portion is from there to some altitude specified for obstacle clearance, usually either 35 or 50 feet. Where ground roll requirements are to be used for analysis, use the sum of ground roll plus rotation plus transition distances—these are the phases of the takeoff segment where the rubber meets the road.

**Ground Roll.** Begin this analysis with a free body of an airplane on the runway with forces acting on it as shown in Figure 44. Then define start and end conditions for each portion of the takeoff segment.

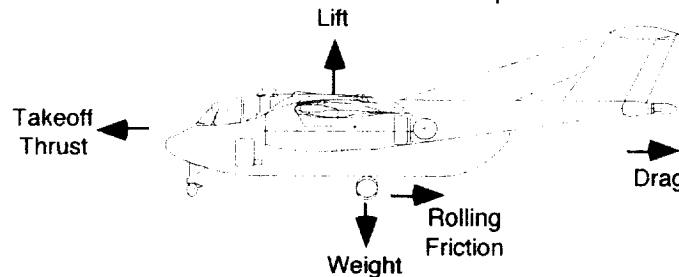


**Figure 44. An Airplane During Takeoff is Acted Upon by Determinable Forces and Accelerations.**

At the beginning of the ground roll, the aircraft is stationary and its full weight rests on its landing gear. initial conditions are:

Speed,	$V$	=	0
Weight,	$W$	=	TOGW
Thrust,	$T$	=	$T_{takeoff}$
Lift,	$L$	=	0
Drag,	$D$	=	0

At the end of the ground roll phase, speed will be some fraction of stall speed, usually assumed to be one-half. Initial acceleration is around 0.3 g for conventional aircraft but may be as high as 0.8 g for super/STOL aircraft and higher for uninhabited air vehicles. Average speed during the ground roll phase, then, will be about one-

quarter stall speed. Note that the stall configuration used here is power on, flaps at takeoff setting, and landing gear down.

$$(V_{\text{ground roll}})_{\text{initial}} = 0$$

$$(V_{\text{ground roll}})_{\text{final}} = 0.5V_{\text{stall}}$$

$$(V_{\text{ground roll}})_{\text{average}} = 0.25V_{\text{stall}}$$

$$\alpha_{\text{ground roll}} = i_{\text{wing}}$$

This angle can be increased by extending the nose gear strut for takeoff (as done on British F-4 Phantom IIs) and, possibly, by raising the wing at the same time (as done on Vought F8U Crusaders). Then

$$\alpha_{\text{ground roll}} = i_{\text{wing}} + \Delta i_{\text{takeoff setting}} + \Delta i_{\text{nose strut}}$$

$$(C_{L_{\text{ground roll}}})_{\text{average}} = (C_{L_c})_{\text{ground effect}} \alpha_{\text{ground roll}}$$

$$(L_{\text{ground roll}})_{\text{average}} = (q_{\text{ground roll}})_{\text{average}} S_{\text{ref}} (C_{L_{\text{ground roll}}})_{\text{average}}$$

$$(C_{D_i})_{\text{average}} = \frac{(C_{L_{\text{ground roll}}})_{\text{average}}^2}{\pi e_{\text{ground roll}} AR}$$

$$(D_{\text{ground roll}})_{\text{average}} = (q_{\text{ground roll}})_{\text{average}} S_{\text{ref}} \left[ (C_{D_0})_{\text{ground roll}} + (C_{D_i})_{\text{average}} \right]$$

$$S_{\text{ground roll}} = \frac{1.44 \frac{W}{S_{\text{ref}}}}{\left\{ \rho g C_{L_{\text{max}}} \left[ \frac{T_{\text{takeoff}}}{W} - \frac{D}{W} - \mu \left( 1 - \frac{L}{W} \right) \right] \right\}}$$

$$t_{\text{ground roll}} = \frac{S_{\text{ground roll}}}{0.5V_{\text{stall}}}$$

$$(W_{fuel})_{ground\ roll} = tsfc_{takeoff} T_{takeoff} t_{ground\ roll}$$

$$(W_{ground\ roll})_{end} = (W_{rotation})_{start} = TOGW - (W_{fuel})_{ground\ roll}$$

**Rotation.** As stated earlier, the rotation phase will take approximately three seconds, so calculating ending conditions will be straightforward. Initial conditions are the final conditions for the ground roll portion. Rotation angle,  $\theta$ , is on the order of ten degrees for most aircraft, so ending angle-of-attack (not corrected for ground effect) will be

$$(\alpha_{rotation})_{end} = \alpha_{ground\ roll} + \theta_{rotation}$$

where  $\theta_{rotation} = 10^\circ$

$$(V_{rotation})_{end} = (V_{transition})_{start} = 0.84V_{stall}$$

$$(V_{rotation})_{average} = (V_{rotation})_{end} - (V_{rotation})_{start} = 0.67V_{stall}$$

$$(q_{rotation})_{average} = \frac{1}{2} \rho (V_{rotation})_{average}^2$$

$$(C_{L_{rotation}})_{average} = (C_{L_{\alpha}})_{ground\ effect} (\alpha_{rotation})_{end}$$

$$(L_{rotation})_{average} = (q_{rotation})_{average} S_{ref} (C_{L_{rotation}})_{average}$$

The weight on the landing gear is:

$$(W_{rotation})_{average} = (W_{groundroll})_{end} - (L_{rotation})_{average}$$

$$(C_{D_i})_{average} = \frac{(C_{L_{rotation}})_{average}^2}{\pi e_{rotation} AR}$$

$$(W_{fuel})_{rotation} = tsfc_{takeoff} T_{takeoff} t_{rotation}$$

$$(W_{rotation})_{end} = (W_{transition})_{start} = (W_{ground\ roll})_{end} - (W_{fuel})_{rotation}$$

**Transition.** The transition phase of the takeoff segment will begin as soon as liftoff angle-of-attack is attained at the end of the rotation phase and will continue until the aircraft lifts off at speed,

$$(V_{\text{transition}})_{\text{end}} = (V_{\text{climbout}})_{\text{start}} = 1.05V_{\text{stall}}$$

$$(q_{\text{transition}})_{\text{average}} = \frac{1}{2}\rho(V_{\text{transition}})_{\text{average}}^2$$

$$\alpha_{\text{transition}} = \alpha_{\text{ground roll}} + \theta_{\text{rotation}}$$

$$(C_{L_{\text{transition}}})_{\text{average}} = (C_{L_{\alpha}})_{\text{ground effect}} \alpha_{\text{transition}}$$

$$(L_{\text{transition}})_{\text{average}} = (q_{\text{transition}})_{\text{average}} S_{\text{ref}} (C_{L_{\text{transition}}})_{\text{average}}$$

$$(C_{D_i})_{\text{average}} = \frac{(C_{L_{\text{transition}}})_{\text{average}}^2}{\pi e_{\text{transition}} AR}$$

Recall that takeoff acceleration was specified,

$$t_{\text{transition}} = \frac{(V_{\text{transition}})_{\text{average}}}{a_i}$$

$$s_{\text{transition}} = (V_{\text{transition}})_{\text{average}} t_{\text{transition}}$$

$$(W_{\text{fuel}})_{\text{transition}} = tsfc_{\text{takeoff}} T_{\text{takeoff}} t_{\text{transition}}$$

$$(W_{\text{transition}})_{\text{end}} = (W_{\text{climbout}})_{\text{start}} = (W_{\text{rotation}})_{\text{end}} - (W_{\text{fuel}})_{\text{transition}}$$

**Initial Climbout.** The initial climbout phase of the takeoff segment starts with zero weight on the aircraft landing gear, although the gear still touch the runway. This portion of the takeoff segment ends at some predetermined altitude close to the ground, usually 35 or 50 feet and the aircraft is assumed to be in takeoff configuration (takeoff flap setting, landing gear down) during this initial climbout. Speed at the end of this portion is

$$(V_{\text{climbout}})_{\text{end}} = (V_{\text{climb}})_{\text{start}} = 1.20V_{\text{stall}}$$

$$(V_{\text{climbout}})_{\text{average}} = 1.12V_{\text{stall}}$$

$$(q_{\text{climbout}})_{\text{average}} = \frac{1}{2}\rho(V_{\text{climbout}})_{\text{average}}^2$$

$$h_{\text{start}} = h_{\text{runway}}$$

$$h_{\text{end}} = h_{\text{runway}} + \Delta h_{\text{obstacle}}$$

The aircraft will transition to climb configuration instantaneously at the end of the initial climbout phase. Climb configuration will be with landing gear up, flaps at climb setting (or retracted), and thrust at climb (maximum continuous) setting. The wing will provide a large fraction of maximum lift at this stage, or

$$C_{L_{\text{climbout}}} = \frac{(C_{L_{\text{max}}})_{\text{takeoff}}}{1.2}$$

$$(L_{\text{climbout}})_{\text{average}} = (q_{\text{climbout}})_{\text{average}} S_{\text{ref}} (C_{L_{\text{climbout}}})_{\text{average}}$$

Parasite drag coefficient will reflect the flight configuration change as will the aircraft efficiency factor used in induced drag coefficient calculations.

$$(C_{D_0})_{\text{climbout}} = (C_{D_0})_{\text{clean}} + \Delta(C_{D_0})_{\text{climb flaps}}$$

$$(C_{D_i})_{\text{average}} = \frac{(C_{L_{\text{climbout}}})_{\text{average}}^2}{\pi e_{\text{climbout}} AR}$$

$$(D_{\text{climbout}})_{\text{average}} = (q_{\text{climbout}})_{\text{average}} S_{\text{ref}} \left[ (C_{D_0})_{\text{climbout}} + (C_{D_i})_{\text{average}} \right]$$

Evaluate performance assuming weight is the weight at the end of the transition portion. The climb angle,  $\gamma$ , can be found through the ratio of basic forces acting on the airplane.

$$\sin \gamma = \frac{T_{\text{climbout}} (D_{\text{climbout}})_{\text{average}}}{W_{\text{climbout}}}$$

$$(R/C)_{\text{average}} = (V_{\text{climbout}})_{\text{average}} \sin \gamma$$

$$s_{\text{climbout}} = \frac{\Delta h_{\text{required}}}{\cos \gamma}$$

$$t_{\text{climbout}} = \frac{s_{\text{climbout}}}{(V_{\text{climbout}})_{\text{average}}}$$

$$(W_{\text{fuel}})_{\text{climbout}} = tsfc_{\text{takeoff}} T_{\text{takeoff}} t_{\text{climbout}}$$

Both thrust and lift will be augmented by momentum terms which will be added later in discussions of specific powered lift approaches.

**Idealized STOL Landing Equations**

Analysis of the landing segment will proceed similarly to that for the takeoff segment. Final landing conditions will occur when the airplane is stationary on the runway. Again, we can divide the landing segment into four phases as shown in Figure 45.

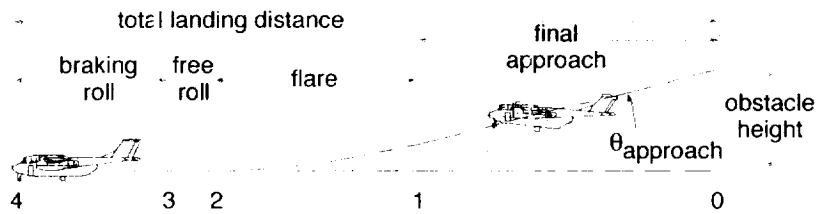


**Figure 45. Landing Analysis is Conceptually Similar to Takeoff Analysis.**

At time,  $t = 0$ , the aircraft is on final approach and in final approach configuration with landing gear down and flaps at landing setting. Configuration will remain constant over the approach and landing run and the segment will end when the aircraft is stationary at the far end of the runway. Forces acting on the aircraft during landing are shown in Figure 46.

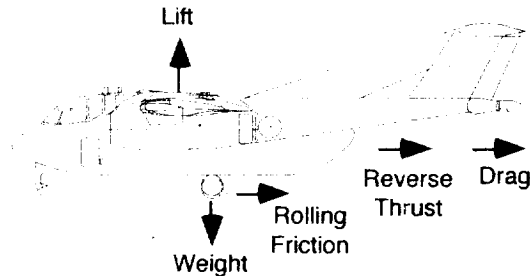


**Figure 46. The Landing Run Freebody Includes Braking.**

**Final Approach.** In the final approach phase of the landing segment, the aircraft is descending toward the runway as speed bleeds off from stabilized approach speed to flare speed in ground effect. Minimum aircraft landing weight will be

$$W_{\text{final approach}} = W_{\text{design landing}} = W_{\text{empty}} + W_{\text{payload}} + 0.03W_{\text{fuel}}$$

although these calculations should also be performed at maximum landing weight as well as any other landing weights specified in mission requirements.

$$(V_{\text{final approach}})_{\text{start}} = 1.30(V_{\text{stall}})_{\text{full flaps}}$$

$$(V_{\text{final approach}})_{\text{end}} = 1.10(V_{\text{stall}})_{\text{full flaps}}$$

$$(V_{\text{final approach}})_{\text{average}} = 1.20(V_{\text{stall}})_{\text{full flaps}}$$

$$(q_{\text{final approach}})_{\text{average}} = 0.5\rho(V_{\text{final approach}})_{\text{average}}^2$$

$$(C_L)_{\text{final approach}} = \frac{W_{\text{final approach}}}{(q_{\text{final approach}})_{\text{average}} S_{\text{ref}}} \quad \text{-- a sink rate decrement since } L < W$$

$$(L_{\text{final approach}})_{\text{average}} = (q_{\text{final approach}})_{\text{average}} S_{\text{ref}} (C_L)_{\text{final approach}}$$

$$(C_{D_i})_{\text{final approach}} = \frac{(C_L)_{\text{final approach}}^2}{\pi e_{\text{landing}} AR}$$

$$(D_{\text{final approach}})_{\text{average}} = (q_{\text{final approach}})_{\text{average}} S_{\text{ref}} \left[ (C_{D_0})_{\text{landing}} + (C_{D_i})_{\text{final approach}} \right]$$

$$\sin \theta_{\text{final approach}} = \frac{(R/D)_{\text{required}}}{(V_{\text{final approach}})_{\text{average}}}$$

$$S_{\text{final approach}} = \frac{\Delta h_{\text{required}}}{\sin \theta_{\text{final approach}}}$$

$$t_{\text{final approach}} = \frac{S_{\text{final approach}}}{(R/D)_{\text{required}}}$$

There will also be a significant thrust term which will be a function of the VTOL or super/STOL.

technology used. Assume for now that thrust is set at idle, then we'll add a finite thrust term in discussions of powered lift technologies later.

**Flare.** At the end of the flare phase of the landing segment, the aircraft makes contact with the runway. For carrier-suitable aircraft and STOL aircraft, there may be no flare phase and the aircraft contacts the runway or deck at a stabilized final approach sink rate. Assume this to be the case here, so time for the flare phase is zero and final flare conditions are the same as initial flare conditions. For conventional aircraft, the flare phase is calculated along a circular arc tangent to the runway at one end and to the final approach path at the other.

**Free Ground Roll.** The aircraft contacts the runway at the end of the flare phase. Starting speed is the full-flap stall speed in ground effect if the aircraft is flared on landing. If not, starting speed for this portion is greater than full-flap stall speed by some fraction, and may be the same as final approach speed. This portion of the landing segment is only long enough for the pilot to begin applying brakes and/or reverse thrust and ends when one or both have been engaged. Referring to the free body in Figure 46, the rolling friction coefficient should reflect either a hard, concrete surface or a steel deck. The initial conditions for this phase of the landing segment are

$$t_{\text{free roll}} = 3$$

$$(V_{\text{free roll}})_{\text{start}} = 1.10(V_{\text{stall}})_{\text{full flaps}}$$

$$(V_{\text{free roll}})_{\text{end}} = (V_{\text{stall}})_{\text{full flaps}}$$

$$(V_{\text{free roll}})_{\text{average}} = 1.05(V_{\text{stall}})_{\text{full flaps}}$$

$$(q_{\text{free roll}})_{\text{average}} = 0.5\rho(V_{\text{free roll}})_{\text{average}}^2$$

$$(C_L)_{\text{free roll}} = \frac{W_{\text{final approach}}}{(q_{\text{free roll}})_{\text{average}} S_{\text{ref}}}$$

$$(L_{\text{free roll}})_{\text{average}} = (q_{\text{free roll}})_{\text{average}} S_{\text{ref}} (C_L)_{\text{free roll}}$$

$$(C_{D_i})_{\text{free roll}} = \frac{(C_L)_{\text{free roll}}^2}{\pi e_{\text{landing}} AR}$$

$$(D_{\text{free roll}})_{\text{average}} = (q_{\text{free roll}})_{\text{average}} S_{\text{ref}} \left[ (C_{D_0})_{\text{landing}} + (C_{D_i})_{\text{free roll}} \right]$$

$$S_{\text{free roll}} = (V_{\text{free roll}})_{\text{average}} t_{\text{free roll}}$$

Rolling friction will be

$$F_{\text{free roll}} = \mu_{\text{free roll}} N_z = \mu_{\text{free roll}} (W_{\text{final approach}} - L_{\text{free roll}})$$

**Ground Roll with Braking.** This phase of the landing segment covers ground roll which is retarded by constant braking and/or reverse thrust. It ends when the aircraft has come to a full stop on the runway. At this point, the aircraft is moving below stall speed and its weight increasingly rests on the landing gear. The braking rolling coefficient should reflect full brakes and either a concrete surface or a steel deck.

$$(V_{\text{braking roll}})_{\text{start}} = (V_{\text{free roll}})_{\text{end}} = (V_{\text{stall}})_{\text{full flaps}}$$

$$(V_{\text{braking roll}})_{\text{end}} = 0$$

$$(V_{\text{braking roll}})_{\text{average}} = 0.50(V_{\text{stall}})_{\text{full flaps}}$$

$$(q_{\text{braking roll}})_{\text{average}} = 0.5\rho(V_{\text{braking roll}})_{\text{average}}^2$$

$$(C_L)_{\text{braking roll}} = \frac{W_{\text{final approach}}}{(q_{\text{braking roll}})_{\text{average}} S_{\text{ref}}}$$

$$(L_{\text{braking roll}})_{\text{average}} = (q_{\text{braking roll}})_{\text{average}} S_{\text{ref}} (C_L)_{\text{braking roll}}$$

$$(C_{D_i})_{\text{braking roll}} = \frac{(C_L)_{\text{braking roll}}^2}{\pi e_{\text{landing}} AR}$$

$$(D_{\text{braking roll}})_{\text{average}} = (q_{\text{braking roll}})_{\text{average}} S_{\text{ref}} \left[ (C_{D_o})_{\text{landing}} + (C_{D_i})_{\text{braking roll}} \right]$$

$$F_{\text{braking roll}} = \mu_{\text{braking}} N_z = \mu_{\text{braking}} (W_{\text{final approach}} - L_{\text{braking roll}})$$

The reverse thrust term will be some fraction of full thrust, or

$$\text{reverse thrust} = T_{\text{reverse}} = R_{\text{reverse thrust}} T_{\text{sea level static}}$$

Deceleration will be less than or equal to takeoff acceleration, or

$$a_{\text{braking roll}} \leq 0.8g$$

Or, deceleration may be considered a variable and braking roll distance can be solved for using a summation of horizontal forces in Figure 46.

$$\Sigma F_x = \frac{W}{g} \frac{dV}{dt} = -T_{\text{reverse}} - F_{\text{rolling}}$$

$$-T_{\text{reverse}} - \mu_{\text{rolling}} W = -\frac{W}{g} \frac{dV}{dt}$$

$$-\frac{T_{\text{reverse}}}{W} - \mu_{\text{rolling}} = -\frac{1}{g} \frac{dV}{dt}$$

$$-\left(\frac{T_{\text{reverse}}}{W} + \mu_{\text{rolling}}\right) = -\frac{1}{g} V \frac{dV}{ds}$$

Integrating, let  $V_0$  = initial speed =  $1.2V_{\text{stall}}$  and  $V_1$  = final speed = 0:

$$\left(\frac{T_{\text{reverse}}}{W} + \mu_{\text{rolling}}\right) s = \frac{V_0^2}{2g} - \frac{V_1^2}{2g}$$

$$\left(\frac{T_{\text{reverse}}}{W} + \mu_{\text{rolling}}\right) s = \frac{V_0^2}{2g}$$

$$s_{\text{total}} = \frac{\frac{(1.2V_{\text{stall}})^2}{2g}}{\left(\frac{T_{\text{reverse}}}{W} + \mu_{\text{rolling}}\right)}$$

$$s_{\text{total}} = \frac{1.44V_{\text{stall}}^2}{2g\left(\frac{T_{\text{reverse}}}{W} + \mu_{\text{rolling}}\right)}$$

$$V_{stall}^2 = \frac{2}{\rho C_{L_{max}}} \frac{W}{S_{ref}}$$

$$S_{total} = \frac{1.44 \frac{W}{S_{ref}}}{\rho g C_{L_{max}} \left( \frac{T_{reverse}}{W} + \mu_{rolling} \right)}$$

$$S_{total} = \frac{1.44 \frac{W}{S_{ref}}}{\rho g C_{L_{max}} \left( R_{reverse \text{ thrust}} \left( \frac{T_{seal \text{ level static}}}{W} \right) + \mu_{rolling} \right)}$$

$$t_{braking \text{ roll}} = \frac{S_{braking \text{ roll}}}{\left( V_{braking \text{ roll}} \right)_{average}}$$

The total ground roll equation is expressed in two basic design parameters, thrust-to-weight ratio and wing loading. However, note that both lift and drag during the landing roll have been neglected here. This equation can be used to create a plot like that in Figure 47 which shows the effect of stopping deceleration on ground roll.

Appendix A presents an alternate set of equations for calculating takeoff and landing performance.

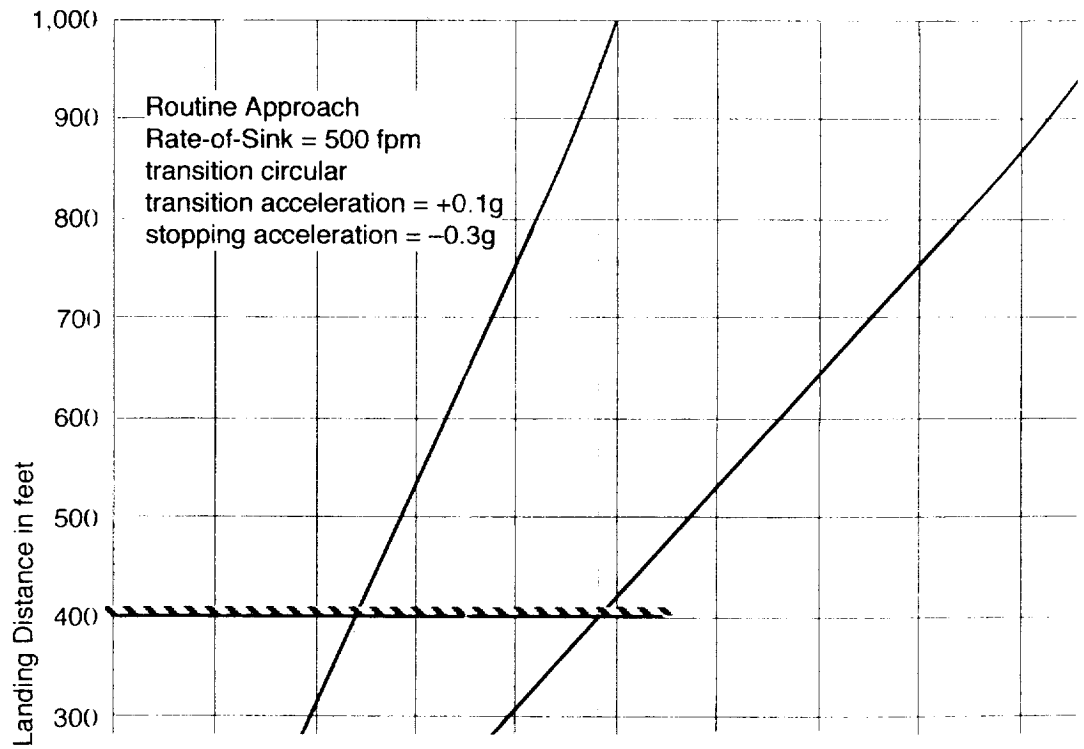


**Figure 47. The Effect of Stopping Deceleration on Ground Roll Can Be Dramatic.**

### Flight Envelopes

Flight envelopes are critical to describing aircraft performance. For every powered aircraft, it is possible to plot thrust available versus airspeed and thrust required versus airspeed on the same graph as shown in Figure 48 left. Each altitude, load factor, landing gear, and lift system configuration will have a set of these curves to describe it. Consider here the 1-g full thrust curves for an airplane in clean configuration.

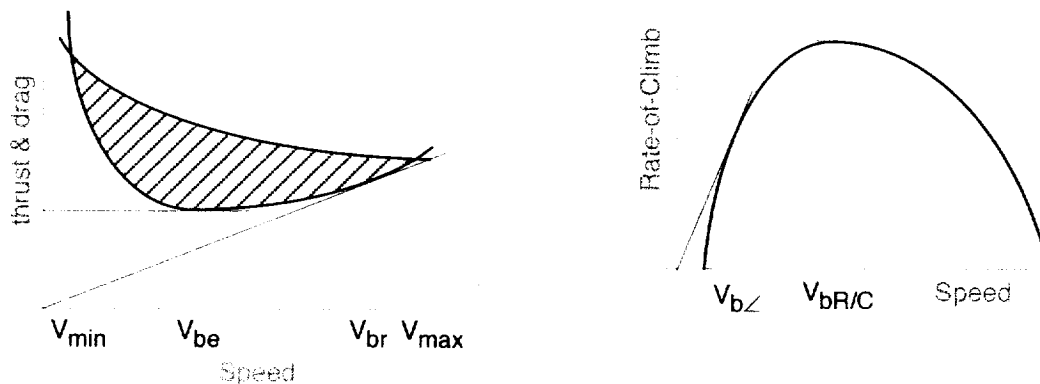


**Figure 48. Thrust or Power Required and Available versus Airspeed (left) Yields Excess Thrust or Power for Climb Rate Determination (right).**

Figure 49 shows the relationship between minimum and maximum speeds for each altitude and how flight envelopes are constructed. For conceptual clarity, also shown is each set of thrust and drag versus airspeed curves used to define the flight envelope. Note that the left side of the flight envelope shows the minimum power-on speed at which an airplane can maintain straight and level flight at each altitude. The right side of the flight envelope shows the maximum level speed an airplane can maintain at each altitude. Figure 50 left shows minimum and maximum level speeds defining the ideal flight envelope. Practically speaking, aircraft flight envelopes are seldom determined solely by minimum and maximum speeds; there are other factors which can sculpt the flight envelope to look like that shown in Figure 48 center. These factors are:

1. High Lift Devices;
2. Nose or Windscreen Dynamic Pressure Limit;
3. Government Imposed Speed Limits at Certain Altitudes;
4. Empennage Flutter Limit;
5. Drag Divergence Mach Number;
6. Cabin Pressurization Limit; and
7. Angle-of-Attack Limit on Stability.

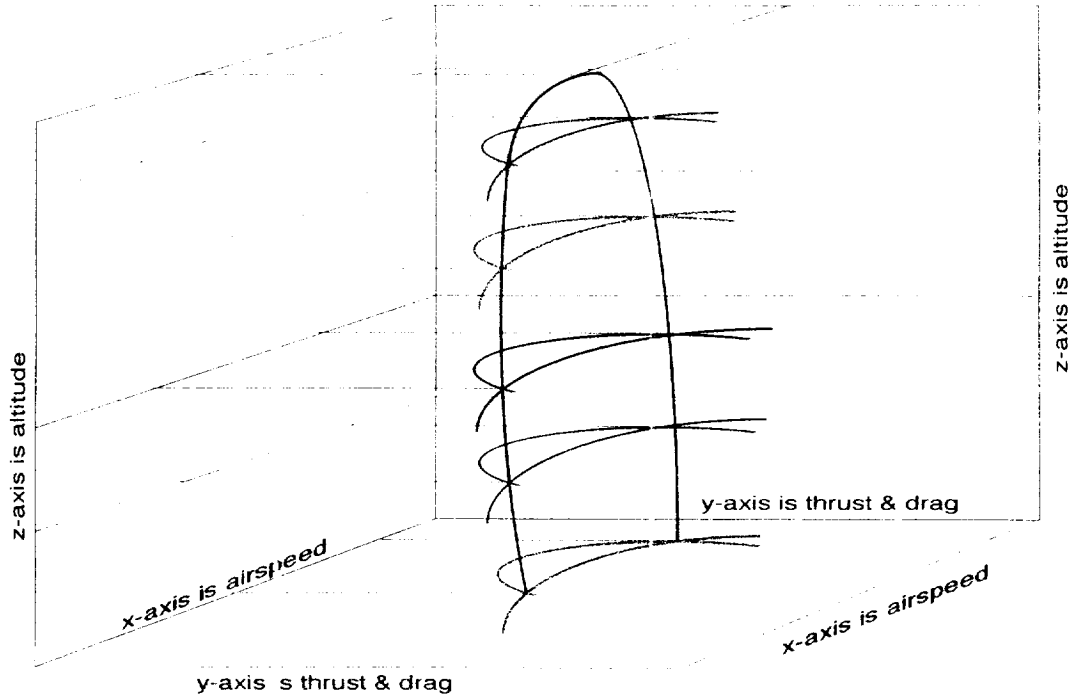
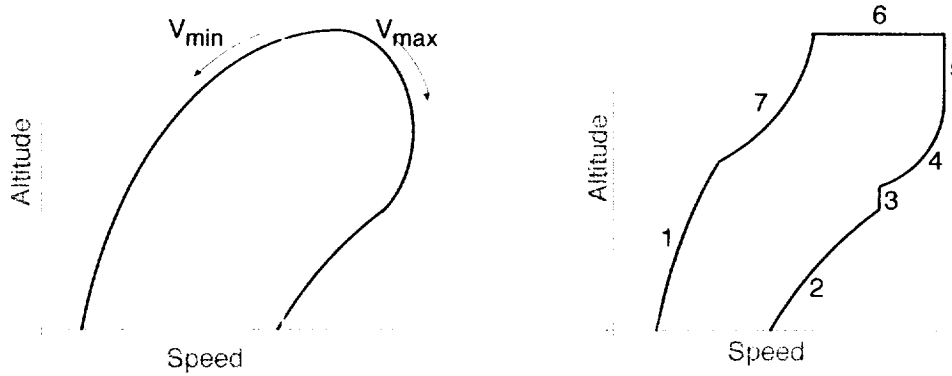
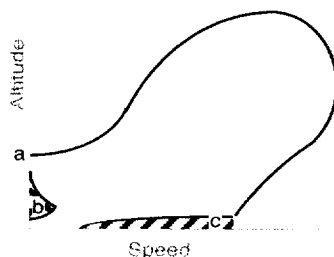


Figure 49. A Flight Envelope is Constructed from Other Sets of Performance Curves.





**Figure 50. A Variety of Factors Determine the Shape of a Flight Envelope.**

### **Avoid Curve Considerations in Flight Envelope Determination**

The following discussion presents basic considerations for transient behaviors and not exact solutions. For VTOL aircraft, the flight envelope is more likely to look like Figure 50 right where the left portion of the curve intersects the y-axis at an altitude greater than zero rather than intersecting the x-axis. This implies that the aircraft has an ability to hover with the maximum hover altitude shown as point a. Point a is the point out of ground effect where thrust and weight are exactly equal and is known as the maximum hover altitude.

The flight envelope will have cutouts indicating areas to be avoided in emergencies. Area b is the low speed avoid zone and can be determined through performance analysis coupled with basic kinematics. Area b takes into account both structural and energy considerations. Area c is the high speed avoid zone and is usually empirically determined.

To determine either of these avoid zones, consider instantaneous and complete engine failure (one engine only) as a starting point for analysis. The lower curve in Figure 51 is where an engine is lost in hover and the aircraft drops to the ground at maximum allowable sink rate with no structural damage—and no injury to crew or passengers, of course. The higher curve describes the combination of altitude and forward speed where the aircraft is capable of pitching down to gain speed and flying away. The two curves meet at that single point where the pilot has either option should an engine fail.

After establishing the lowest safe hover point, calculate the lowest altitude/airspeed combination where the pilot has time to pitch over, flare, and land. Then calculate the set of points where the pilot reacts, pitches over, gains flying speed and climbs out.

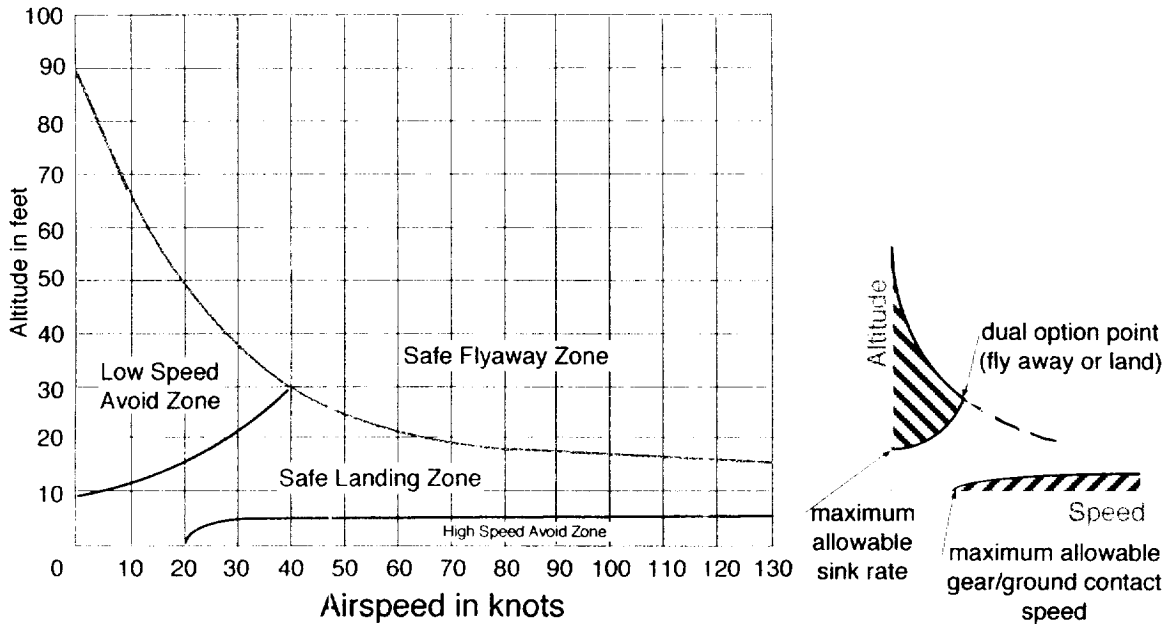


Figure 51. Avoid Zones Are Both Kinematically and Aerodynamically Determined.

**Case 1: Engine Loss at Hover**

The first case to be considered is the simplest and can be solved with basic kinematics. Given a starting altitude, calculate the ending speed if powered lift fails. In a single engine VTOL, vertical thrust would decrease to zero, but in a multiple engine VIOL, engine thrust would decrease to a number greater than zero. In either case, turbine engines operating in hover would be putting out maximum takeoff thrust. Practically speaking, should one engine fail, it isn't likely to fail instantaneously. It would spool down over several seconds, thus providing some thrust cushion while the crew ponders their options. Consider the worst case, though: complete and instantaneous engine failure.



$$E_{total} = E_{potential} + E_{kinetic}$$

$$E_{total} = Wh + \frac{1}{2} mV^2$$

$$E_{total} = W \left( h + \frac{V^2}{2g} \right)$$

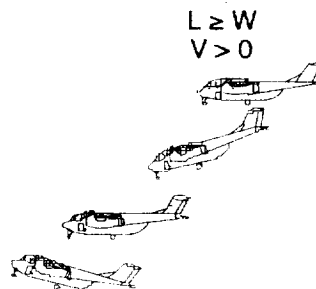
$$(E_{total})_{@V=0} = Wh_{@V=0} = \frac{W}{2g} (V_{R/S})_{max}^2$$

$$h_{@V=0} = \frac{(V_{R/S})_{max}^2}{2g}$$

This equation quantifies point a in Figure 43 right.

#### Case 2: Engine Loss at Low Speed, Low Altitude

This case corresponds to a VTOL having lifted off and initiated transition just as an engine fails. Note that a pilot would make as few changes to the status quo as possible in order to maintain control; therefore, airspeed would be held constant by lowering the nose in order to trade potential energy for kinetic. The nose would be raised prior to impacting the ground, or rather, before a very hard but damage-free landing. The free body in Figure 52 applies.



Before engine loss,  $L \geq W$ ,  $T \geq D$ ,  $a_x \geq 0$ , and  $a_z \geq 0$ . Calculate initial conditions including total thrust just before and just after engine failure.

$$T_i = \phi T \cos(\delta_{flap} + \alpha_{t=i})$$

Calculate dynamic pressure at engine failure (the pilot holds airspeed constant during descent).

$$V_z \leq (V_{R/S})_{max} = V_\infty \sin \gamma$$

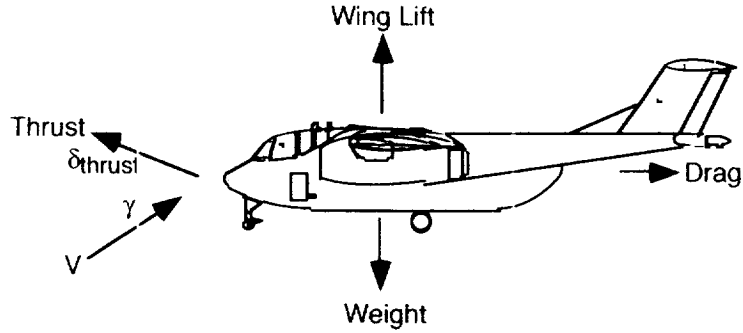


Figure 52. Angle-of-Attack Plays an Important Role in Avoid Curve Determination.

$$q_{\infty} = \frac{1}{2} \rho V_{\infty}^2$$

$$q_{t=0} = \frac{TOGW - \phi T \sin(\delta_{flap} + \alpha_{t=0})}{4.6 \delta_{flap} S_{jet} + C_{L_{\alpha}} \alpha_{t=0} S_{ref}}$$

Test  $q$  at time = 0. If  $q \leq 0$ , then  $V$  at time,  $t = 0$  is zero.

$$\text{If } q \geq 0, V_{t=0} = \sqrt{\frac{2q}{\rho}}$$

Calculate free stream dynamic pressure at any time

$$q_i = \frac{1}{2} \rho V_i^2$$

$$L_{t=0} = 4.6 \delta_{flap} S_{jet} q_{t=0} + \phi T \sin(\delta_{flap} + \alpha_{t=0}) + C_{L_{\alpha}} \alpha_{t=0} q_{t=0} S_{ref}$$

$$D_{t=0} = C_{D_0} S_{ref} q_{t=0} + \frac{2.176 S_{flap} q_{t=0} \delta_{flap}}{1.5707963} + \frac{(L_{t=0})^2}{\pi AR + 2\phi T}$$

$$a_x = \frac{T - D_{t=0}}{W} g$$

$$a_z = \left( \frac{L_{t=0}}{W} - 1 \right) g$$

Increment time and repeat.

$$t_i = t_{i-1} + \Delta t$$

$$V_{x_i} = V_{x_{i-1}} + a_{x_{i-1}} \Delta t$$

$$V_{z_i} = V_{z_{i-1}} + a_{z_{i-1}} \Delta t$$

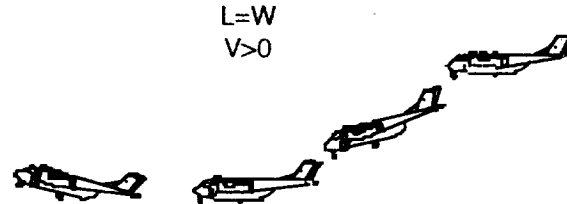
Then position at this time will be

$$x_i = x_{i-1} + \frac{V_{x_i} + V_{x_{i-1}}}{2} \Delta t$$

$$t_i = t_{i-1} + \frac{V_{z_i} + V_{z_{i-1}}}{2} \Delta t = h_i$$

### Case 3: Engine Loss at Low Speed, Low Altitude

At some initial combinations of airspeed and altitude, the pilot will be able to lower the nose and gain enough airspeed to fly away on the remaining engine(s).



To begin, calculate initial conditions for time, angle-of-attack, flight path angle, horizontal position, height, horizontal and vertical speeds. Then calculate aerodynamics.

$$L_{t=0} = 4.6 \delta_{flap} S_{jet} q_{t=0} + \phi T_{n-1} \sin(\delta_{flap} + \alpha_{t=0}) + C_{L\alpha} \alpha_{t=0} q_{t=0} S_{ref}$$

$$D_{t=0} = C_{D0} q_{t=0} S_{ref} + \frac{2.176 S_{flap} q_{t=0} \delta_{flap}}{1.5707963} + \frac{(L_{t=0})^2}{(\pi A R q_{t=0} S_{ref} + 2 \phi T_{n-1})}$$

The rate of sink will be:

$$V_{z_i} = -V \sin \gamma$$

Accelerations will be:

$$a_x = \frac{\left\{ \left[ \phi T_{n-1} \cos(\delta_{flap} + \alpha_{t=0}) \right] - D_{t=0} \right\} \cos \alpha - L_{t=0} \sin \gamma}{W} g$$

$$a_z = \frac{\phi T_{n-1} \cos(\delta_{flap} + \alpha_{t=0}) \sin \gamma + L_{t=0} \cos \gamma}{W} g$$

Now increment time and repeat.

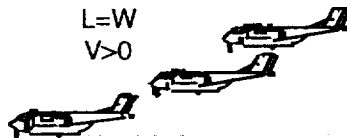
$$t_i = t_{i-1} + \Delta t$$

$$V_{x_i} = V_{x_{i-1}} + a_{x_{i-1}} \Delta t$$

$$V_{z_i} = V_{z_{i-1}} + a_{z_{i-1}} \Delta t$$

#### Case 4: Engine Loss at High Speed, Low Altitude

This case covers the high speed, low altitude avoid zone and its boundaries are usually empirically determined. Story: I met John Spencer at North American Aviation/Columbus Aircraft Division in 1972. John's civilian flying career had started at Bell Helicopter where he was a test pilot on UH-1s in charge of establishing this portion of its flight envelope. According to John, the series of tests involved landing the UH-1 from increasing combinations of altitude and airspeed until landings damaged the skids. Then they'd back off one point, plot it on the flight envelope graph, replace the skids and move to the next combination.



That being the case, how could we analyze this particular avoid zone? We would first need structural impact values for the landing gear. Then kinematics would assist in calculating descent rates. When the two are equal, back off a tad and plot it.

#### Lift Engine Operational Considerations

For a configuration that uses lift engines, it's important to note that they don't run throughout most of the mission, just at takeoff and landing. Figure 53 presents the thrust versus time characteristics for a Rolls Royce lift engine which was developed in the 1970s. Note the spool-up and spool-down times which are part of each duty cycle and have a profound effect on how the engines are used.

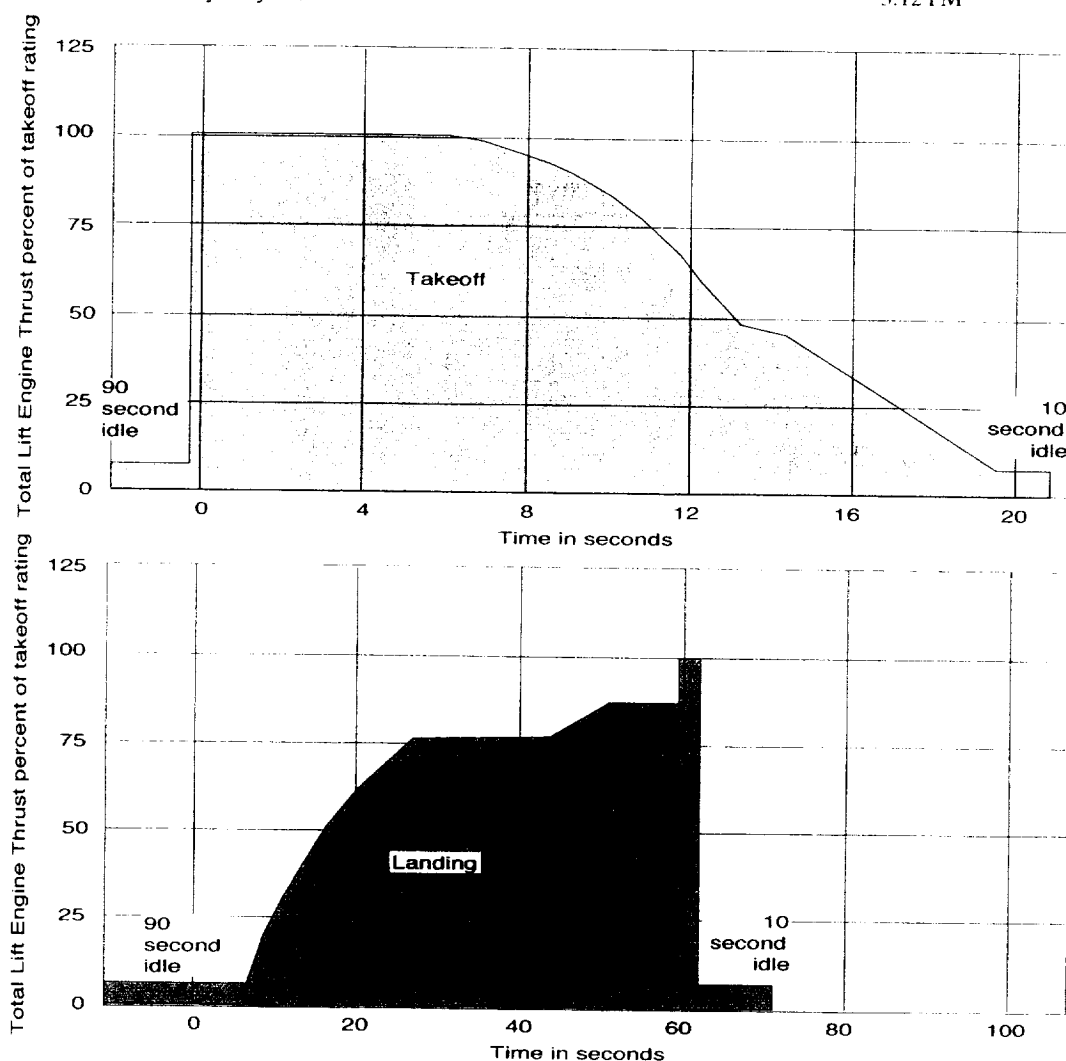


**Figure 53. Lift Engines Run for only a Small Portion of Total Flight Time.**

Losing an engine will affect lateral/directional stability in that asymmetric vertical thrust will cause an unbalanced rolling moment and asymmetric horizontal thrust will cause an unbalanced yawing moment. If engine loss occurs during transition, this may set up a spin entry. There are four solutions. One is to rely on a single engine and adjust flight operations to minimize exposure to avoid zones. This may be a viable solution for small, cheap VTOLs as well as for VTOLs using complicated vertical lift systems.

A second solution is to increase the number of engines so that losing one can be accommodated by spooling up the others. Obviously, the more engines, the less the impact of losing one; however, the more engines, the more costly and complicated the airplane becomes. To illustrate, losing one engine in a twin engine design cuts available thrust to half the all-up total; losing one engine in four cuts thrust to three-quarters the all-up total; and losing one engine in eight cuts thrust to seven-eighths the all-up total. If the remaining engines can be spooled up a certain percent over takeoff rating to temporarily deliver the missing thrust, then the percentage they can be spooled up may determine the number of engines, and the size and shape of flight envelope avoid zones.

### Vertical Lift Stability and Control Considerations

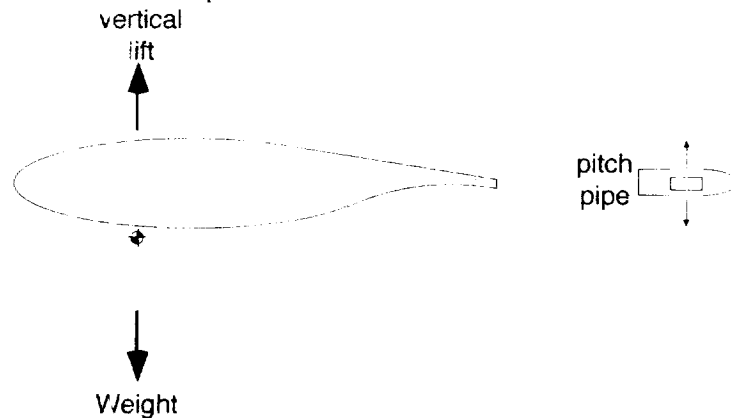
A third solution is to cross-link engines so that loss of one can be made up for by borrowing power from the others to maintain symmetrical horizontal and vertical thrust. Mechanical cross-linkages are series of shafts and gears which can get complicated and heavy depending upon distance of runs, power transferred, and engine speed. The V-22 uses extensive mechanical cross-shafting. Air or exhaust gas cross-feeds require ducting and valving to transfer air to the vicinity of the dead engine. These systems could be lossy depending upon duct turns and distances. In either of the latter cases, engines may talk to one another and adjust back pressures to be roughly equal from all engines regardless of what the pilot wants.

A fourth solution is to arrange engines to dump exhaust gas into a common plenum chamber and duct air from there to all vertical lifting surfaces. This avoids cross-ducting, but losing one engine will still change back pressures on the others and may cause engine surge or stall in the operating engines.

Any time engine air is ducted, flow temperature becomes an important structural consideration. Flow temperature will decrease with increasing engine bypass ratio in a mixed flow engine and will increase with increasing fan pressure ratio. Figure 54 shows how this can affect aircraft size.

Some form of attitude control must be provided for the period between initial liftoff and transition to wingborne flight. Puffer pipes are frequently used in this capacity in much the same way they're used on spacecraft. Pitch pipes are placed at the extreme nose and/or tail to balance the airplane fore and aft and to provide trim as well as to facilitate pitch-up or pitch-down maneuvers. This is the same function the horizontal tail serves in conventional flight. Puffer pipes can also be placed at the wingtips, but only if absolutely necessary, to provide lateral control.

Three puffer pipe sizing cases will be discussed here, the first being where the center of vertical lift and the center-of-gravity are coincident and the pitch pipe is only needed for control. In this case, no steady-state engine bleed air is required and thrust available for powered lift isn't affected.



The second case is where the center of vertical lift is ahead of the center-of-gravity. Pitch pipes using steady-state engine bleed air are required for trim as well as for control, so using the aft pitch pipe to correct trim with a vector in the vertical lift direction is the most desirable solution.

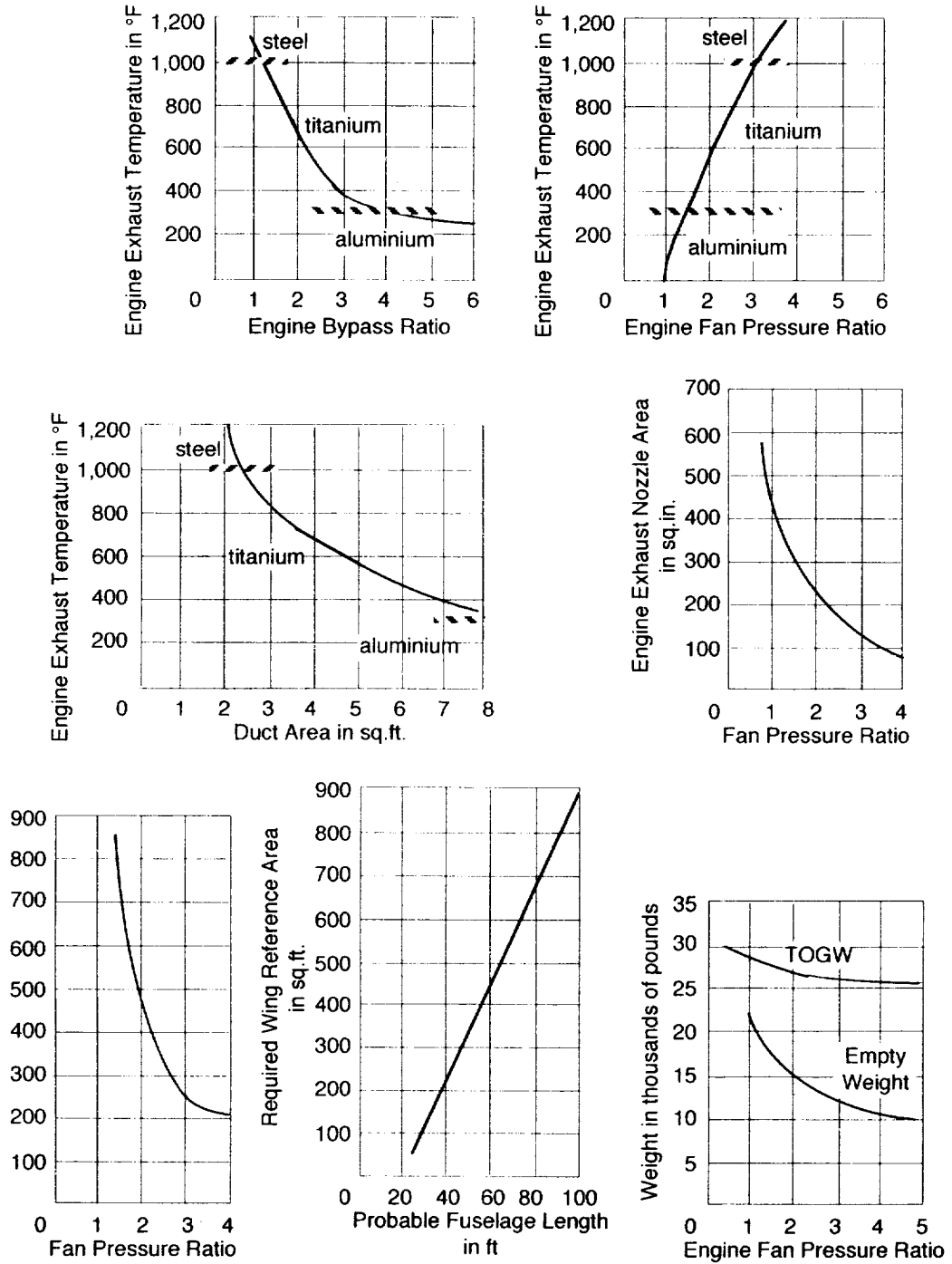
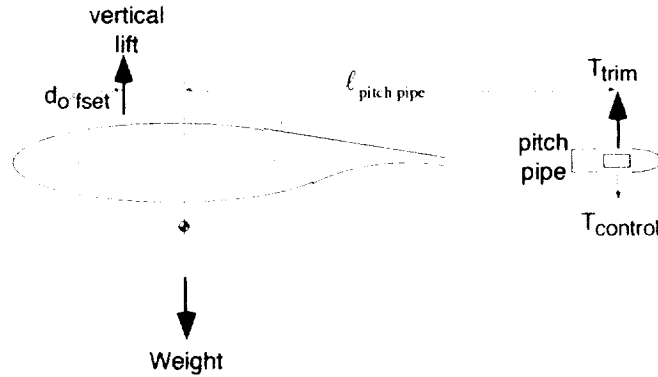


**Figure 54. Engine Bypass Ratio and Fan Pressure Ratio Affect Aircraft Design as Shown by This F100/F401 Class Turbofan.**



$$\Sigma M_{c.g.} = -L_{vertical} d_{offset} + T_{trim} \ell_{pitch\ pipe} \equiv 0$$

$$T_{trim} = \frac{d_{offset}}{\ell_{pitch\ pipe}} L_{vertical}$$

$$\Sigma F_{vertical} = L_{vertical} + T_{trim} - (TOGW)_{vertical} = 0$$

$$(TOGW)_{vertical} = \left( 1 + \frac{d_{offset}}{\ell_{pitch\ pipe}} \right) L_{vertical}$$

For an augmenter wing:

$$L_{vertical} = \phi(T - L_{pitch\ pipe})$$

$$\Sigma M_{c.g.} = -\phi(T - L_{pitch\ pipe})d_{offset} + T_{trim} \ell_{pitch\ pipe} \equiv 0$$

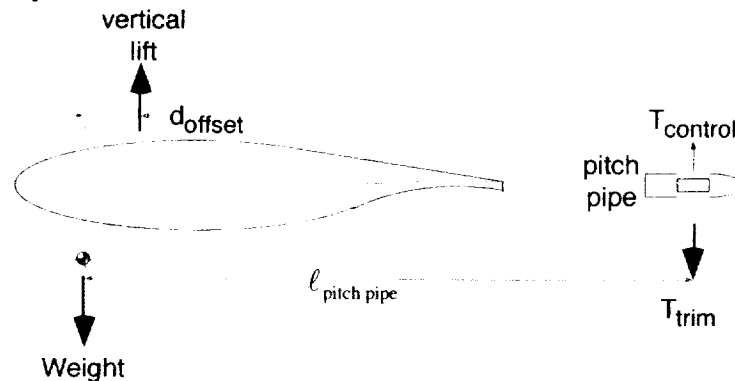
$$T_{trim} = \frac{\phi T d_{offset}}{\ell_{pitch\ pipe} + d_{offset}}$$

$$\Sigma F_{vertical} = \phi(T - T_{trim}) + T_{trim} - (TOGW)_{vertical} = 0$$

$$(TOGW)_{vertical} = \phi T + (1 - \phi)T_{trim}$$

$$(TOGW)_{vertical} = \phi T + (1 - \phi) \frac{\phi T d_{offset}}{\ell_{pitch\ pipe} + d_{offset}}$$

The third case is where the center of vertical lift is aft of the center-of-gravity. Again, steady-state engine bleed air is required for trim. If the aircraft has pitch pipes at both the nose and tail, trim will provide vertical lift when coming from the forward pipe; however, if the only pitch pipe exists at the tail, vertical lift will be decreased by the amount of the steady-state trim.



For an augmeter wing:

$$\Sigma F_{vertical} = L_{vertical} - L_{pitch\ pipe} - (TOGW)_{vertical} = 0$$

$$(TOGW)_{vertical} = \left( 1 - \frac{d_{offset}}{\ell_{pitch\ pipe}} \right) L_{vertical}$$

$$L_{vertical} = \phi(T - L_{pitch\ pipe})$$

$$(TOGW)_{vertical} = \phi T + (1 - \phi)L_{pitch\ pipe}$$

$$\Sigma F_{vertical} = \phi(T - L_{pitch\ pipe}) - L_{pitch\ pipe} - (TOGW)_{vertical} = 0$$

$$(TOGW)_{vertical} = \phi T - (\phi + 1) \frac{\phi T d_{offset}}{\ell_{pitch\ pipe} + d_{offset}}$$

### Effect of Ground Plane

Engine exhaust air in a VTOL system will point straight down in hover and may cause erosion problems on surfaces from flow pressure and/or temperature. Flow speeds can be anywhere from 0.4 Mach to sonic and pressures can be three times ambient in spots. The eroding effect of hot gas streams will lessen with nozzle height above ground so maximizing that height will reduce footprint erosion. Maximizing surface hardness will minimize deleterious effects as will mixing hot exhaust flows with ambient air. Surfaces can also be perforated (vented) to duct away exhaust gases.

As shown in Figure 55, ground plane proximity causes several things to happen to the VTOL flow, one of the worst of these being hot gas reingestion by air intakes.

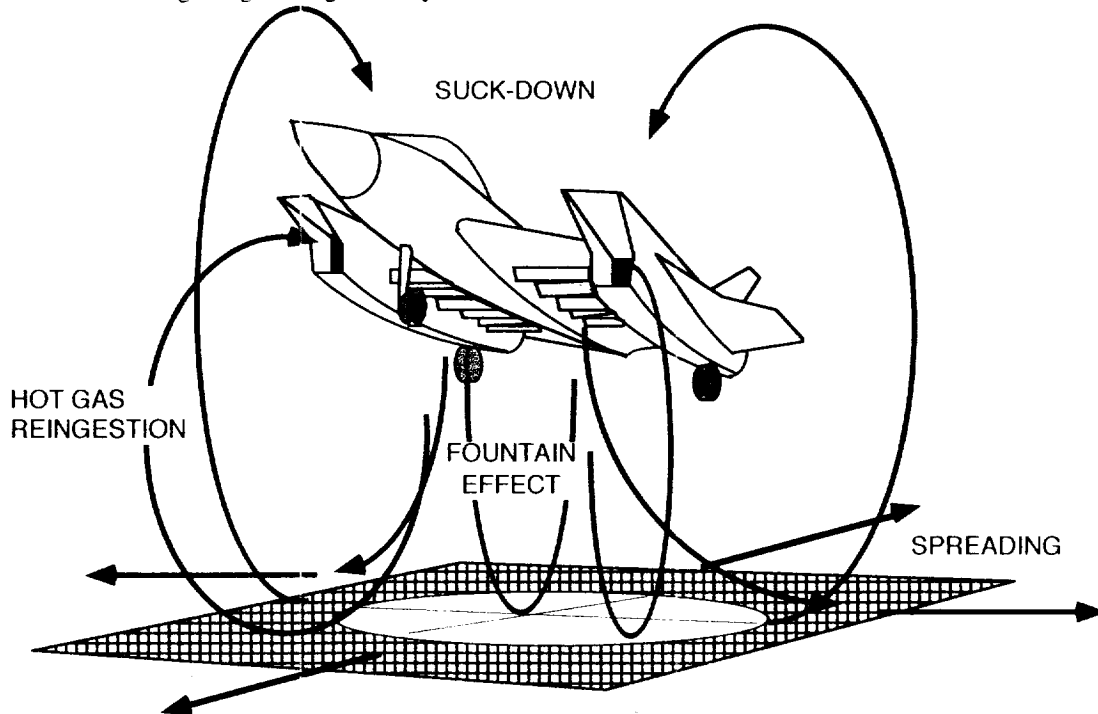


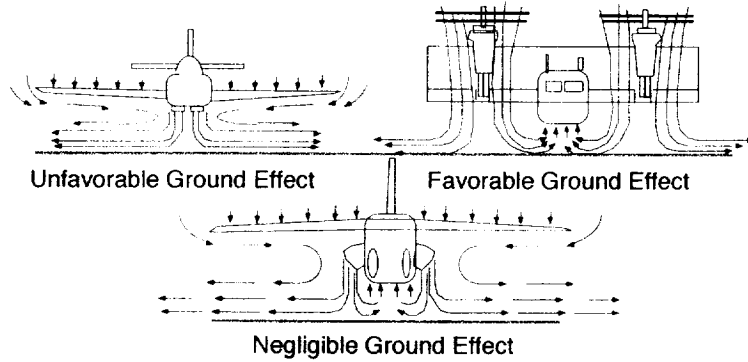
**Figure 55. Blowing Hot, High Pressure Gas at a Hard Surface Causes a lot of Things to Happen.**

A vertical stream hitting a flat surface spreads more-or-less uniformly in a circular pattern. Flow will also be turned back upward and enter the augmenters mixed with ambient, entrained air. As an example, flow hitting the ground from a nozzle five feet in the air will spread outward about 60 feet before turning back in. As this air is reingested into the engine, exhaust gas temperatures may rise 2% or about 20°F. Wind will cut the horizontal spreading distance in half on the upwind side and will ensure hot gas is reingested into the engine. In this case, exhaust gas temperature may rise 3% to 8%, or 30°F to 80°F.

Air that doesn't enter the augmenters may rise, come back around, and press down on the lifting surfaces, causing a suck down effect when coupled with vertical streams of exhaust gases under the aircraft pulling air away and outward. However, air will also get turned back under the aircraft by part of the exhaust gas stream and will cause a fountain effect as it rises under the center of the aircraft. This is only a possibility, though, with multiple lift engines or nozzles. Poor placement of exhaust gas nozzles may lead to little or no fountain effect and additional hot gas and debris being sucked back into the engine. This will cause exhaust gas temperature to rise 8% to 12%, or 80°F to 120°F as the aircraft hovers. Dams could be judiciously placed on the underside of the fuselage to trap the fountain effect gases and the AV-8B may be an example of this type of fix.

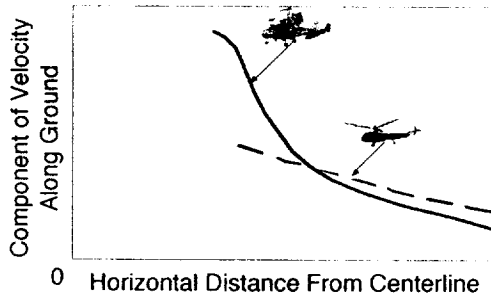
Some general configuration-related observations may be made at this point. Refer to Figure 56 which presents three VTOL aircraft configuration types and qualitatively shows their effect on flow patterns in the presence of a ground plane. The Bell X-14 exhibited unfavorable ground effect interactions in hover and the only solution was to launch and recover the aircraft from a steel mesh screen over a pit—a solution also used for some models of the

Harrier/ Kestrel family.



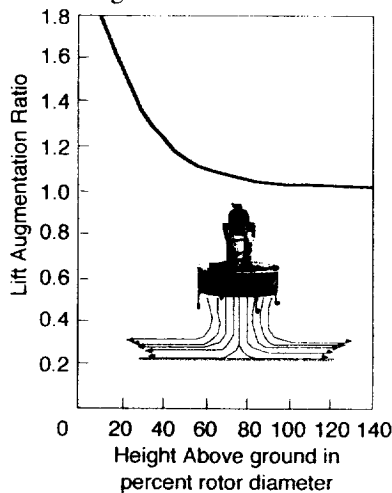
**Figure 56. Configuration Plays a Role in Ground Effect Patterns.**

Figure 57 presents another oddity of hovering flight for various disc loadings—flow velocities outward from center tend to reach the same range of values for all types of hovering vehicles. The two shown here are tilt-wings and helicopters.



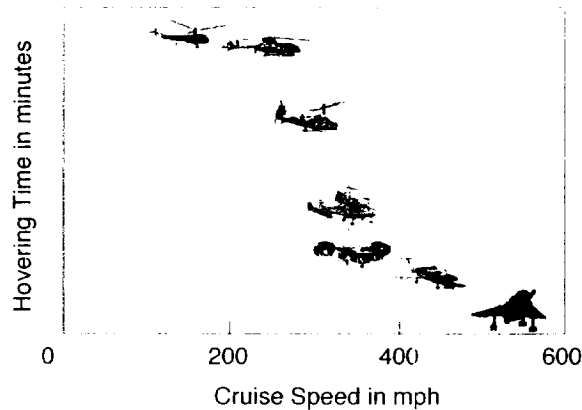
**Figure 57. Beyond a Certain Distance, Flow Velocities Tend to Become Uniform.**

Figure 58 presents one indication of how strong the fountain effect can be under a hovering VTOL, the example being for a ducted fan. The lift augmentation ratio is the ratio of the vertical lift provided to the aircraft weight and reaches respectable values close to the ground.



**Figure 58. Fountain Effect Can Increase Apparent Lift in Hover.  
Disc Loading Effects**

Disc loading is defined as the ratio of aircraft weight to rotor, propeller, or compressor face area depending upon the type of VTOL propulsion system being considered. Observation of various types of historical VTOLs shows that hover time lessens with aircraft cruise speed, as shown in Figure 59. More importantly, the relationship is with disc loading and cruise speed is a fallout of high disc loading machines. Another reason for higher cruise speeds with high disc loading VTOLs is that installed engine power increase with disc loading, which is intuitively obvious but doesn't go without saying, as shown in Figure 60.



**Figure 59. Hover Time Varies Inversely With Cruise Speed.**

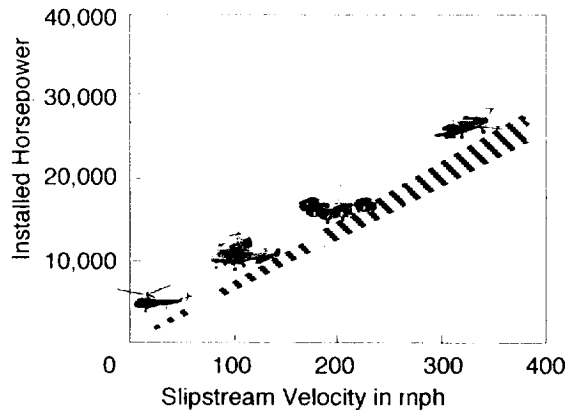


**Figure 60. High Disc Loading VTOLs Tend to Have Large Engines.**

**Hover Performance**

The size, shape and speed of exhaust and entrained air directly under a VTOL affects its ability to hover for long periods of time. Since installed power tends to rise with disc loading, so, too, does fuel consumption and total propulsion system weight. Given a theoretically constant 40,000 vertical takeoff gross weight for VTOLs using a variety of lift systems, Figure 61 shows the effect of slipstream velocity under each vehicle on its hover

performance. Also shown is the variation of rotor diameter to achieve low values of slipstream velocity. The final set of curves in Figure 61 shows the pronounced effect of hover time on total propulsion system weight including the fuel required to hover.

A cautionary note on these curves is in order. Figures 56 through 64 were taken from reference 2 which was published in 1962. Enough technologies have changed in the intervening 38 years that a renewed look at these conclusions is in order.

### **Minimizing Power Required**

Continuing this discussion, note that the power required curve for a VTOL will look different at its low end than that for a conventional aircraft as Figure 62 shows for a tilt-wing VTOL. This reflects the propulsion system's ability to produce sizable amounts of static thrust. Figure 63 continues the graphical presentation of ways to decrease power required at low speed, some of which are configuration dependent such as tailoring the lift distribution, and some are operational as in avoiding transitioning with the wing aerodynamically stalled.

Last but not least, Figure 64 presents the effect of engine loss on choice of operating speed for three different types of VTOL aircraft. Operationally, the aircraft would accelerate as rapidly as possible to this minimum engine out speed to minimize exposure to catastrophe.

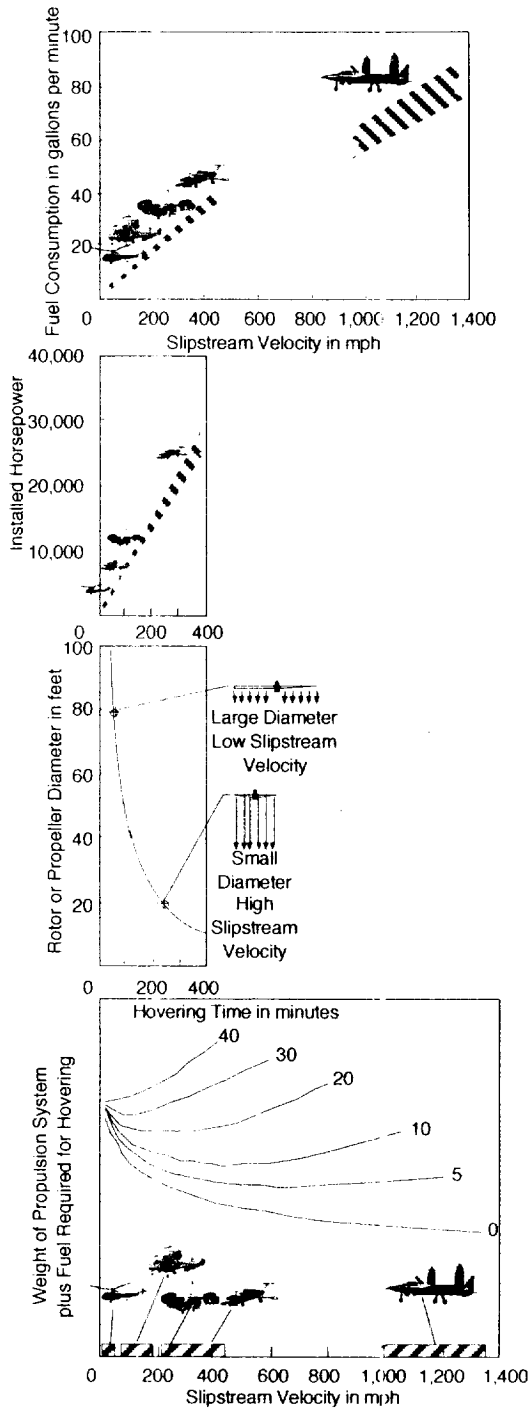


Figure 61. Slipstream Velocity Directly Under a Hovering VTOL Affects Its Performance.

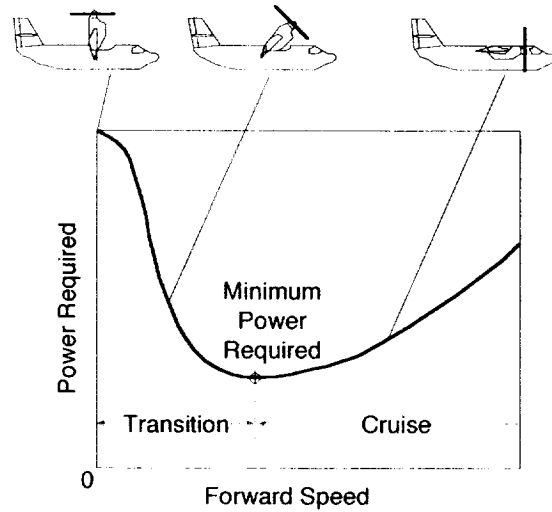


Figure 62. Power Required Reaches a Minimum at the End of Transition from Hover.

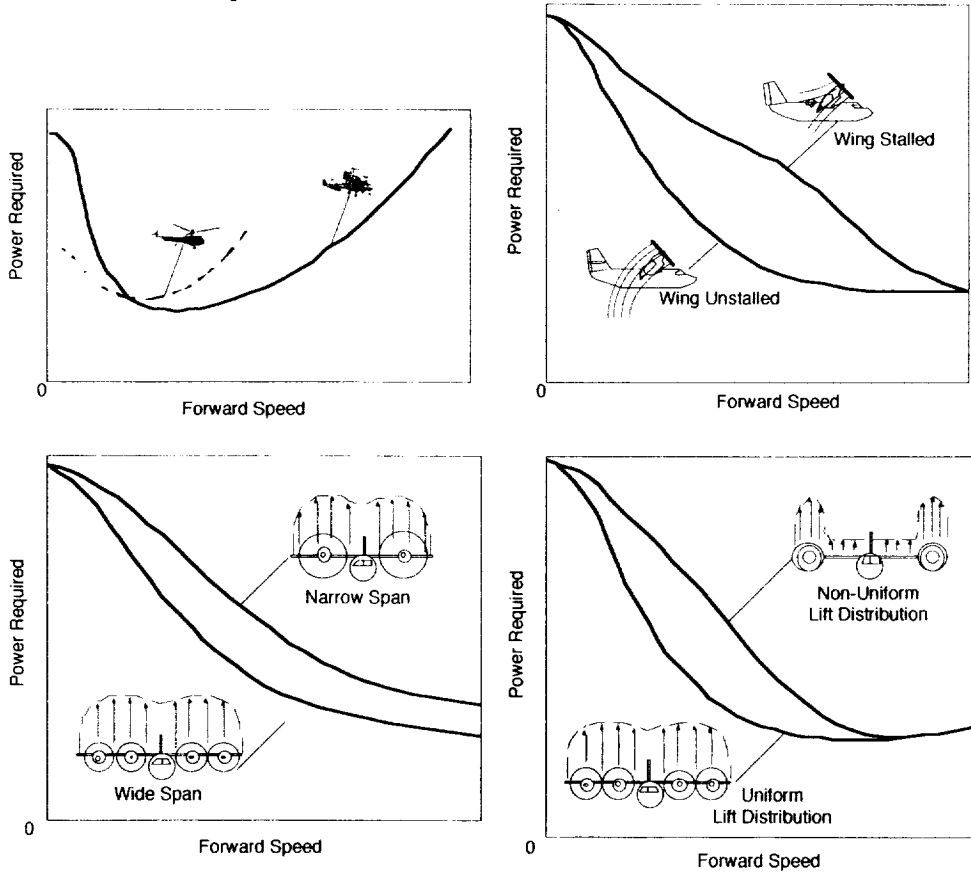
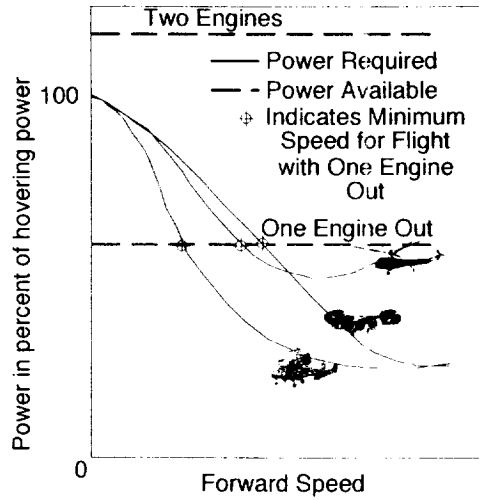


Figure 63. Designers Can Improve Low Speed Performance of VTOLs.



**Figure 64. VTOL Aircraft Engines Must Be Sized to Take Engine-Out Performance Into Consideration.**

**STOL and Super/STOL Flow Considerations**

Define a blowing coefficient, actually a momentum coefficient,  $C_\mu$ , as

$$C_\mu = \frac{\dot{m}_{blowing} V_{ejector}}{q(S_{flap})_{jet}} \Rightarrow \dot{m}_{blowing} = \frac{C_\mu q(S_{flap})_{jet}}{V_{ejector}}$$

At forward speed, the aircraft generates a lift coefficient that is a combination of aerodynamic lift and powered lift. For an augmenter wing:

$$C_L = C_{L_a} \alpha + 4.6 \frac{S_{jet}}{S_{ref}} + \phi C_\mu \sin(\delta + \alpha)$$

where mass flow is in slugs per second. For conventional aircraft  $C_\mu$  might be around 0.5, but for STOL and Super/STOL  $C_\mu$  might be on the order of 5.0.

**THEORETICALLY ELEGANT VTOL CONCEPTS—FLUIDIC AMPLIFICATION**

Fan-in-wing and thrust augmenters are both fluidic amplifiers and are conceptually the same between the engine and the fan or augmenter in terms of analyzing internal ducting losses.

**Fan-In-Wing**



Fan-in-wing performance may be estimated by treating it as a vertically oriented shrouded propeller where the blades are turned by blowing ducted engine exhaust gas past tip turbines. The energy-depleted exhaust gas must then be vented overboard. Covering doors should be oriented perpendicular to the cruise direction and parallel with cruise airflow.

The amount of thrust provided by the fan is ratioed to the jet thrust used to turn it to calculate an augmentation ratio.

$$\phi = \frac{\text{Total Lift from Fan}}{\text{Jet Thrust at Fan}} = \frac{\dot{m}_{\text{fan}} V_{\text{fan}}}{\dot{m}_{\text{jet}} V_{\text{jet}}} = \frac{(\dot{m}_{\text{primary flow}} + \dot{m}_{\text{secondary flow}}) V_{\text{fan}}}{\dot{m}_{\text{jet}} V_{\text{jet}}}$$

$$\phi = \frac{\dot{m}_{\text{primary flow}} V_{\text{fan}}}{\dot{m}_{\text{jet}} V_{\text{jet}}} + \frac{\dot{m}_{\text{secondary flow}} V_{\text{fan}}}{\dot{m}_{\text{jet}} V_{\text{jet}}}$$

$$\phi = \frac{V_{\text{fan}}}{V_{\text{jet}}} \left( 1 + \frac{\dot{m}_{\text{secondary flow}}}{\dot{m}_{\text{jet}}} \right)$$

Low fan pressure ratios ( $1.1 \leq fpr \leq 1.4$ ) seem to work best and augmentation ratio will decrease as fan pressure ratio increases. Disc loading, the thrust per unit fan planform area, has an inverse effect on augmentation ratio as well; the more heavily loaded the blades are, the less efficient they are. Figure 65 presents this effect.

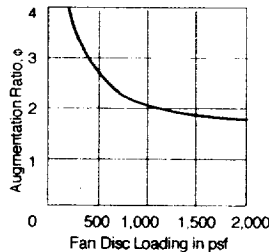


**Figure 65. Fan Disc Loading is a Strong Determinant of Augmentation Ratio.**

As with other fluidic amplifiers, the depth of the cavity directly affects efficiency; hence, a thicker airfoil section is more beneficial than a thinner one for a given chord length in order to incorporate a deeper fan.

### Thrust Augmentor Wing



This approach to fluidic amplification relies on entrainment of outside air with no mechanical accelerator, as in a fan-in-wing. Coanda Effect is used on forward and aft surfaces to force outside air into a gap between exhaust gas nozzles. Augmentation ratio is defined as before, a ratio of entrained flow to primary flow, and will vary from  $1 \leq \phi \leq 2$ .

This particular approach was demonstrated on a DeHavilland/Canada Buffalo in the 1970s and the aircraft is still stored at NASA/Ames Research Center. It proved reasonably efficient for improving STOL performance but was incredibly noisy.

### Thrust Augmentor Wing

#### Overview

Consider the augments arrangement of Figure 66.

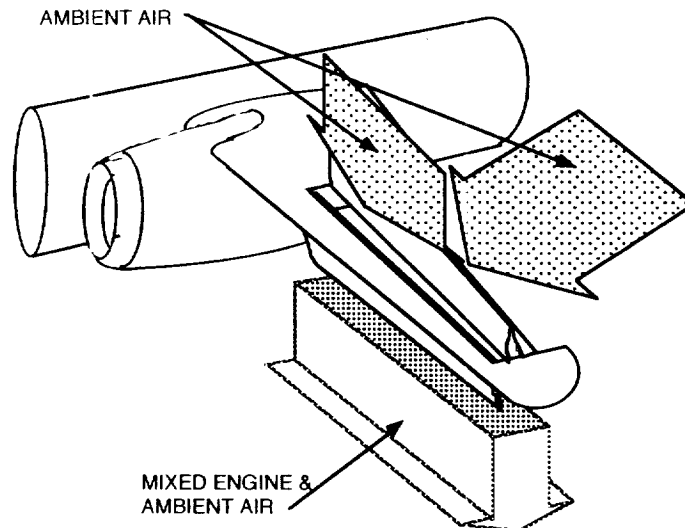


**Figure 66. Spanwise Augments Bays Entrain Large Amounts of Ambient Air.**

Semantics often play a pivotal role in engineering and here's a prime example. This particular approach to fluidic amplification differs in two respects from the previous one: First, the fluidic amplifier takes up most of the wing cross-section instead of just the trailing edge; second, it's spelled differently. Other than that, analyses are similar. Note, however, that this approach employs a center injector in each augments bay as well as forward and

aft nozzles, the exhaust gas split being 25%-50%-25% of total engine mass flow. Refer to Figure 67 for definition of terms. For a constant span, areas can be defined as

$$A_2 = b_{\text{augmenter bay}} D_2$$

$$A_3 = b_{\text{augmenter bay}} D_3$$

$$D_3 = D_2 + 2L \tan \delta_{\text{flap}}$$

$$\frac{A_3}{A_2} = \frac{D_3}{D_2} = 1 + 2 \frac{L}{D_2} \tan \delta_{\text{flap}}$$

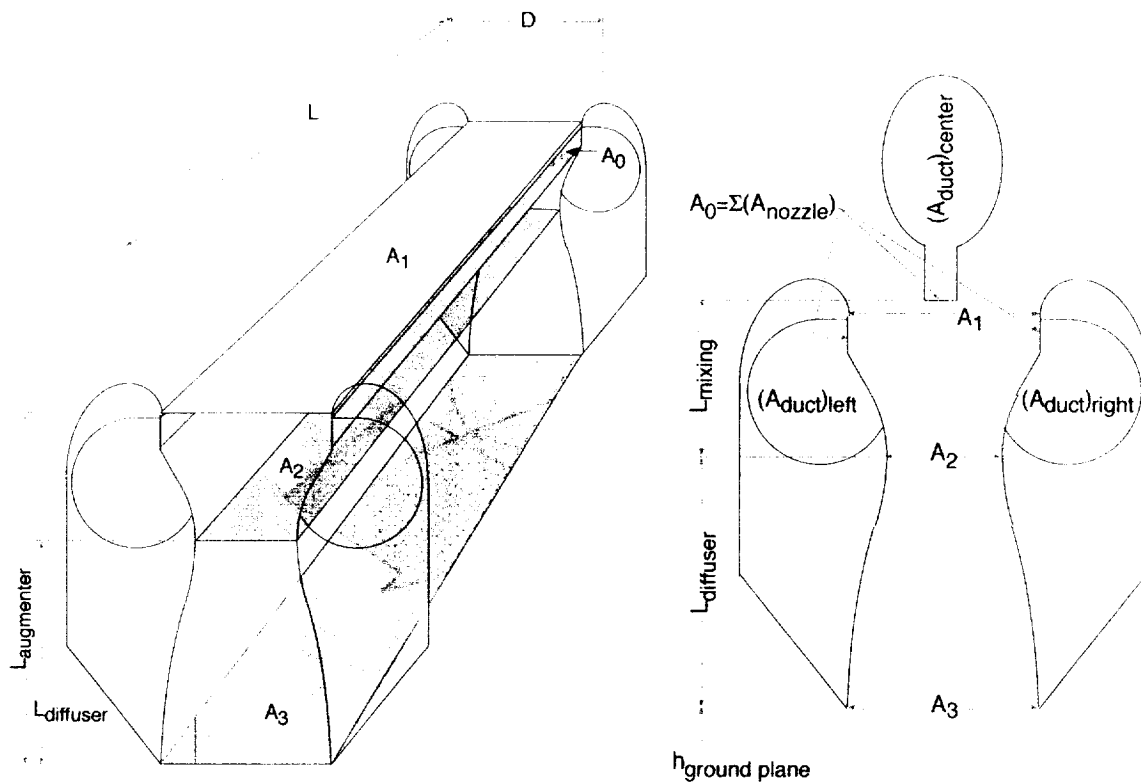


Figure 67. Relative Geometries Play a Significant Role in Determining Augmentation Ratio.

Thrust augmenter efficiency, then, is a function of the following:

- $\frac{r}{D}$

- $\frac{h}{D}$
- $\frac{L}{D}$
- $\frac{A_3}{A_2}$
- $\frac{A_2}{A_0}$
- flow properties
- wing planform geometry (I, I., AR)
- end blowing
- end plating

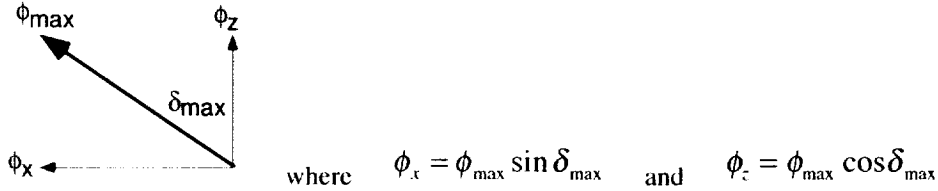
One can define properties of a theoretically efficient augmenter as being rectangular (no taper) with no sweep (perpendicular to the cruise airflow direction), full length end plates, end blowing, and the following:

- $\frac{L}{D} > 3$
- $\frac{r}{D} > 0.1$
- $\frac{h}{D} > 2$
- $AR > 5$
- $\frac{A_2}{A_0}$  large

This particular type of fluidic amplification has the advantage that vertical lift is spread out over the entire wing. The exit flow is relatively cool compared to engine nozzle flow and, therefore, has a lower exhaust footprint than vectored thrust approaches. Engines can be sized closer to cruise requirements as well. Some attitude control can be had by varying augmenter flap settings to produce differential augmentation ratios, but the most practical form of instantaneous control is still judiciously placed puffer pipes.

One big disadvantage of augmenters is that they require a lot of internal plumbing. There is a narrow choice of engines because only certain ranges of fan pressure ratio and thrust will be acceptable for given missions. Exhaust gas ducts are long and, therefore, more lossy. Engine-out cases may be hard to handle in a practical, operational aircraft, and long pressurized internal ducts don't themselves well to damage.

For angling augmenters to provide super/STOL performance, the augmentation ratio will have both horizontal and vertical components.



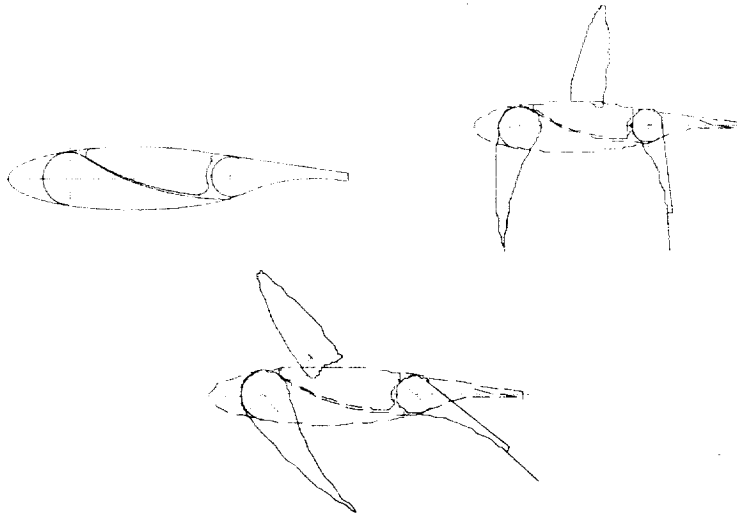
To illustrate, consider the STOL application of augmenters in Table 3 where the first column is flap deflection off horizontal.

**Table 3. Augmenter Flap Deflection Determines Thrust Available for Direct Acceleration.**

$$\delta_{\max} \quad \phi_{\max} \quad \phi_x \quad \phi_z \quad T_x \quad T_z = \phi_x T \quad T_z = \phi_z T$$

90°	1.80	0	1.80	100%	0%	180%
75	1.77	0.46	1.71	100%	46	171
60	1.68	0.84	1.46	100%	84	146
45	1.57	1.11	1.11	100%	111	111
30	1.44	1.25	0.72	100%	125	72
15	1.29	1.25	0.33	100%	125	33

As can be seen, fifteen to thirty degrees of augmenter flap deflection provides maximum horizontal augmentation ratio and, therefore, maximum acceleration in STOL mode.



**Cruise Position**

**Vertical Takeoff Position**

**Transition and/or STOL Position**

Augmenters may be laid out in a variety of orientations, the primary determinant being ease of fitting them within desired aircraft mold lines that are determined by other mission requirements. Figure 68 presents an augmenter arrangement similar to the one used in the North American Aviation/ Rockwell XfV-12A except that augmenters bays are not tapered.

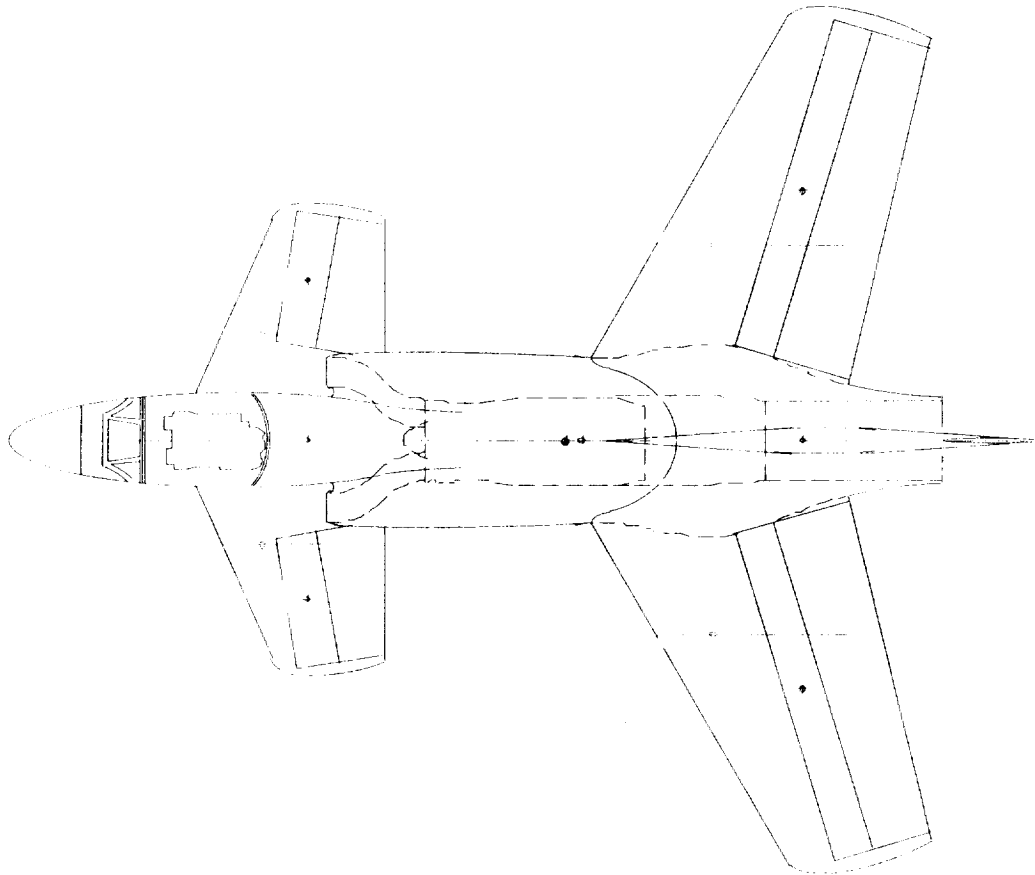


**Figure 68. This Augmenter Layout is Similar to That on the XFV-12A.**

Figure 69 shows an alternative arrangement where augmenters are placed inboard and spanwise adjacent to the engine compartment and consist of several small, rectangular sets of bays and doors with fuselage and nacelle sides providing end plating. A third arrangement is to align augmenters bays chordwise as shown in Figure 70.

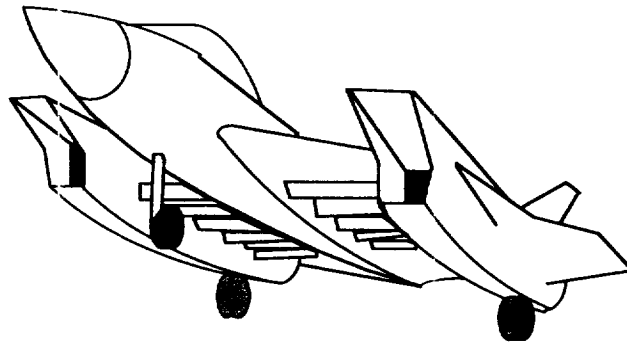


**Figure 69. Augmenter Bays May Be Placed Spanwise Inboard in Small Sets.**

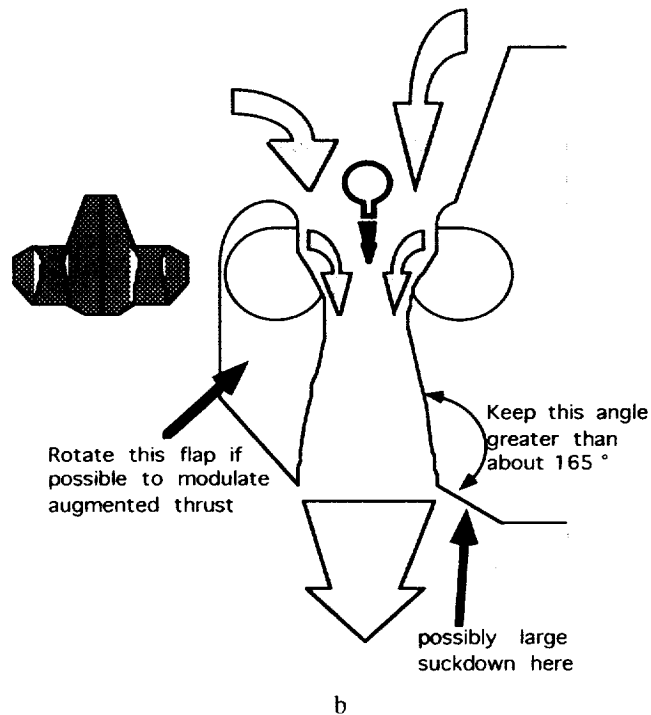
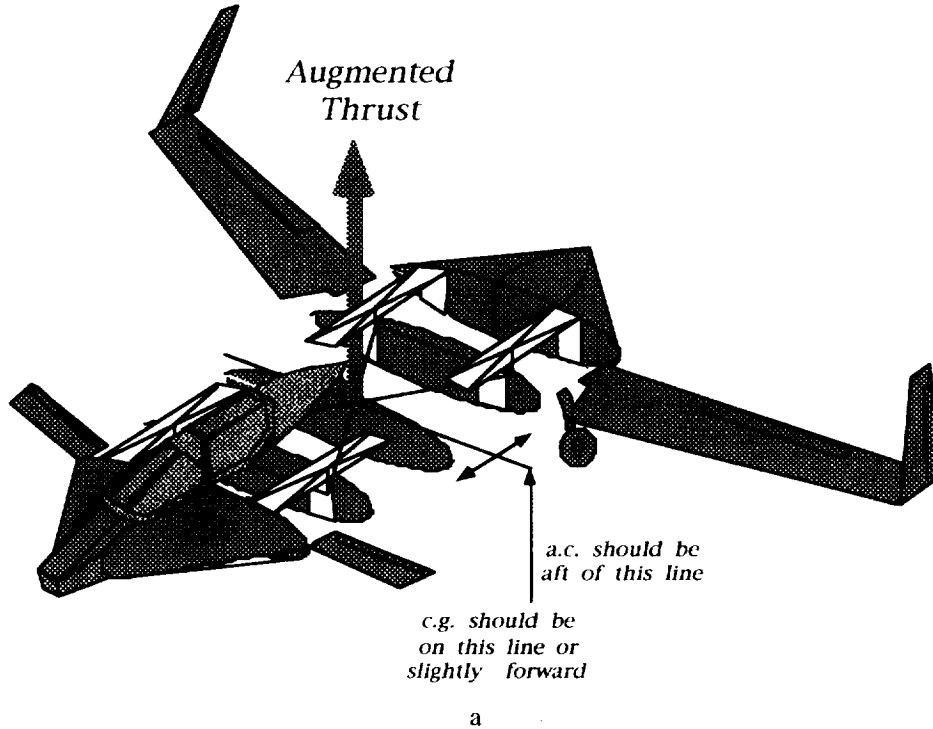


**Figure 70. Augmenter Bays can be Arranged Chordwise as well as Spanwise.**

Regardless of augmeter bay orientation, the underlying principles are the same. Engine exhaust air is routed from the fan and core through ducts to nozzles positioned along each side of each augmeter bay. Coanda effect turns the hot flow along curved flaps and this entrains ambient air. The mixture of ambient air and exhaust air exits the augmeter bay and, hopefully, produces more thrust than the engine would alone if pointed vertically downward.

Begin analysis by defining the entire exhaust gas flow route from engine nozzle to augmeter bay exit at the bottom of the augmeter skirts. Define lengths, angles of turns, and duct cross-sectional shapes and areas. One possible layout is shown in Figures 71 and this will be analyzed here.

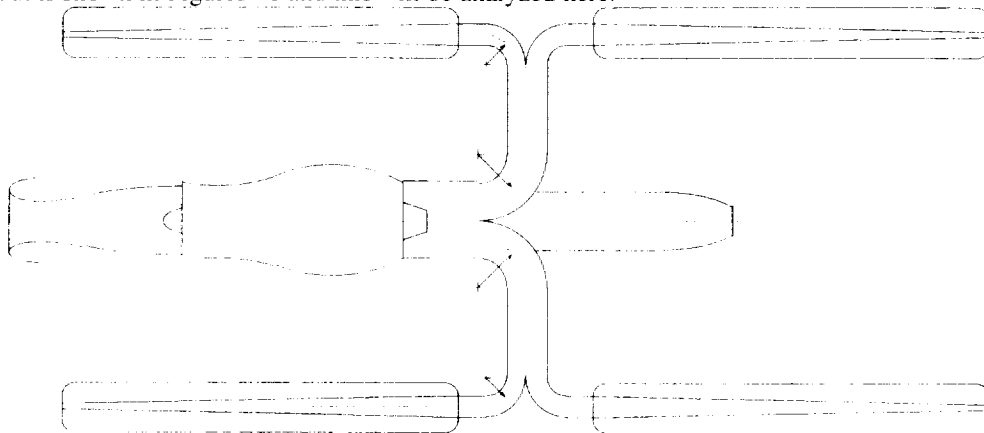


Figure 71a. This Four-Poster Augmeter Arrangement is Practical and Efficient.

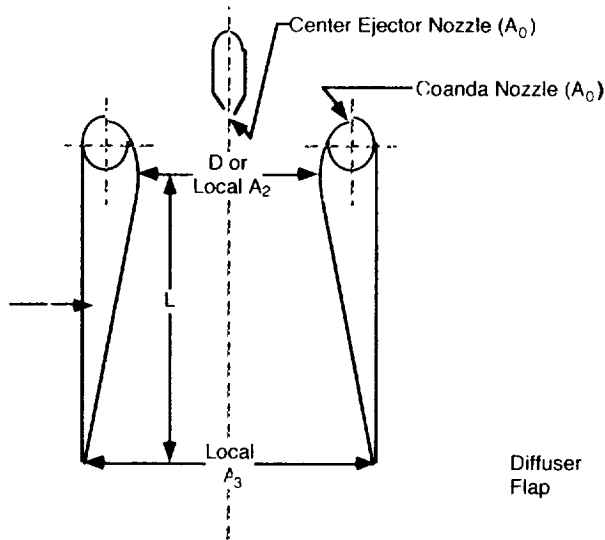


Figure 71b. Cross-Section Geometric Relationships Define Augmeter Performance.

Empirical testing of thrust augmentor configurations has provided a wide range of design parameter cross-plots with which to create conceptual designs. Unfortunately, no substantive design development work has been done since the end of the 1970s on this approach to vertical flight and the current state-of-the-art reflects 1979 technology as shown in Figures 72.

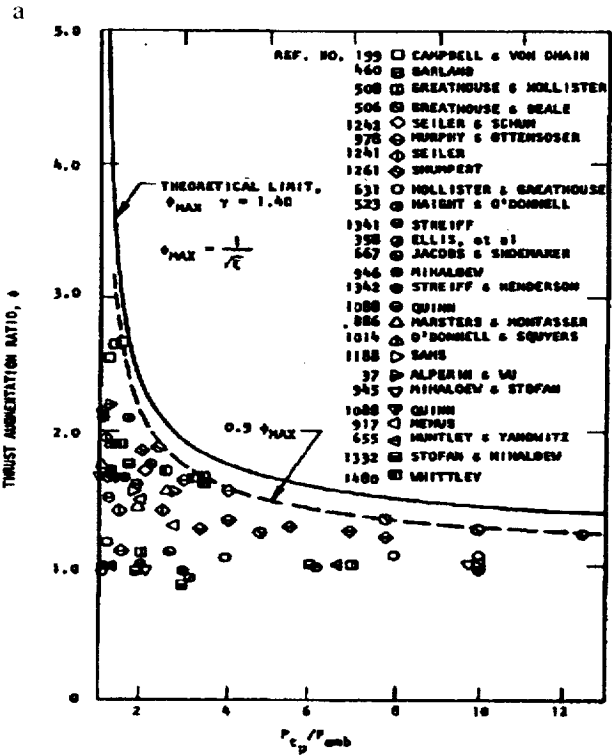
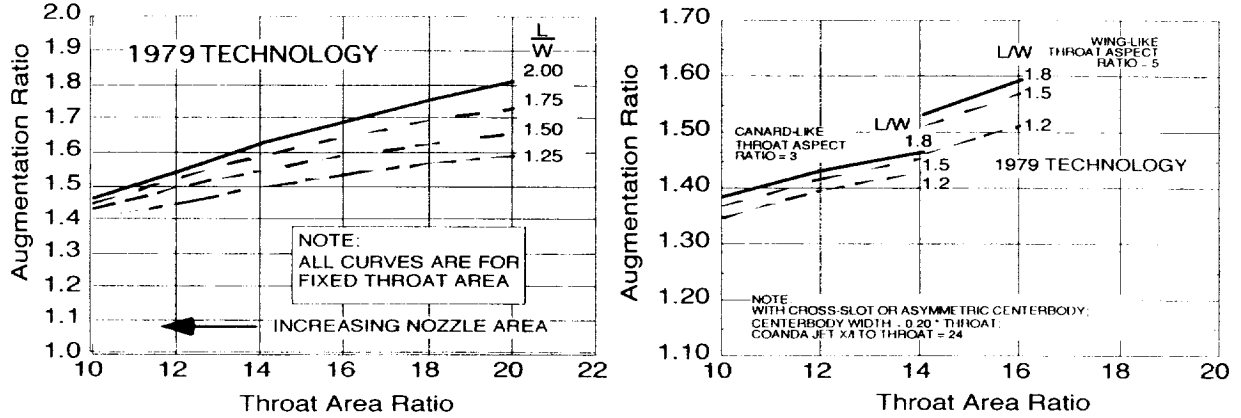


FIGURE 6. SUMMARY OF RECENT THRUST AUGMENTOR TESTING.

Figure 72. 1979 Marked the Final Year for Substantive Augmentor Development.

## **SUMMARY**

The extensive foregoing discussion first centered on the long and colorful history of V/STOL aircraft development and then presented analytical methods which could be applied to parametric analyses of takeoff and landing requirements as well as development of avoid curves in the VTOL flight envelope. Finally, this paper looked at several alternative methods of achieving vertical or super STOL flight.

Little research and development has been done on most of the sixteen methods presented here since the late 1970s and the neglected approaches could benefit from renewed examination in the light of a quarter century of progress in related technologies such as composite structures, engines, electronics, guidance and control algorithms, and the increasing operational database available on uninhabited aerial vehicles. If simplicity is a key criterion, vectored thrust is still the VTOL method of choice but thrust may be vectored using free-wing technology to effectively point the propulsion system/fuselage wherever it's needed. Augmentors and augmenters still look viable on paper and have yet to be demonstrated or operationally fielded. Tilt rotors are under full-scale development in several aircraft and will shortly enter military and then civilian operational environments. Tilt wings look promising, particularly for super STOL operation where a full 90 degree pivot isn't necessary. Finally, stowed rotors weren't discussed but may offer a suitable compromise of long hover time and high cruise speed, particularly if coupled with UAV technologies.

## **Comments on the Appendices**

The following appendices present, first, an alternate takeoff and landing method to the one described in an earlier section. Appendix B presents some augmentor design guidelines compiled from people involved in testing them at North American Aviation/Columbus Aircraft Division in the 1970s.

## REFERENCES

1. Taylor, John W.R., *Helicopters and VTOL Aircraft*, Doubleday & Company, Inc., Garden City New York, 1968.
2. Campbell, John Paul, *Vertical Takeoff and Landing Aircraft*, The Macmillan Company, New York City New York, 1962 (LoFC Number: 62-8553).
3. Symposium on Vertical & Short Take-off and Landing Aircraft, AGARDograph, Part 1, Jun 1960.
4. Shanahan, R.J., compiled by, "Advisory Group for Aerospace Research and Development, Bibliography 2, Second Supplement 1963/64/65, VTOL/STOL AIRCRAFT, 1966."
5. Janes' All the World's Aircraft, various issues.
6. Anderson, Seth B., Historical Survey of Flight-Testing Accidents, ARC-13330, NASA Tech Briefs, NASA Ames.
7. Bright, George, "VJ-101C Supersonic VTOL Program," SAE 650087, International Automotive Engineering Congress, Jan 11-15, Detroit, MI. Jan 11-15, 1965.
8. Driver, Cornelius, & M. Leroy Spearmen, "Stability and Control Characteristics at a Mach Number of 2.01 of a Supersonic VTOL Airplane Model Having a Broad Fuselage and Small Delta Wings, " NASA Technical Memorandum X-441, Feb 1961, 27 pgs.
9. Fuhrman, et al, Systems Analysis Report on USAF Model X-13 Airplane Stabilization System, Ryan Report No 6955-1, 15 Mar 1956.
10. Lovell, Powell M., Jr, Robert H. Kirby, and Charles C. Smith, Jr., "Flight Investigation of the Stability and Control Characteristics of a 0.13-scale Model of the Convair XFY-1 Vertically Rising Airplane During Constant-Altitude Transitions ", NACA RESEARCH MEMORANDUM, TED No. NACA DE 368, May 21, 1953.
11. Rolls, L. Stewart, "Operational Experiences With the X-14A Deflected-Jet VTOL Aircraft," NASA Ames, pp 299-307.
12. Smith, Charles C., Jr, and Powell M. Lovell, Jr., "Vertical Descent and Landing Tests of a 0.13-Scale Model of the Convair XFY-1 Vertically Rising Airplane in Still Air," National Advisory Committee for Aeronautics Research Memorandum, TED No. NACA DE 368, 1954.
13. Stevens, James Hay, compiled by, VTOL Aircraft 1965.
14. Tuttle, D.T., Monthly Progress Report, X-13, Vertical Take-Off Research Airplane (Ryan Model 69), Ryan, 1 Jul 1956.

**APPENDIX A**  
**Alternate Method of Calculating Takeoff and Landing Performance**

**Super STOL Takeoff Distance Equations**

$$(s_{ground})_{takeoff} = \frac{13.08 \frac{W}{S_{ref}}}{\frac{(C_{L_{max}})_{power\ off}}{\left(\frac{V_{takeoff}}{V_{stall}}\right)^2} \left(\frac{T}{W} - 0.1\right)}$$

**Super STOL Landing Distance Equations**

Air Distance Over a Fifty Foot Obstacle (flight path along straight line at constant velocity)

$$\sin \theta = \frac{C_{D_r}}{C_L} - \frac{T}{W}$$

$$s_{air} = \frac{50}{\sin \theta}$$

$$K = \frac{V}{(V_{stall})_{power\ off}}$$

Rate of Descent =  $1.68889V_{spec} K \sin \theta$

Ground Roll Distance without Brakes (velocity interval from  $V$  to  $V_{brake}$  with retarding forces drag and unbraked friction where  $(C_{D_r})_{taxi} > \mu C_L$ )

$$P_1 = \frac{\left[ \sigma (C_{D_r})_{taxi} - \mu (C_L)_{taxi} \right]}{295 \mu \frac{W}{S_{ref}}}$$

$$(s_{ground})_{no\ brakes} = \frac{0.0443}{\mu\sqrt{P_1}} \ln\left(\frac{1 + P_1V^2}{1 + P_1V_{braking}^2}\right)$$

$$(t_{ground})_{no\ brakes} = \frac{0.0523}{\mu\sqrt{P_1}} \left[ \text{Tan}^{-1}(V\sqrt{P_1}) - \text{Tan}^{-1}(V_{braking}\sqrt{P_1}) \right]$$

Ground Roll Distance with Brakes (velocity interval from  $V_{brake}$  to  $V_{reverse\ thrust}$  with full brakes applied over time interval)

$$P_2 = \frac{-\sigma(C_{D_r} - \mu_{braking}C_{L_r})}{295\mu_{braking} \frac{W}{S_{ref}}}$$

$$(s_{ground})_{braking} = \frac{0.0443}{\mu_{braking}P_2} \ln\left(\frac{1 - P_2V^2}{1 - P_2V_{braking}^2}\right)$$

$$(t_{ground})_{braking} = \frac{0.0262}{\mu_{braking}\sqrt{P_2}} \ln\left[\frac{1 + (V_{braking} - V_{reverse\ thrust})\sqrt{P_2} - P_2V_{braking}V_{reverse\ thrust}}{1 - (V_{braking} - V_{reverse\ thrust})\sqrt{P_2} - P_2V_{braking}V_{reverse\ thrust}}\right]$$

Ground Roll Distance with Brakes and Reverse Thrust (velocity interval from  $V_{reverse\ thrust}$  to 0 with reverse thrust decreasing linearly with velocity)

$$P_3 = \mu_{braking} + \frac{T_{reverse}}{W}$$

$$P_4 = \frac{K_{reverse\ thrust}}{W}$$

$$P_5 = \sqrt{P_4^2 + 4\mu_{braking}P_2P_3}$$

$$(s_{ground})_{reverse\ thrust} = \frac{0.0443}{\mu_{braking}P_2} \left\{ \frac{P_4}{P_5} \ln\left[\frac{2P_3 + (P_4 + P_5)V_{reverse\ thrust}}{2P_3 + (P_4 - P_5)V_{reverse\ thrust}}\right] - \ln\left[1 + \frac{P_4V_{reverse\ thrust} - \mu_{braking}P_2V_{reverse\ thrust}^2}{P_3}\right] \right\}$$

Other Equations

$$\gamma = 0.0523 = \tan^{-1} \left[ \frac{V\sqrt{P_1} - V_{braking}\sqrt{P_1}}{1 + P_1 V V_{braking}} \right]$$

$$\frac{T\mu\sqrt{P_1}}{\gamma} = \tan^{-1}(V\sqrt{P_1}) - \tan^{-1}(V_{braking}\sqrt{P_1})$$

$$(1 + P_1 V V_{braking}) \tan \gamma = V\sqrt{P_1} - V_{braking}\sqrt{P_1}$$

$$(P_1 V V_{braking}) \tan \gamma + V_{braking}\sqrt{P_1} = V\sqrt{P_1} - \tan \gamma$$

$$V_{braking} = \frac{V\sqrt{P_1} - \tan \gamma}{P_1 V \tan \gamma + \sqrt{P_1}}$$

$$\tan^{-1}(V\sqrt{P_1}) - \gamma = \tan^{-1}(V_{braking}\sqrt{P_1})$$

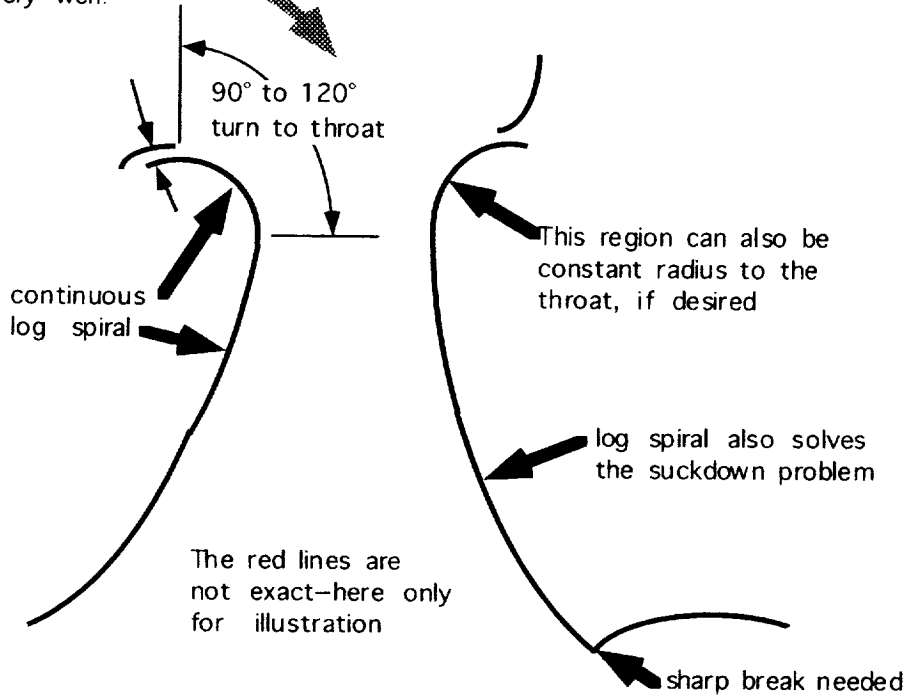
$$V_{braking}\sqrt{P_1} = \tan \left[ \tan^{-1}(V\sqrt{P_1}) - \gamma \right]$$

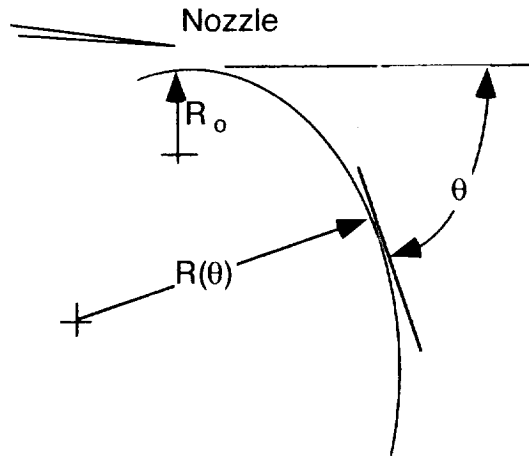
$$V_{braking}\sqrt{P_1} = \frac{V\sqrt{P_1} - \tan \gamma}{1 + V\sqrt{P_1} \tan \gamma}$$

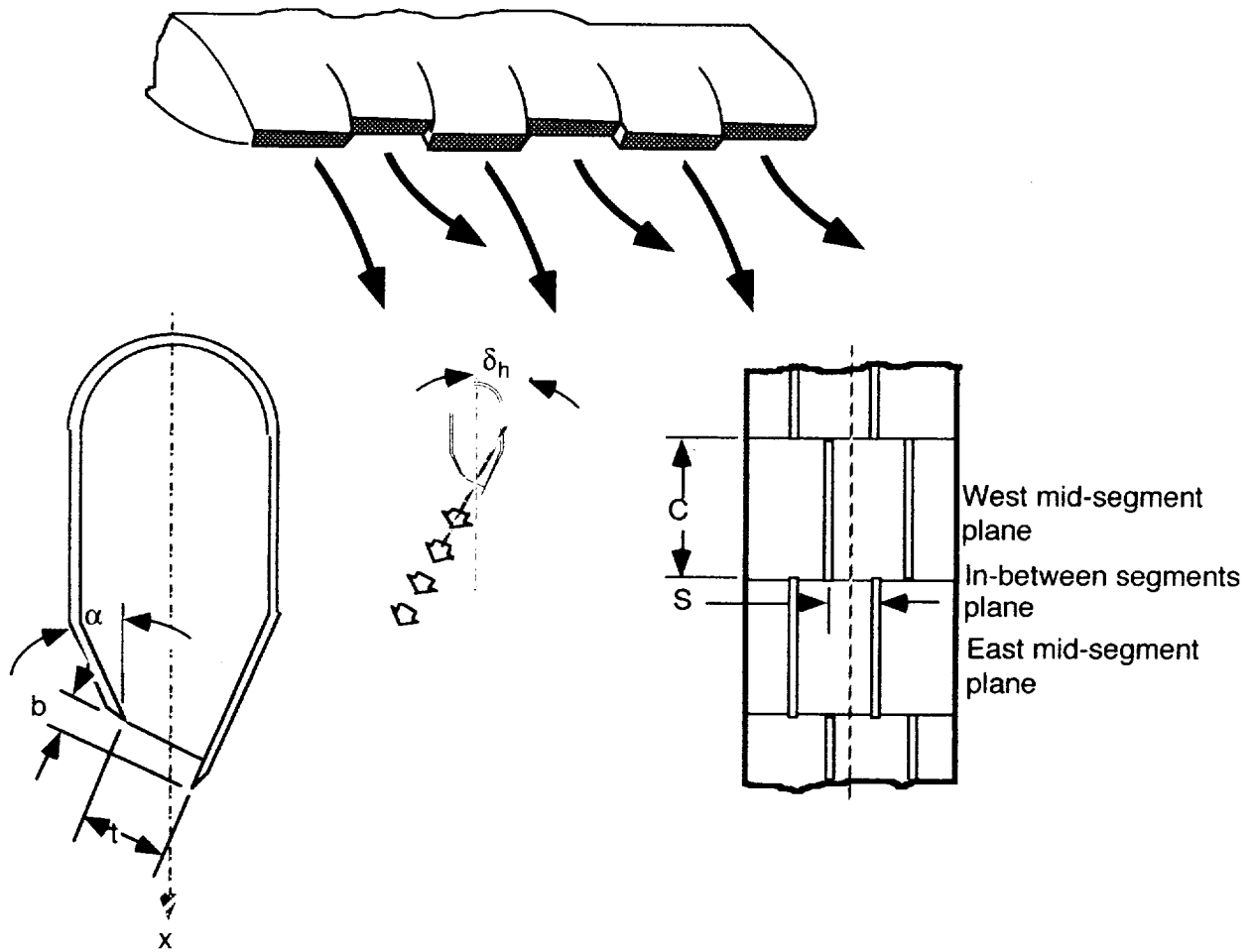
$$V_{braking} = \frac{V\sqrt{P_1} - \tan \gamma}{\sqrt{P_1} + V\sqrt{P_1} \tan \gamma}$$

### APPENDIX B Conceptual Design Guidelines

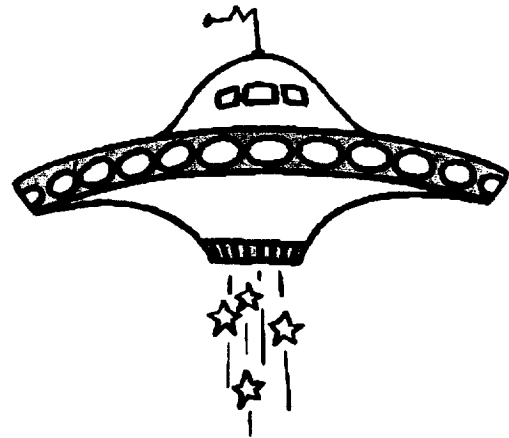
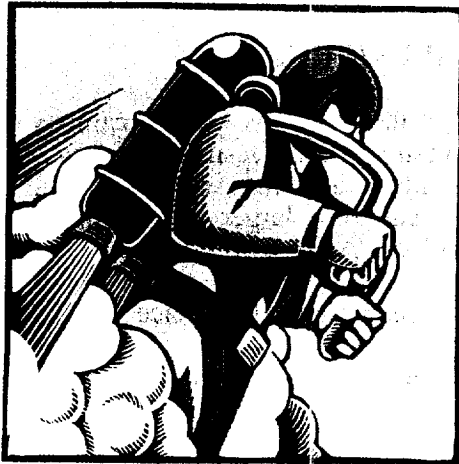
We did successfully test flaps like this. They worked very well!







# Feasibility of Personal Air Vehicles



performed for

Mark D. Moore  
PERSONAL AIR VEHICLE EXPLORATION PROJECT LEADER  
Systems Analysis Branch  
NASA/Langley Research Center

by

David W. Hall, P.E.  
Research Associate Professor  
California Polytechnic State University  
Aerospace Engineering Department  
San Luis Obispo, California

on

March 26, 2002

## FEASIBILITY OF PERSONAL AIR VEHICLES

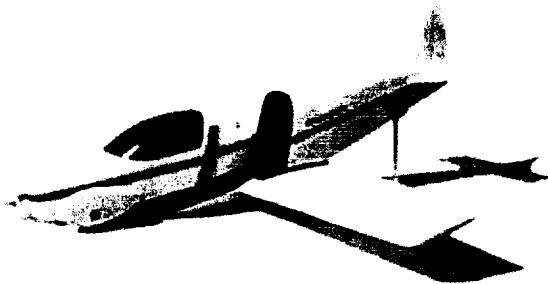
Students in the aerospace engineering department at the San Luis Obispo campus of the California Polytechnic State University (Cal Poly/SLO) investigated the feasibility of four types of personal air vehicle (PAV) for NASA/Langley Research Center's Systems Analysis Branch under the Personal Air Vehicle Exploration (PAVE) project. As part of a larger team of universities, Government organizations, and industry, Cal Poly examined five PAVE options:

- Conventional TakeOff and Landing (CTOL), single-mode, four place;
- Conventional TakeOff and Landing (CTOL), dual-mode, four place;
- Short TakeOff and Landing (STOL), single-mode, four place;
- Short TakeOff and Landing (STOL), dual-mode, four place; and
- Vertical TakeOff and Landing (VTOL), single-mode, four place.

Work began in late summer 2001 with a small team of undergraduate students, most of whom had not yet taken Cal Poly/SLO's award-winning senior aircraft design sequence. This report will present highlights of their work and then discuss two other intriguing options for PAVs.

### Historical Approaches to PAVs

While students acclimated themselves to potential PAV technologies, faculty examined the colorful history of PAVs in order to help structure student work. The resulting white paper on personal air vehicles appears in Appendix A. Approaches to PAV configurations can take one of several tacks, all of which have been either proposed or attempted in the past. Beginning the discussion of the most promising approaches, not in any particular order, is Roger Williamson's *Roadrunner*.



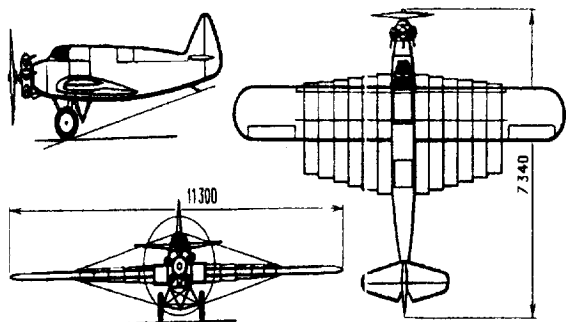
#### Removable Tail on the Roadrunner

- Easy Roadability
- Road travel between different airports a problem
- Possible to tow the tail
- Ruled unfeasible by Cal Poly at the present time

Figure 1. The Roadrunner is a Novel Dual-Model PAV.

Of all the dual mode approaches, this appears the most simple. The RK of the mid-twentieth century is a partial solution to wing stowage as is extreme variability in wing sweep. Moller's

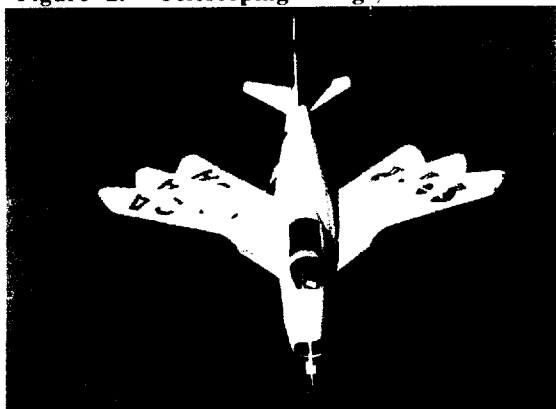
lifelong work in dual mode PAVs represents another approach but there are many practical engineering problems to be solved before it can be fielded to the general public, not the least of which is cost.



**Telescoping Wing on the RK**

- Easy Storage for NHTSA defined car lane width
- Structure Problems

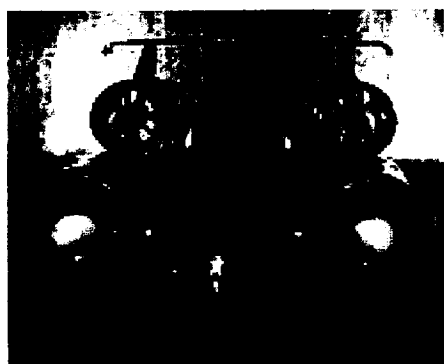
**Figure 2. Telescoping Wings, as on the RK, Help PAVs Meet Highway Lane Width Requirements.**



**“Switchblade” Wings on the Bell X-5**

- Easy Storage for NHTSA roadways
- Leads to a longer vehicle
- Possible to combine with telescoping aspect of wing

**Figure 3. Another Wing-Stowage Approach Would Be Variable Sweep.**



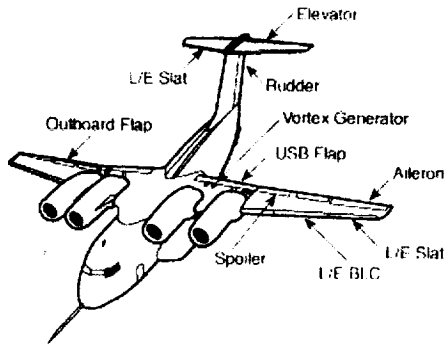
**Ducted Fans shown on the Moller M400**

- Saves weight
- Horizontal Flight Drag from large nacelles
- Easily rotated for vertical and horizontal flight

**Figure 4. Moller’s Ducted Fan Approach Promises Highway Compactness and Acceptable In-Flight Performance.**

The next set of solutions which show potential deal with aerodynamic/airframe/engine integration. In order to produce large values of thrust-to-weight for extremely short takeoff, engines and wings

must be carefully integrated to maximize efficiency. One historically successful approach has been upper surface blowing (USB), but this has never been applied to PAVs and does not solve the roadability challenge necessary for dual mode operation.



### Upper Surface Blowing on the ASKA

- Short Takeoff and Landing
- Induced moments on the wing increase induced drag

Figure 5. For Dedicated Single-Mode PAVs, USB Provides Acceptable Short Takeoff Performance.

One approach to airframe/aerodynamic integration which has applicability to PAV mission is to make the fuselage a lifting body. Moller has done this to some extent, but an extreme example is the Burnelli CBY-3. Propulsion must also be integrated and the ValueJet presents an example of well thought out airframe/propulsion integration.

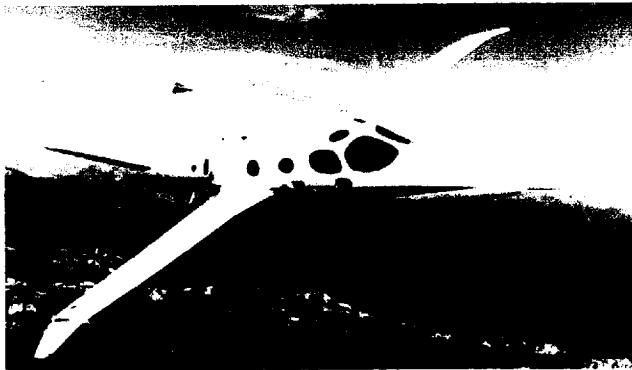


Burnelli CBY-3 Loadmaster

### Burnelli Lifting Body on the CBY-3

- Shorter wings for roadability
- Small wings have bad stall characteristics
- Tough engine placement
- Leads to a smaller vehicle
- Basis for Cal Poly's conceptual designs
- Feasible for NHTSA 102" lane widths and parking spaces

Figure 6. Integrating Lifting Surfaces with the Fuselage Theoretically Improves Airframe Efficiency.



### Body Integrated Engines on the V-Jet II

- Less Structure in Wings
- Vehicle doesn't have to be as wide
- Cleaner Design with smooth lines
- Lighter

Figure 7. Integrating Propulsion with the Fuselage Theoretically Improves Airframe Efficiency.

## Research Approach

Once students had examined historical work and determined promising alternatives, they next defined the design domains applicable to the five PAVs assigned to them. A standard grid of thrust-to-weight ratio and wing loading presents the domains for the five types of vehicle starting with the conventional takeoff and landing PAV. Range is 400 nautical miles (n.mi.), takeoff and landing distance is 2,000 feet, and Part 23 of the Federal Aviation Regulations (FARs) presents stall requirements. Table 1 cites design requirements for each PAV type assigned to Cal Poly.

Table 1. Cal Poly Examined Five Types of PAV.

ITEM	CTOL	STOL	SSTOL	VTOL
Number of Passengers	4	4	4	4
Range in n.mi.	400	400	400	400
Takeoff and Landing Distance in ft.	3,000	1,000	500	250

### Constraint Plots

These vehicles most closely approximate the retractable gear, four place general aviation category whose takeoff gross weights (TOGWs) fall in the range 2,200 # to 2,650 #, wing loadings are on the order of 15 to 20 psf and power-to-weight ratios are on the order of 0.07 to 0.09 HP/# (0.13 to 0.17 #/# thrust-to-weight ratio).

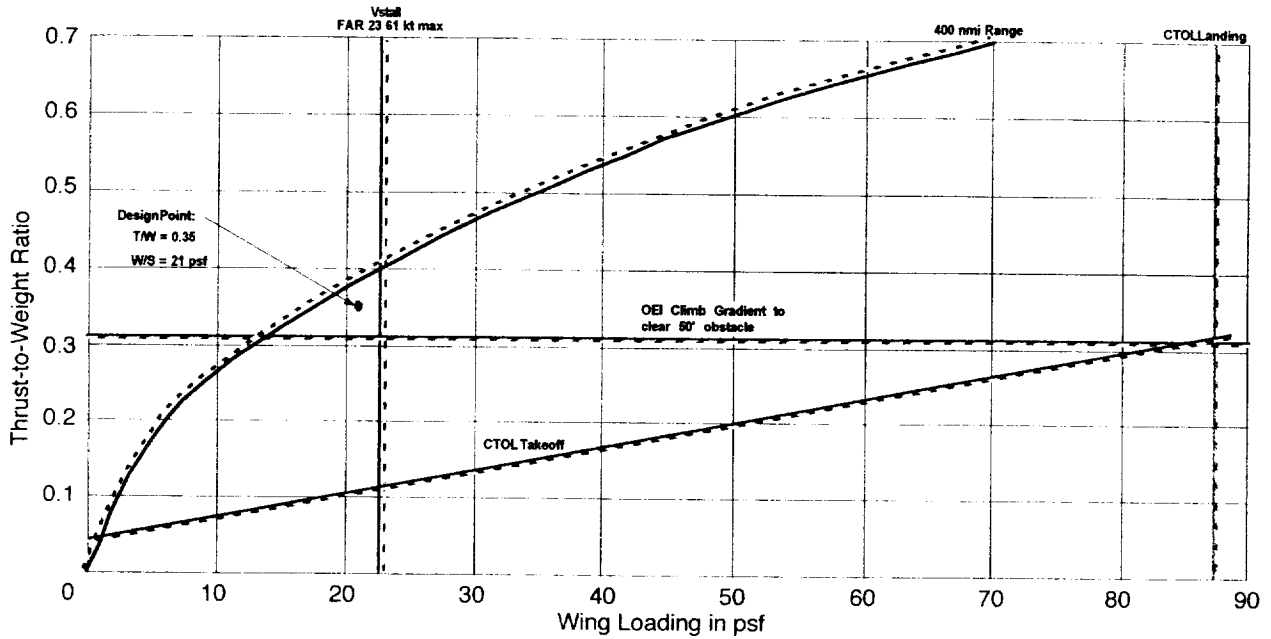


Figure 8. The Design Domain for a CTOL PAV is Small but Finite.

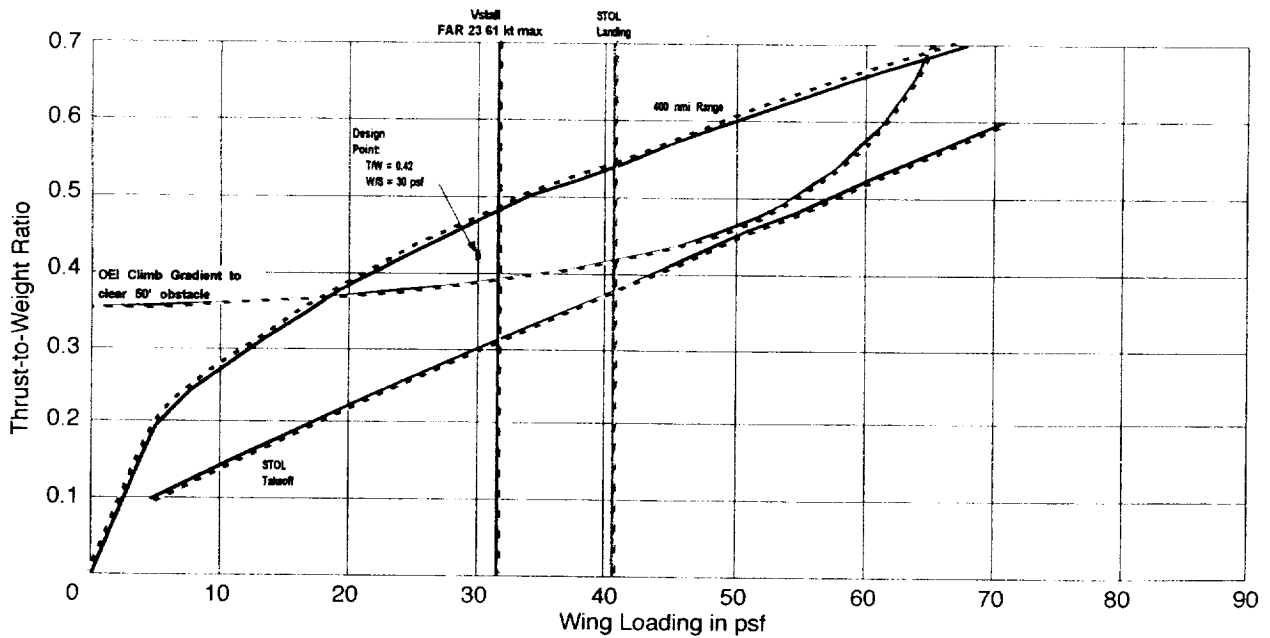


Figure 9. The Design Domain for a STOL PAV is Small but Finite.

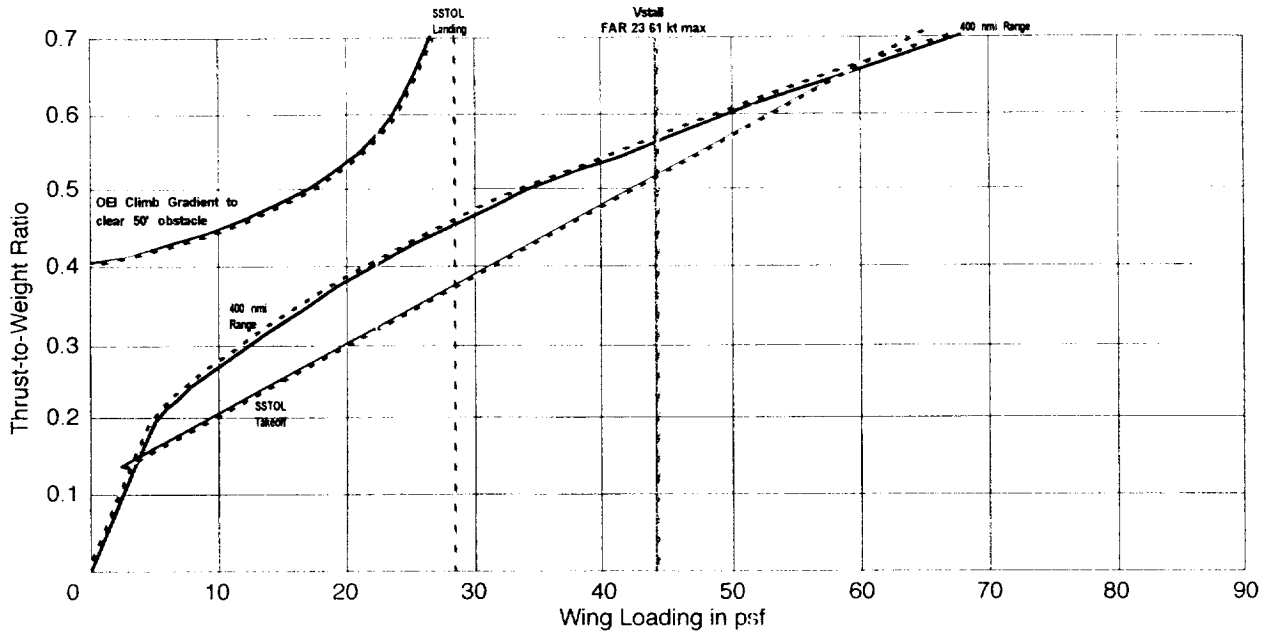


Figure 10. The Design Domain for a SSTOL PAV is Nonexistent.

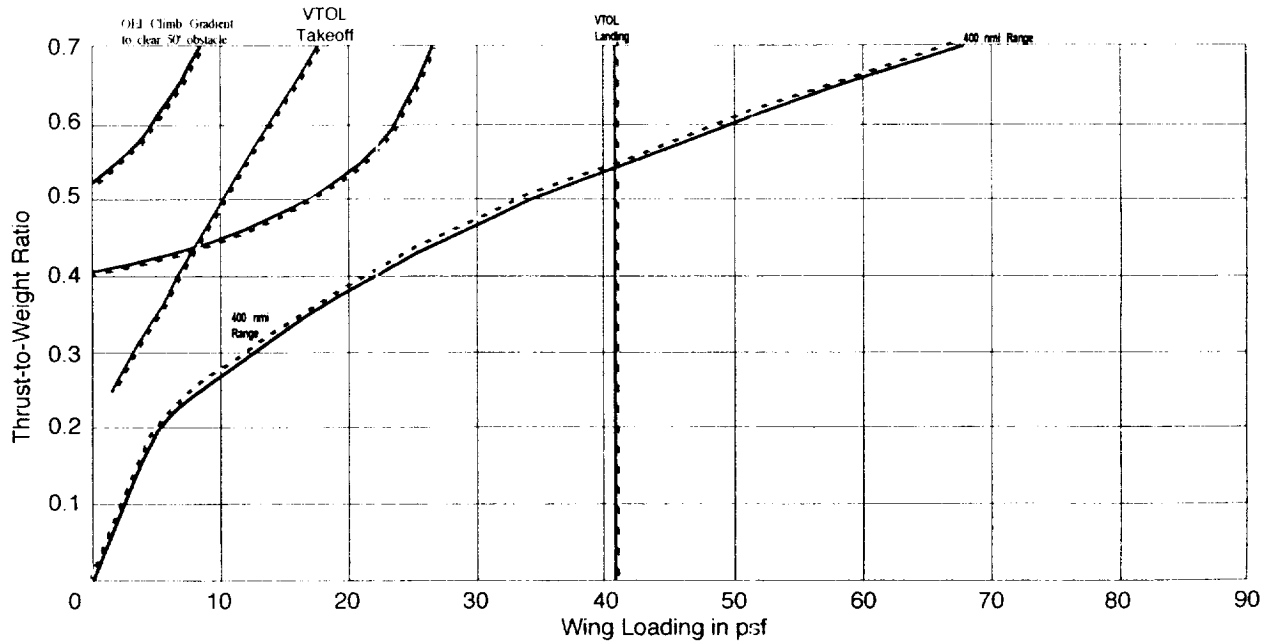


Figure 11. The Design Domain for a VTOL PAV is Nonexistent.

The preceding plots consider only brute force approaches to powered lift. If circulation control can be combined with powered lift to relieve the amount of lift coefficient the wing must develop, then the design domains open up for shorter takeoff and landing distances.

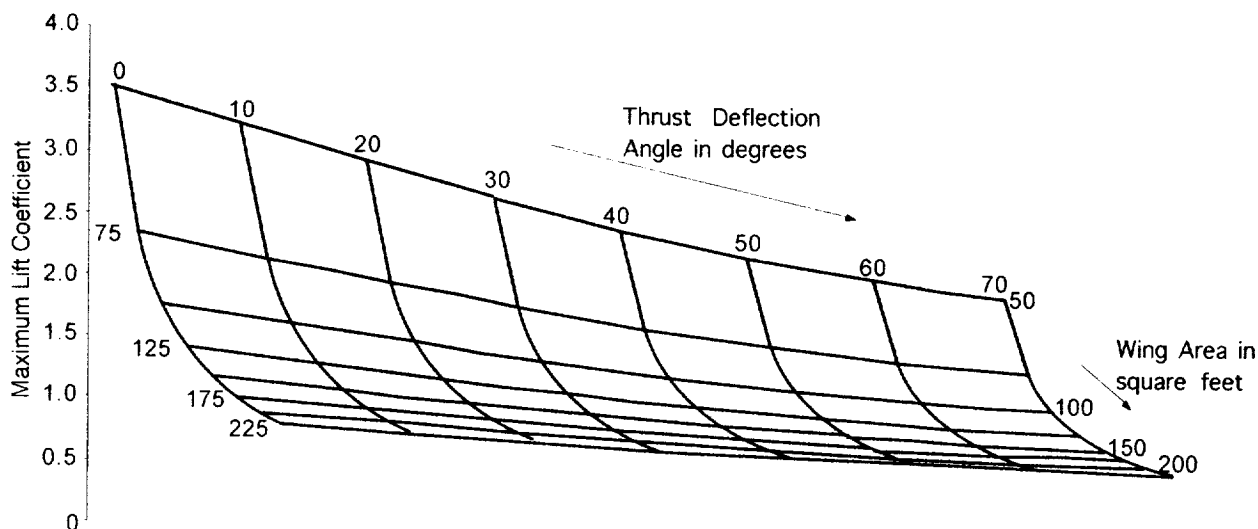


Figure 12. Thrust Deflection Offsets the Amount of Work the Wing Must Do.

Given a combination of thrust deflection and wing lift, the SSTOL approach becomes feasible but the VTOL approach does not. reducing takeoff and landing distance to zero (pure VTOL) actually simplifies the problem.

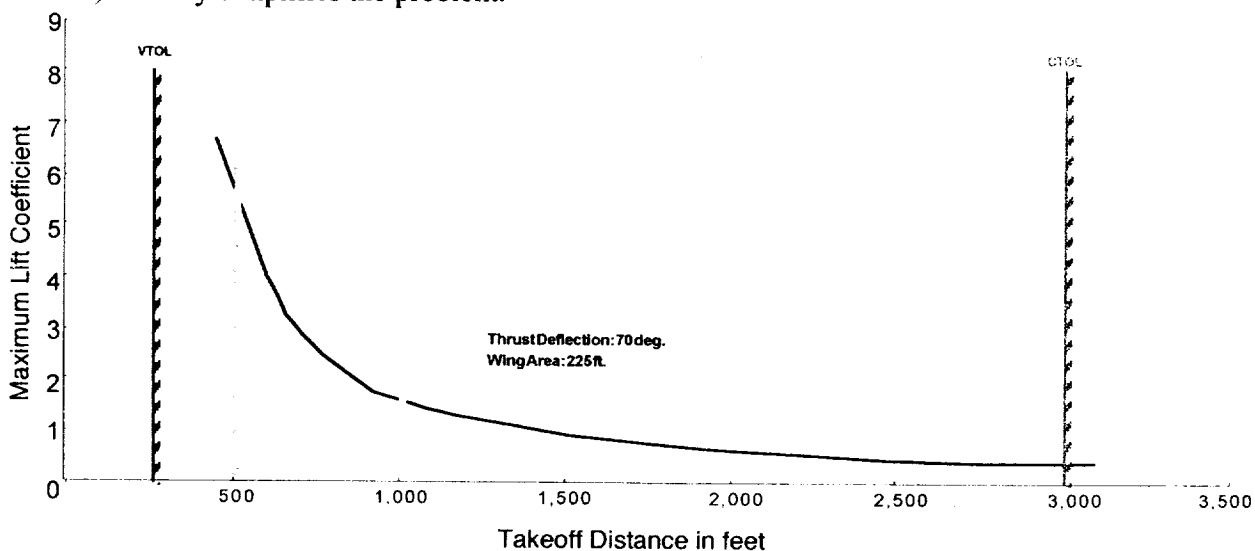


Figure 13. Thrust Deflection Is Necessary to Attain SSTOL Performance.

**Generic Load Diagram**

All of the PAVs examined here were designed to a consistent set of regulatory requirements. For instance, each used the same basic loads diagram.

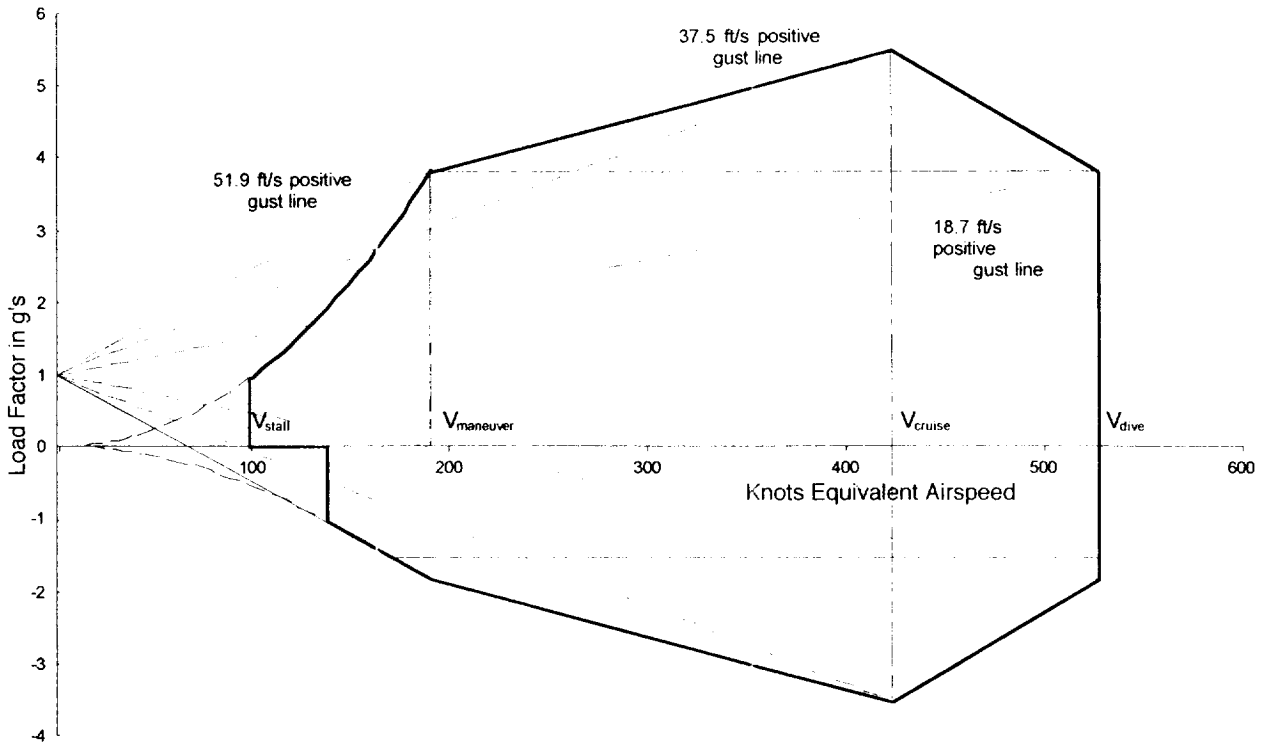


Figure 14. All PAVs Examined in This Study Used the Same Loads Diagram for Sizing Structure.

### Configurations

Students used SolidWorks and Ashlar Vellum Solids CAD applications to create three-dimensional solid models of each configuration and then later transferred these to Rapid Aircraft Modeler (RAM) before sending them to Langley. Each vehicle shown was dual mode unless otherwise specified and it's interesting to compare weight to what was cited earlier for existing four place general aviation aircraft. Of interest, too, is that all of these configurations are multiengine.

## CTOL Dual-Single Mode General Arrangement

- **Wingspan**            20 ft
- **Overall length**    10 ft
- **Roadable Width** 6.5 ft
- **TOGW**                3500 lb

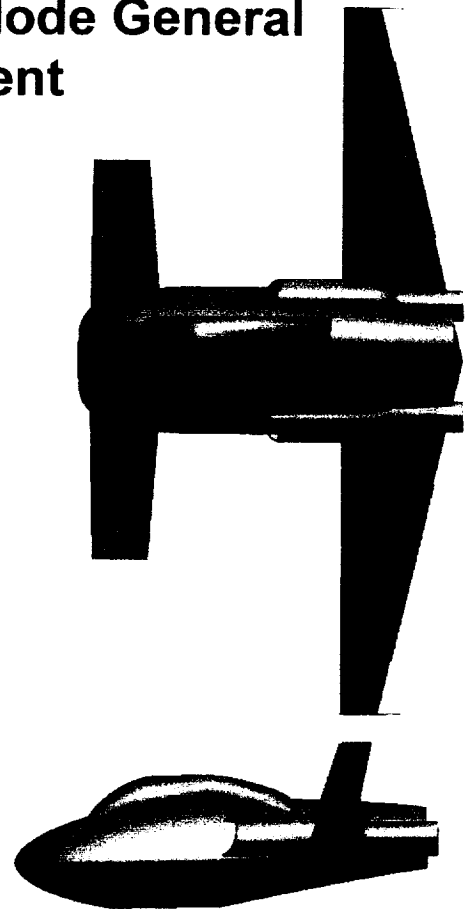
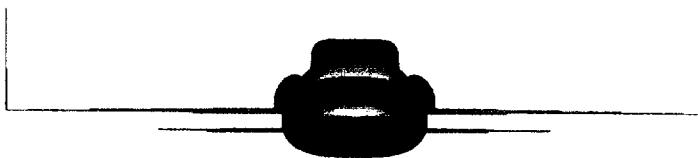
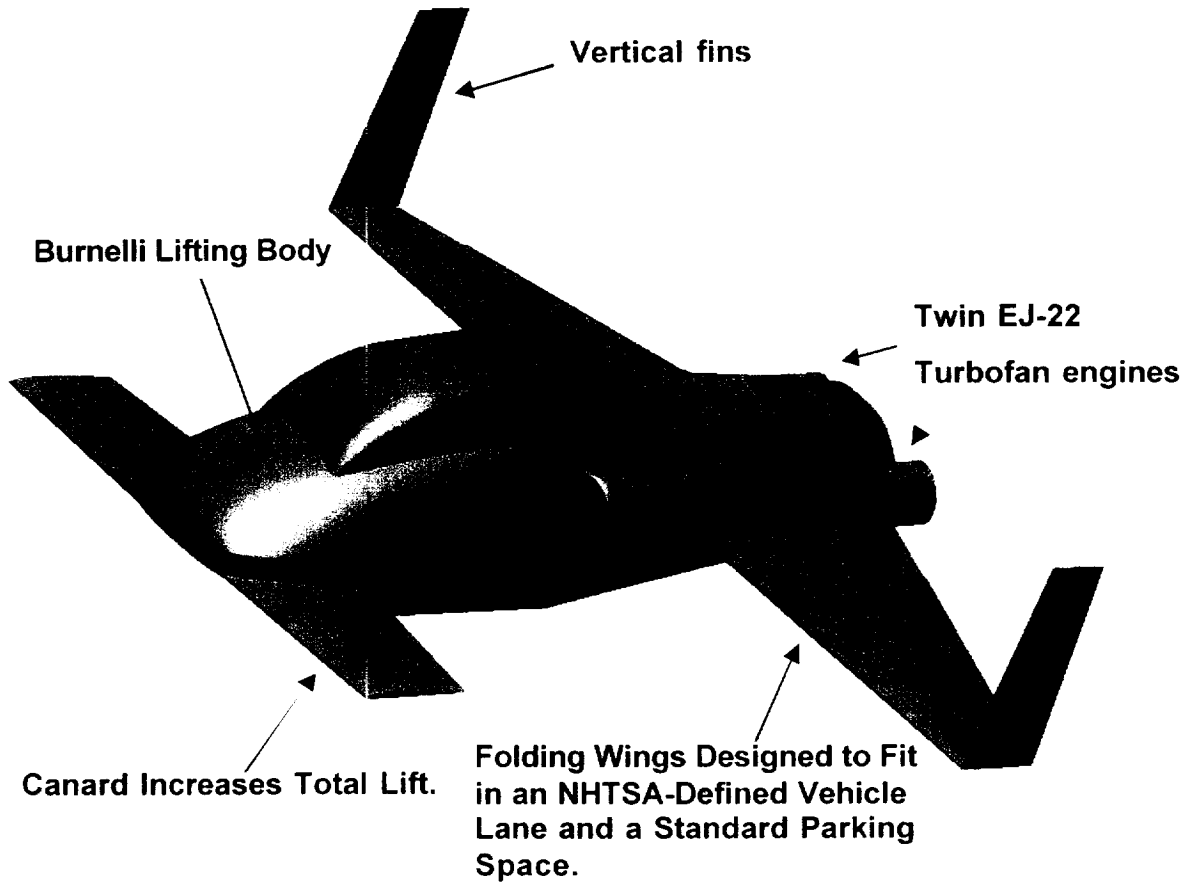
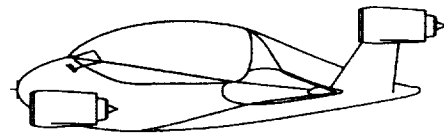
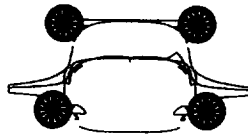
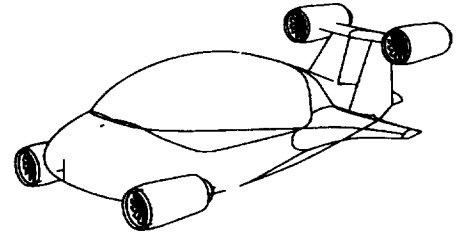
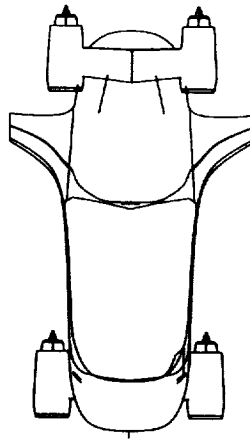


Figure 15a. The CTOL PAV is a Canard Layout with Foldable Surfaces.



**Figure 15b. The CTOL PAV is a Canard Layout with Foldable Surfaces.**

**Length – 19.15 ft**  
**Span – 10.83 ft**  
**Height – 5.71 ft**  
**TOGW – 3000 lbs**



**Figure 16a. The STOL/SSTOL PAV is a Canard Layout with Foldable Surfaces.**

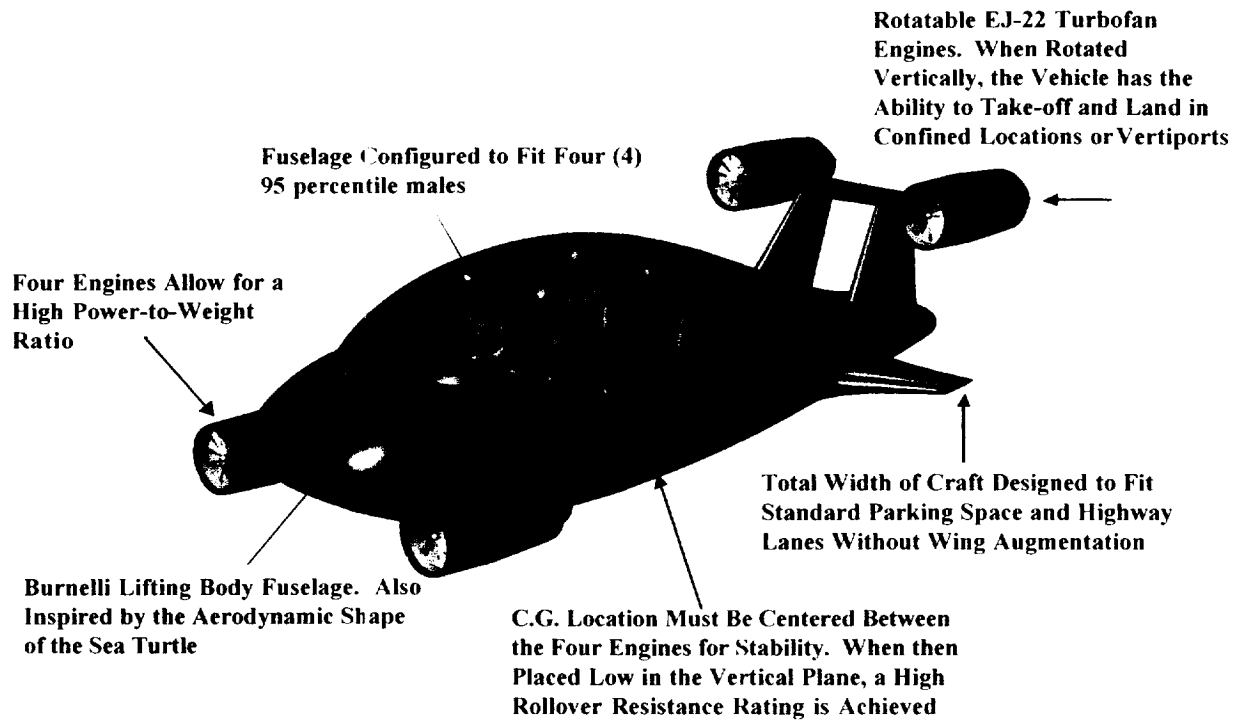
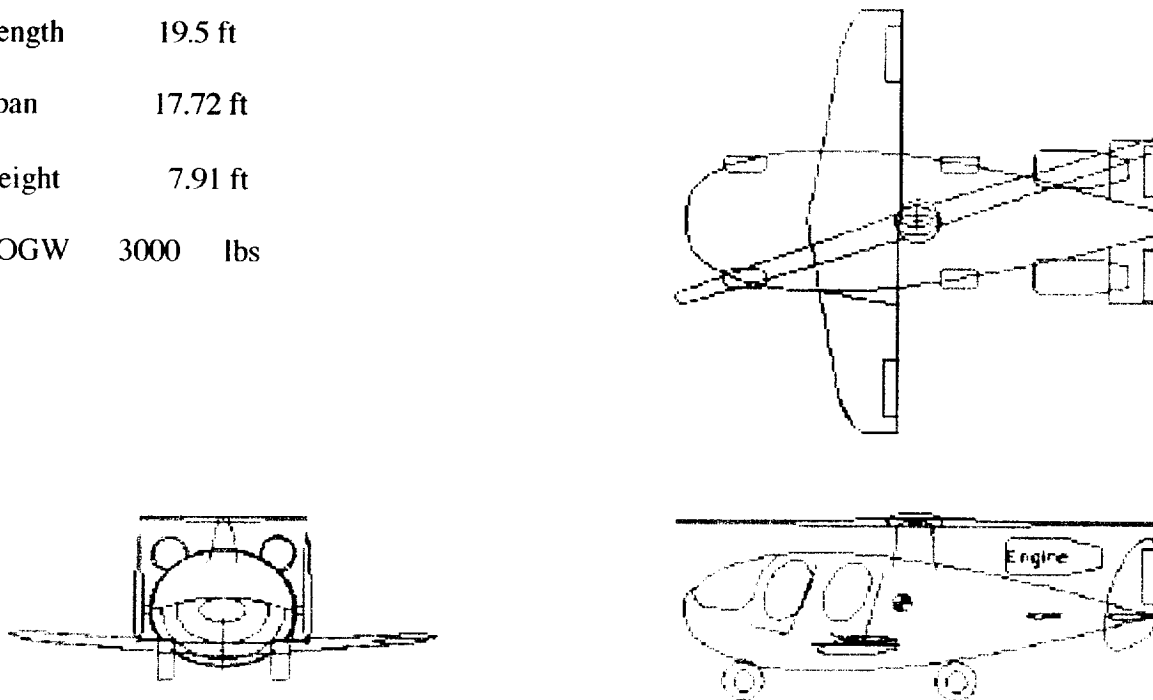
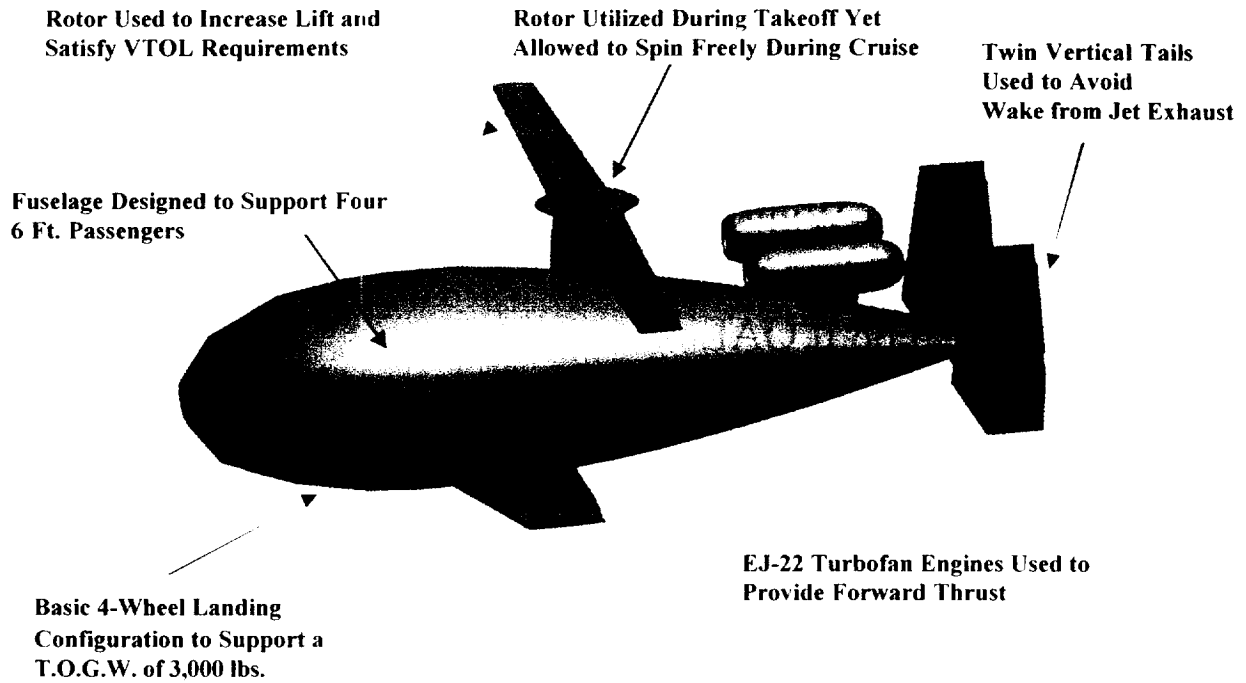


Figure 16b. The STOL/SSTOL PAV is a Canard Layout with Foldable Surfaces.

Length 19.5 ft  
Span 17.72 ft  
Height 7.91 ft  
TOGW 3000 lbs



**Figure 17a. The VTOL PAV is a Gyrocopter Layout with Foldable Surfaces.**



**Figure 17b. The VTOL PAV is a Gyrocopter Layout with Foldable Surfaces.**

#### **Additional Configuration Approaches**

While this work progressed, the applicability of previous studies performed by Battelle Columbus Laboratories (BCL) for NASA's Langley and Dryden became evident. Four previous studies of free-wing and free-wing/free-stabilizer general aviation aircraft were performed during

the 1970s by BCL staff and showed the feasibility of this interesting approach to improving safety and ride quality. With application to PAV missions, the wing hinge pin joint could be modified to act as a Grumman-style wing fold for a potential roadable free-wing, as shown below.

**Foldable Free-Wing Two Place  
Roadable Aircraft**

**25.88 ft OAL**

**25.5 Wingspan**

**1,539# TOGW**

**Theoretical Free-Wing  
Groundwork Laid in  
CR1523, CR2046,  
CR2946, CR3135**

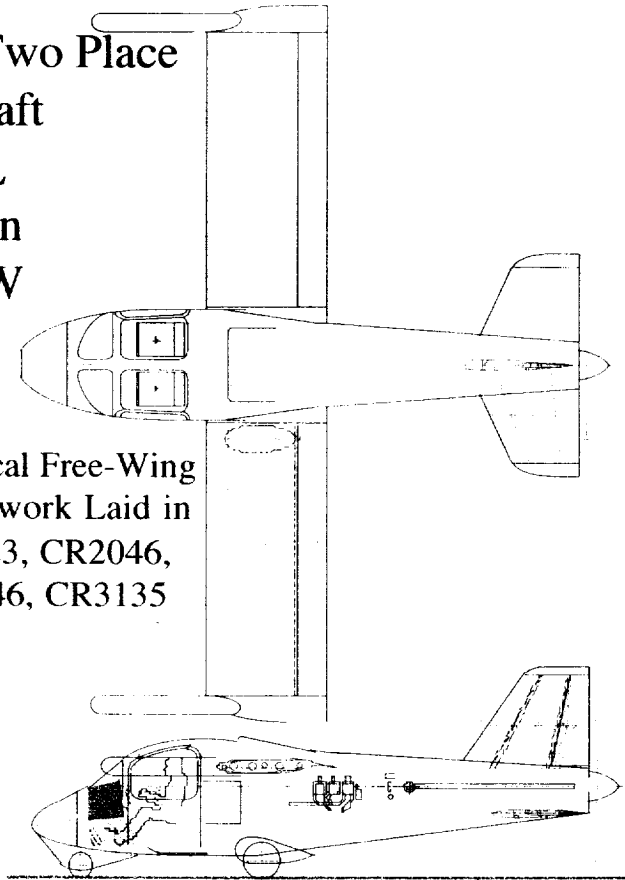


**Figure 18. A Free-Wing PAV Would Exhibit Airliner Ride Quality.**  
Several months of approaching the design of personal air vehicles (PAVs) from the

perspective of an aerospace industry configurator produced extensions of the current state-of-the-art in aircraft which were heavy, expensive, and not truly innovative. Vehicles were large, fitted with aircraft turbine engines or aviation-rated reciprocating engines and produced aviation-rated amounts of thrust or power to fly conventionally. In short, a pedestrian approach produced pedestrian results, no transportation-related pun intended. But what if the answer lies at the end of another thought train?

Consider the desired end result which is a small personal air vehicle to replace, augment, or supplement other forms of personal transportation to travel from Point A to Point B. Driving 200 miles from San Luis Obispo on U.S. 101 to Long Beach on a weekday evening produced reinforcement that the vast majority of cars on the freeway (currently the quickest route between Points A and B) were carrying one person—the driver. This has been a typical observation on most urban freeways in a variety of locales and appears that it can be safely generalized to the country at large.

So the logical place to start this creative project is with what serves the public best and that's a quicker way from A to B tailored for the most frequent number of occupants—one. What other features should this vehicle have?

- It should be affordable, as in the price range of compact and alternate fuel automobiles. That puts a cap of around \$25,000 on list price.
- It should be safe and quiet enough to operate in neighborhoods with low ambient noise levels.
- It should be lightweight with the majority of the weight being payload (occupant, baggage, fuel).
- It should be simple, reliable, and rugged.
- It should be comfortable, as small as possible, and aesthetically pleasing.

Of these five sets of features, the first two will be the most difficult to quantify.

**Low Cost.** Novel manufacturing methods and materials will assist in keeping PAV first cost down to levels comparable with current personal transportation. Instead of building these vehicles like automobiles out of steel or aluminum or like aircraft out of aluminum or composite layups, they could be manufactured like plastic model aircraft—in halves glued at major seams—out of high impact plastics. Parts counts could be kept low by injection molding subassemblies as one part each instead of dozens or hundreds, eliminating fasteners or rivets as well. Injection molding with impact resistant plastics would permit the use of sculpted surfaces which could carefully tailor airflow to maximize aerodynamic performance and to maximize strength from impacts or flight loads.

Low cost would also mean not duplicating systems. This means designing PAVs to be for one purpose—the transfer of occupants from Point A to Point B at speeds indicative of the mode of

transportation. For air vehicles, this means a speed about four times block speed in traffic, or about 160 mph. PAVs would be capable of vertical takeoff and landing (VTOL) to mitigate the need for use of dedicated runways at airports or in special roadside areas and the first generation of PAVs would be single mode with limited dual mode use. This reduces the need for duplicate ground and air drive trains, reduces parts count, simplifies control, lowers cost, and limits certification of the PAV to one set of regulations.

Finally, low cost means developing a propulsion system for an airborne aircraft similar in cost to today's automotive engines but with tomorrow's approach to energy conservation and efficiency. Ideally, the propulsion system would help wean the American public from fossil fuels by using alternate cycles such as hydrogen/air fuel cells where the only replaceable fuel would be hydrogen. Eventually, PAVs could be designed to run on water and the only fuel preparation necessary would be filtration and distillation to remove impurities. Hydrogen/air fuel cells would provide electrical energy to turn motors which, in turn, would provide propulsive thrust. Even with today's standards in fuel cells, motors, and gearboxes, fuel-filler-cap-to-fan efficiency would be on the order of 60% as opposed to a fossil fuel engine's 30% propulsive efficiency.

**Lightweight.** Development effort must be put into construction methods to achieve the low parts counts just discussed, a goal being a two order of magnitude reduction in parts count. New materials capable of replacing aluminum and composite layups will have to be developed and a new approach to fabrication will have to be developed around them. The goal should be to produce a single occupant vehicle weighing 1,000 # or less with structure weight being no more than 25% of TOGW with a goal of 18%.

The single mode propulsion system must provide propulsive thrust multiplication; that is, for a given installed thrust or power, propulsive thrust would be some multiple of it. A goal would be propulsive thrust equal to three times installed thrust. That implies some form of augmentation, either by fluidic amplifier or low disc loading fan.

**Safe and Quiet.** Safety will be provided by a combination of resilient structures, naturally protective molded shapes, low impact speeds, and reliability of major components. Low impact speeds can be assured by taking off and landing vertically with a rapid transition to/from wingborne flight, if wings will be used at all. Incorporation of safety parachutes sized to deploy quickly in emergencies and bring the entire vehicle down with a low ground-contact speed will be a necessary feature. Operational safety can be improved with the use of an augmented reality headset for the pilot which mixes information in the visual range with computer-generated graphics to direct flight.

Quiet operation comes from two approaches. The first is to minimize the use of high tip speed rotors or fluidic amplifier cavities which resonate in the audible range. Second, and perhaps more important, is the incorporation of active noise cancellation tuned to mask propulsion sounds.

**Reliable.** Reliability will come from minimizing moving components and subsystems, all of which have finite mean times between failure (MTBF) which multiply as systems become more and more complex. Minimum parts counts with robust materials will also add to reliability.

Engines or motors will be as reliable as automobile engines of today and capable of functioning with the same amount of neglect most personal owners give their automotive drive trains.

**Comfort and Size.** If the PAV were sized for one person, TOGW would be 1,000# or less with approximately 250# set aside for the occupant and personal stuff. Personal stuff includes baggage and all the assorted items found in personal cars including maps, cables, tools, and any other miscellaneous items important to the owner which have finite weights and volumes. So an important goal would be to size the PAV to include just the occupant and personal stuff plus fuel, propulsion system, and necessary VTOL and forward flight components. Visibility must be at least as good as in most automobiles and existing general aviation airplanes with a goal of improving and augmenting it further. The PAV must also be compact and capable of storage in existing garages to minimize non-flight related costs other than insurance.

### **Summary**

- Creation of the five assigned configurations prompted added explorations, some of which were dead-ends;
- Some components could be common to all configurations such as avionics and dual-mode suspension schemes;
- Single-Mode PAVs can be created by removing dual-mode-specific items;
- Aviation history provided some intriguing starting points, as in what goes around comes around.
- CTOL and STOL dual-mode PAVs look feasible with single-mode PAVs being simplifications of the dual-mode approach;
- VTOL PAVs will require development;
- More exotic collapsing mechanisms need development;
- As a teaching tool, PAVs are not yet a well-enough bounded design problem.